ROYAUME DU MAROC
Université Mohammed V - RABAT -
جامعة محمد الخامس – الرباط –
Faculté des sciences
كلية العلوم

CENTER OF DOCTORAL STUDY - SCIENCES AND TECHNOLOGIES

N° of order: 3151

THESIS

Presented at the faculty to obtain the grad of: ***Doctor***

Structure of Research: Laboratory of Condensed Matter and Interdisciplinary Sciences (LaMCScI)

Discipline: Physics Informatics

Specialty: Condensed Matter and Modelling Systems

Defended on: 17/11/2018 By:

Mohamed HOUMAD

Thesis topic:

Study of physical properties of Siligraphene and its derivatives for different applications

JURY

BENYOUSSEF Abdelilah	*PES, Hassan II Academy of Science and Technology, Rabat*	***President***
EL KENZ Abdallah	*PES, University Mohammed V, Faculty of Sciences, Rabat*	***Director of Thesis***
AINANE Abdelmajid	*PES, University Moulay Ismail, Faculty of Sciences, Meknes*	***Reviewer***
EZ-ZAHRAOUY Hamid	*PES, University Mohammed V, Faculty of Sciences, Rabat*	***Reviewer***
LOULIDI Mohammed	*PES, University Mohammed V, Faculty of Sciences, Rabat*	***Examiner***
MASROUR Rachid	*PES, University Cadi Ayyad, National School of Applied Sciences, Safi*	***Examiner***

Academic year: 2018/2019

DedicationTo

- God who has me shown me the good way.
- The heart of My father, my companion as a recognition.
- My mother, for her constant support, and never ending sacrifices.
- My sisters, for being always by my side.
- My cousin Ahmed Hommadi and her wife Meriam
- AbdelAziz Hommadi my dear cousin.
- Mohamed Hommadi and her wife Yatou.
- To Professor Sara hemmi.

To my big family to whom, I owe a debt of gratitude for providing me with much love and support throughout the years of my study.

Acknowledgement

This thesis has been prepared out at the Laboratory of Condensed Matter and Interdisciplinary Sciences (LaMCScI), Faculty of Science, Mohammed V University– Rabat, under the supervision of Prof. **Abdallah EL KENZ**.

First and foremost, praises and thanks go to Allah, the Almighty, for his unlimited and uncountable blessings in my whole life and throughout my research work in particular. Second, I would like to express my great appreciation, deep gratitude and sincere thanks to my supervisor Prof. **Abdallah EL KENZ**, for giving me this opportunity to learn from his valuable expertise and fruitful discussions with him. He has always had time to answer my questions and he patiently provided much vision, encouragement and advise necessary to proceed throughout my research period. It is my privilege to be his student.

I would also like to extend my acknowledgment to **the chairman** of the jury Prof. **Abdelilah BENYOUSSEF** from Hassan II Academy of Science and Technology Rabat, for reviewing my thesis.

Besides my supervisor, I also would like to offer my thanks to the thesis committee for reviewing my thesis and providing me with their insightful and useful comments.

I also would like to express my thanks to Prof. **Abdelmajid AINANE** from University of Moulay Ismail, Faculty of Sciences, Meknes, for reporting and reviewing this PhD thesis.

I also would like to thank Prof. **Hamid EZ-ZAHRAOUY** from Faculty of Science Rabat, for reporting and reviewing this PhD thesis.

I also would like to acknowledge Prof. **Mohamed LOULIDI** from Faculty of Science Rabat, for reporting and reviewing this thesis.

I also would like to thank my Prof. **Rachid MASROUR** from University Cadi Ayyad, National school of Applied Sciences, Safi, for reviewing this thesis.

I would like also express my recognition to offer my thanks to Prof. **Mohammed HALOOL AL-ABBOODI** from Southern Illinois University, Carbondale, IL USA.

I would also like to extend my thanks to Prof **Saaid AMZAZI** the **Chairman of university Mohammed V Rabat;** for selected my article (accepted at carbon journal impact factors 7.02) the best paper on science at University Mohammed V on 2016.

I would also like to extend my thanks to all researchers at Laboratory of Condensed Matter and Interdisciplinary Sciences (LaMCScI).

Abstract

The aim of this thesis is to study the siligraphene and its derivatives and give a prediction of the possible use of this material in the photovoltaic cells or like anode of the Lithium batteries. We used the methods of the linearized increased plane waves (FP-LAPW) and the functional theory of the density to deduce the properties optoelectronics from the siligraphene. These methods are implemented in the codes Wien2k and Quantum espresso. Our work focuses on the siligraphene and its derivative and treats also the answers to the following open questions:1) How to open the band gap of the graphene?2) how to control the band gap of the graphene by doping with silicon?3) How to open and control the band gap of the graphene by constraints?4) Which are the magnetic properties of silicon nanosheet carbide doped by manganese?5) Is the siligraphene can be used as anode in the batteries of Lithium or others? To answer of these questions, we dope the graphene by selected silicon concentrations to open and control its gap. We have shown that it is possible to open the gap of the graphene by doping silicon and we controlled the gap of the graphene by silicon concentration. This doping gives new types of materials which are called the siligraphene. Also we applied a compression or a dilatation to open or control the gap siligraphene. This modified material has a potential of application as anode of battery of Li-ion. In this case, how to improve the diffusion of the Li ions about the anode of siligraphene? To answer this question we calculated the diffusion barriers of this material.

Key Words:siligraphene, graphene, anode of the Lithium batteries, Ab initio calculations, FP-LAPW, Wien2k, Quantum espresso, photovoltaic cells, compression, dilatation.

Résumé

Le but de cette thèse est d'étudier le siligraphene et ses dérivées et donner une prédiction de l'utilisation possible de ce matériau dans les cellules photovoltaïques ou comme anode dans des batteries de Lithium. Nous avons utilisé les méthodes des ondes planes augmentées linéarisées (FP-LAPW) et la théorie fonctionnelle de la densité pour déduire les propriétés optoélectroniques du siligraphene. Ces méthodes sont implémentées dans les codes Wien2k et Quantum espresso. Nos travaux se focalisent sur le siligraphene et ses dérivées et traitent aussi les réponses aux questions ouvertes suivantes :1) comment ouvrir le gap du graphene?2) comment contrôler le gap du graphene par dopage avec le silicium? 3) comment ouvrir et contrôler le gap du graphene par des contraintes ?4) Quelles sont les propriétés magnétiques du carbure de silicium nanosheet dopé par le manganèse ? 5) Est-ce que le siligraphene peut être utilisé comme anodes dans les batteries de Lithium ou d'autres ? Pour répondre à ces questions: Nous avons choisi de doper le graphene par différentes concentrations de silicium pour ouvrir et contrôler son gap. Nous avons montré qu'il est possible d'ouvrir le gap du graphene par le silicium dopé et on a contrôlé le gap en fonction de la concentration de silicium. Ce dopage donne de nouveaux types de matériaux qui s'appellent les siligraphenes. Aussi nous avons appliqué une compression ou une dilatation pour ouvrir ou contrôler le gap du siligraphene. Ce matériau modifié a un potentiel d'application comme anode de batterie de Li-ion. Dans ce cas on pose la question comment améliorer la diffusion des ions de Li sur l'anode de siligraphene ? Pour répondre à cette question nous avons calculé les barrières de diffusion de ce matériau.

Mots clé: siligraphene, graphene, anode of the Lithium batteries, Ab initio calculations, FP-LAPW, Wien2k, Quantum espresso, photovoltaic cells, compression, dilatation.

Résumé détaillé

Dans ce mémoire de thèse de doctorat, nous avons étudié le siligraphene et ses dérivées et nous avons aussi présenté une proposition de l'utilisation possible de ce matériau dans les cellules photovoltaïques ou comme anode dans des batteries de Lithium. Le manuscrit est divisé en trois parties.

la première partie présente une introduction générale sur les propriétés physiques et les méthodes de fabrication du graphene et aussi leurs applications. On a aussi introduit le siligraphene et ses dérivés. Dans cette partie, Nous avons présenté quelques formes allotropiques de carbone allant du diamant jusqu'au siligraphene. Ce dernier est un nouveau type de matériaux 2D qui se construit à partir du graphene en le dopant par diffèrentes concentrations des atomes de silicium. Le dopage du graphene par le silicium change leur caractère métallique vers le caractère semi-conducteur.

La deuxième partie traite les méthodes ab initio qui sont basées sur la résolution de l'équation de Schrödinger. Dans cette partie, nous avons utilisé les ondes planes augmentées linéarisées (FP-LAPW) et la théorie fonctionnelle de la densité pour déduire les propriétés optoélectroniques du siligraphene. Ces méthodes sont implémentées dans les codes Wien2k et Quantum espresso.

La troisième partie est dédiée à l'étude des propriétés physiques de Siligraphene et ses dérivés pour des applications sur la pile solaire ou la Li-Batterie ou les matériaux flexibles. Nos travaux de recherche se sont focalisés sur le siligraphene et ses dérivées et traitent aussi les réponses aux questions ouvertes suivantes :1) comment ouvrir le gap du graphene? 2) comment contrôler le gap du graphene par le dopage avec le silicium? 3) comment ouvrir et contrôler le gap du graphene par des contraintes ? 4) Quelles sont les propriétés magnétiques du carbure de silicium nanosheet dopé par le

manganèse ? 5) Est-ce que le siligraphene peut être utilisé comme anodes dans les batteries de Lithium ou d'autres ?

Pour répondre à ces questions: Nous avons choisi de doper le graphene par différentes concentrations de silicium pour ouvrir et contrôler son gap. Nous avons montré qu'il est possible d'ouvrir le gap du graphene en le dopant par le silicium et on a contrôlé ce gap en fonction de la concentration de silicium. Ce dopage donne de nouveaux types de matériaux qui s'appellent les siligraphenes. Aussi nous avons appliqué une compression ou une dilatation pour ouvrir ou contrôler le gap du siligraphene. Ce matériau modifié a un potentiel d'application comme anode de batterie de Li-ion. Dans ce cas on pose la question : comment améliorer la diffusion des ions de Li sur l'anode de siligraphene ? Pour répondre à cette question nous avons calculé les barrières de diffusion de ce matériau.

Cette partie se divise en huit chapitres:

Le premier chapitre présente les propriétés optiques du nanosheet de carbure de silicium. Ainsi, nous calculons dans ce chapitre la fonction diélectrique, le spectre de réflectivité, le coefficient d'absorption, la conductivité optique et la réfraction suivant les polarisations perpendiculaires et parallèles du champ électrique. Nous avons trouvé que les propriétés optiques des nanosheet du carbure de silicium sont intéressantes et en accord avec les propriétés optiques du graphene. C'est pourquoi le nanosheet du carbure de silicium peut être remplacé par le graphene à cause de sa stabilité chimique plus élevée. Enfin, ce nanosheet de SiC peut être employé pour fabriquer des appareils nano-optoélectroniques.

Dans le deuxième chapitre de cette partie nous traitons théoriquement la réponse à la question comment ouvrir le gap du graphene et comment améliorer sa conductivité optique ? Nous avons choisi de doper le graphene par des

différentes concentrations du silicium. Pour cela, nous avons étudié la structure électronique du graphene pur et du graphene dopé par le silicium et ceci par trois approximations GGA, TB-mBJ et GW. A cause de la symétrie hexagonale, toutes les propriétés optiques du graphene, quand on applique le champ électrique suivant la direction parallèle ou la direction perpendiculaire, sont différentes. Par conséquent, le graphene est un matériel anisotrope. Aussi nous avons montré qu'on peut contrôler le bandgap du graphene par le dopage avec le silicium.

En conséquence, nous avons répondu à un certain nombre de questions de trouver en premier lieu que la conductivité électrique de g-SiC3 est meilleure que la conductivité électrique de g-SiC7. À cet égard, nous supposons que le siligraphene a un potentiel d'être employé dans l'application de pile solaire. Dans le chapitre 5 par exemple, nous avons étudié les propriétés électroniques et la conductivité électrique du siligraphene (g-SiC3) en employant des paquets de Boltztrap dans le quantum espresso. En second lieu, les divers pourcentages de la contrainte ont affecté les propriétés électroniques. Ainsi, la bande interdite électronique s'ouvrira sous l'application de -9% et -10% contraintes.

Cependant, la géométrie de la structure a également changé. Nous avons observé que la longueur de liaison entre les atomes Carbone-Silicium a une augmentation de10%, qui est mène à boucler la structure géométrique du g-SiC3.Un autre résultat fascinant est que la conductivité électrique de g-SiC3 augmente aussi, quand nous appliquons de divers pourcentages de contrainte. Alors nous pourrions obtenir une valeur plus élevée de la conductivité électrique à la contrainte égale à -9 % quand le siligraphene (g-SiC3) change ses propriétés semi-métal vers un semi-conducteur. Le résultat trouvé est que le siligraphene (g-SiC3) est un nanomatériau flexible et il peut être employé dans le smartphone.

Dans le chapitre 6, nous avons étudié théoriquement les propriétés électriques et la stabilité des structures du siligraphene en utilisant les codes de Boltztrap et le quantum espresso. Ainsi, nous avons constaté que la bande interdite de siligraphene change sous des contraintes (compressives et de tension) bi-axiales. En d'autres termes, elle diminue sous des contraintes bi-axiale (compressif et de tension). La conductivité électrique de Siligraphene g-SiC7 devient plus grande sous ces contraintes (compressif et de tension) comparé à celle sans contraintes.

Par la suite, dans le chapitre 7 nous avons proposé une nouvelle anode basée sur le siligraphene et qui peut être industrialisées dans les batteries de Li-ion. En se basant sur le premier principe de calcul, nous avons constaté que cette anode a une diffusion des batteries d'ion de Li importante. Ces résultats théoriques poussent les chercheurs expérimentaux à fabriquer cet anode.

List of Publications

- **Houmad, M., H. Zaari, A. Benyoussef, A. El Kenz, and H. Ez-Zahraouy. "Optical conductivity enhancement and band gap opening with silicon doped graphene." *Carbon* 94 (2015): 1021-1027.**

- **HOUMAD, M., MOHAMMED, Mohammed H., MASROUR, R., et al. Electronic and electrical properties of siligraphene (g-SiC3) in the presence of several strains. Journal of Physics and Chemistry of Solids, 2019, vol. 127, p. 231-237.**

- **HOUMAD, M., ESSAOUDI, I., AINANE, Abdelmajid, A., El Kenz, A., Benyoussef, A., Ahuja, R. Improving the electrical conductivity of Siligraphene SiC7 by strain. Optik, 2019, vol. 177, p. 118-122.**

- **Houmad, M., O. Dakir, A. Abbassi, A. Benyoussef, A. El Kenz, and H. Ez-Zahraouy. "Optical properties of SiC nanosheet." *Optik-International Journal for Light and Electron Optics* 127, no. 4 (2016): 1867-1870.**

- **Houmad, M., A. Abbassi, A. Benyoussef, H. Ez-Zahraouy, and A. El Kenz. "Optical properties of Ni doped 3C-SiC with ab initio calculations." In *Renewable and Sustainable Energy Conference (IRSEC), 2014 International*, pp. 596-601. IEEE, 2014.**

- **Houmad, Mohamed, Halima Zaari, Abdelilah Benyoussef, and Abdelah El Kenz. "Optical properties of titanium and iron doped 3C-SiC behaviors TB-mBJ." *Chinese Journal of Physics*54, no. 6 (2016): 960-967.**

- **Houmad, M., Z. Zarhri, Y. Ziat, Y. Benhouria, A. Benyoussef, and A. El Kenz. "Ferromagnetism induced by double impurities Mn and Cr in 3C-SiC." *Chinese Journal of Physics*(2017).**

- **Houmad, M., O. Dakir, H. Benzidi, O. Mounkachi, A. El Kenz, and A. Benyoussef. "Magnetic behavior of Mn-doped silicon carbide nanosheet." *International Journal of Modern Physics B*(2017): 1750163.**

- **Houmad, M., A. El Kenz, and A. Benyoussef. "Thermal and Electrical properties of Siligraphene and its derivatives." *Optik-International Journal for Light and Electron Optics* (2017).**

- **Houmad, M., A. Benyoussef, and A. El Kenz. "Optical and magnetic properties of Mn doped 4H-SiC: First principal calculations." In *Renewable and Sustainable Energy Conference (IRSEC), 2016 International*, pp. 698-703. IEEE, 2016.**

- **Dakir, O., M. Houmad, A. Benyoussef, and A. El Kenz. "Absorption of visible light by GaAs and GaN nanosheets." *Optik-International Journal for Light and Electron Optics* 141 (2017): 60-65.**

- **Ziat, Younes, Abderrahman Abbassi, Amine Slassi, Maryama Hammi, Abderrahim Ait Raiss, Omar El Rhazouani, Mohamed Houmad, Siham Echihi, and Abdallah El Kenz. "First-principles investigation of the electronic and optical properties of Al-doped FeS2 pyrite for photovoltaic applications." *Optical and Quantum Electronics* 48, no. 11 (2016): 511.**

- **Ziat, Younes, Amine Slassi, Zakaryaa Zarhri, Maryama Hammi, Mohamed Houmad, Abderrahim Ait Raiss, Younes Sbai, Siham Echihi, Abdallah El Kenz, and Abdelilah Benyoussef. "First-principles study of magnetic and electronic properties of fluorine-doped Sn0. 98Mn0. 02O2 system." *Journal of Superconductivity and Novel Magnetism* 29, no. 11 (2016): 2979-2985.**

- **Zarhri, Z., M. Houmad, Y. Ziat, O. El Rhazouani, A. Slassi, A. Benyoussef, and A. El Kenz. "Ab-initio study of magnetism behavior in TiO 2 semiconductor with structural defects." *Journal of Magnetism and Magnetic Materials* 406 (2016): 212-216.**

- **BENHOURIA, Y., KHOSSOSSI, N., HOUMAD, M., et al. Dynamic magneto-caloric effect of a multilayer nanographene: Dynamic quantum Monte Carlo. Physica E: Low-dimensional Systems and Nanostructures, 2019, vol. 105, p. 139-145.**

Submitted

M. Houmad et al. "Stana-Silicene is a Novel 2D Nanomaterial" 2018

M. Houmad et al. "Siligraphene as anode novel Materials for Rechargeable Lithium Batteries" to Journal of energy storage, 2019

M. Houmad et al. "Detection various properties of two Single-layer Tetragonal Silicon Carbides" Chemical Physics Letter, 2019

M. Houmad et al. "Effect of inter-distance on band gap of silicon carbide Bilayers" Advance Nanomaterials and Technologies For Energy Sector - NanoEnergy, 2019

جامعة محمد الخامس بالرباط
Université Mohammed V de Rabat

Attestation

Cérémonie de l'Excellence du 14 janvier 2016 sous le thème :
Le Rendez-Vous de l'Excellence de l'UM5 de Rabat

Je soussigné Professeur ***Saaïd AMZAZI****, Président de l'Université Mohammed V de Rabat, atteste que :*

La publication intitulée :

« Optical conductivity enhancement and band gap opening with silicon doped graphene »

Parue dans la revue Carbon au titre de l'année 2015 et dont les auteurs sont :

Mouhamed Houmad, Halima Zaari, Abdelilah Benyoussef, Abdellah El Kenz, Hamid Ez-Zahraouy

a reçu le prix de ***la Meilleure Publication 2015*** *pour le domaine Sciences, Technique et Ingénierie*

Fait à Rabat, le 25 Mai 2017

Signature du Président
Le Président de l'Université
Saaïd AMZAZI

Reviewer for journal of Applied Surface Science

ELSEVIER

Applied Surface Science

certifies that

"Houmad Mohamed"
has acted as a reviewer for the journal during 2017

The Editors of Applied Surface Science
Elsevier, Amsterdam, The Netherlands

Tables and Figures

General Introduction

The key of nano-technologies and their success of application in several Nano-devices is the discovery of graphene, the latter pushed science to find others materials alternative to graphene. 2D-materials are new area of materials constituting of a single layer or few layers. The research in 2D-materials is motivated by the success of application of graphene and by their unique physical and chemical properties due to their dimensionality. The recent development in scientific research is the synthesis and the characterization of an isolated or few layers of 2D-materials.After extracting graphene, it is necessary to measure and manipulate this material at the nanometer scale. The first allotrope of carbon, discovered by Kroto in 1985 in nanotechnology, is the fullerene having a 0D dimension[1]. The second allotrope of carbon in 1D dimension, discovered by SumioIijima in 1991, is Nanotube of carbon[2].

Before 2004, the vision of science was synthesized and characterized a new material having a two dimensional structure order to deduce their physical properties. This objective has been realized at the Centre for Mesoscopic and Nanotechnology of Manchester University, UK by A. Geim et al. [3, 4, 5]. This group used the micro-mechanical cleavage of graphite to produce graphene. This discovery of a new material having two-dimensions is called graphene. The success of the application of graphene in many areas such as electronic, optoelectronic and spin-tronic devices, catalysis, sensors, high performance electrodes and nano-composites, was the reason why Andre Geim and Konstantin Novoselov were awarded the noble prize of physics in 2010. The monolayer of graphene is only a plan of graphite. The graphene has higher physical properties compared to graphite because its 2D hexagonal structure differs from graphite (3-dimensions). The carbon atom in graphene is surrounded by three atoms of carbon in planar sheet. The bond length between two carbon atoms (sp2 bonded carbon atoms) is equal to 0.14nm, being measured by Geim et al. using the transmission electron microscope (TEM). Schniepp et al. and Berger et al. produced experimentally the isolated graphene[6, 7].The recent research confirmed that graphene has high electron mobility[8, 9, 10, 11, 12, 13]. The mechanical, electronic, optical and magnetic properties of graphene have been studied in these refs [14, 15, 16, 17, 18]. The graphene has been

introduced in several applications of nanotechnology such as the fabrication of nano-transistors [19]. After synthesizingthe graphene by several groups, the difficulty of using graphene in solar cell or in the field of semi-conductors lies in the semi-metallic character of graphene. This property limits its applications, as it leads the researchers and the experts to ask the following question: How to open the gapless of graphene?

The method of calculations being based on quantum mechanical modeling is used for the prediction of equilibrium structures and the calculations of energies of solid state. The physical properties associated to the materials can be predicted quantitatively by the modeling. In this thesis, we used Density Functional Theory (DFT) methods in the field of quantum mechanical modeling to determine the physical properties of siligraphene and its derivatives for the application to solar cell or Li-battery or mechanical applications (flexible materials). These materials are produced using graphene doped by silicon atoms for different concentrations. This doping of graphene with silicon atoms permits to open the band gap of graphene.

Firstly, the group of Denis et al. has demonstrated theoretically that the band gap of graphene (monolayer or bilayer) is possible to be opened with silicon, aluminium, phosphorus and sulfur [20]. The formation of the band gap in graphene with silicon doped has been analyzed by Escaño et al. and Azadeh et al. [21, 22]. Furthermore, in this thesis we are doping graphene with silicon for opining its band gap. [23]. Likewise, other methods can be used for opening the band gap of graphene such as functionalized graphene with hydrogen or molecule adsorptions [24].

This work is divided into three parts: in the first Part, we are going to present Generalities on synthesis and applications of the graphene, siligraphene and its derivatives. The second Partis going to deal with the methods of modeling and simulation. The final Part is eventually going tofocus on the siligraphene and its derivatives and treats the answers to the following open questions:1) How to open the band gap of graphene? 2) How to control the band gap graphene by doping with silicon?3) How to open and control the band gap graphene by constraints?4) Which are the magnetic properties of silicon nanosheet Carbide doped by manganese?5) The siligraphene can be used as anodes in the batteries of Lithium or others?

To answer of these questions we structure this part by several chapters: In chapter 1, we dope the graphene by various silicon concentrations to open and control its gap. We have shown that it is possible to open the gap of graphene by doped silicon and we controlled the gap of graphene by silicon concentration. This doping gives new types of materials which are called the siligraphene. Also, we applied a compression or an attraction to open or control the gap siligraphene. In chapter 8, we answer to the question how to improve the diffusion of the Li ions about the anode of siligraphene?

The organizations of these chaptersare as follows:

Chapter 1 will treat theoretically the Optical Conductivity enhancement and band gap opening With Silicon doped graphene

Chapter 2 will give the optical proprieties of Silicon Carbide nanosheet.

Chapter 3 will investigate Magnetic behavior of Mn doped silicon carbide nanosheet

Chapter 4 will focus on the Electrical property of Siligraphene and its derivatives.

Chapter 5 will investigate Electronic and Electrical properties of Siligraphene (g-SiC3) in The Presence of Various Strains

Chapter 6 will treat Detection various properties of two Single-layer Tetragonal Silicon Carbides

Chapter 7 will treat the improving the electrical conductivity of Siligraphene SiC7 by strain

Chapter 8 will focus Siligraphene as anode novel Materials for Rechargeable Lithium Batteries

Part I: Generalities on Siligraphene

I. Some allotropes of carbon

Lavoisier discovered Carbon in 1789. It exists largely in the nature. Carbon canform several allotropes such as graphite, graphene, diamond and carbon nanotubes. They require a high temperature for reaction and they are thermodynamically stable. The possibilities of carbon to form sp2 and sp3 bonds give its interesting electronic and structural properties[25]. This contributes to increase the range of transport and magnetic properties offered by carbon.

I.1. Diamond

The term diamond comes from a modification of the Greek word "adamastos", invincible. The first Western texts that made mention of it date from the first century. Diamond has a metastable crystalline form at the ordinary temperature, which allows it to be preserved without transformation. The diamond lattice, being formed by carbon atoms in a diamond crystal, is composed of face centered cubic Bravais lattices (figure 1). Each atom of carbon in diamond is surrounded by four nearest neighbors of other atoms. Graphite is stable at averaged pressures but diamond is stable at higher pressures.

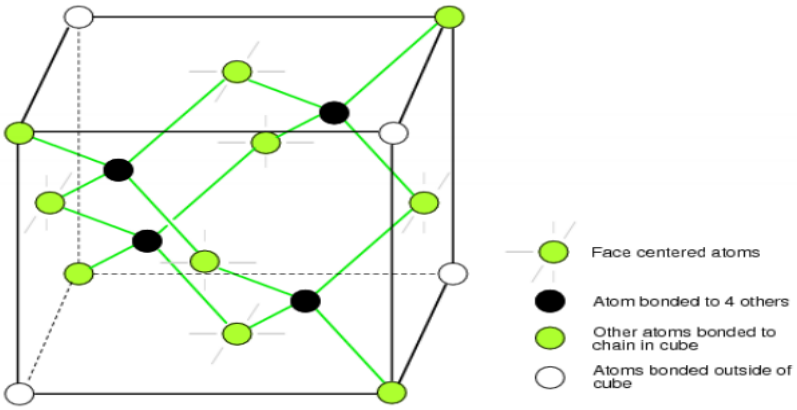

Figure 1: scheme of diamond in cubic structure

Diamond has cubic structure in three dimensions. The sp^3 represents the bonding hybridization in diamond structure. The band gap of diamond is equal to 5.47eV. This permits us to consider that diamond is an insulator material at room temperature.

Diamond has strong physical properties because of its Young's modulus of 1050 GPa and high bulk modulus of 442 GPa, Its density is in the order of 3.515g $cm^{-3}$and its thermal conductivity ranges fromfrom 900 to 2300W $m^{-1}K^{-1}$, which shows lower

electrical conductivity. Diamond is used for industrial purposes due to the fact that its electrical conductivity is lower and its hardness is employed for cutting.

I.2. Fullerene

The Nobel Prize for Chemistry in 1996 was granted to H. Krotofrom Sussex University, R. Smalley and R. Curl of the University of Rice in Houston [1]for their discovery, synthesis and identification of fullerene (C60) in 1985. The molecule of fullerene (name buckyball) is a spherical-shaped molecule composed of carbon atoms only. Each carbon atom is attached to three others with a bonding type sp^2 hybridized. It consists of both pentagonal and hexagonal carbon rings (20 hexagonal and 12 pentagonal rings) (see figure 2).

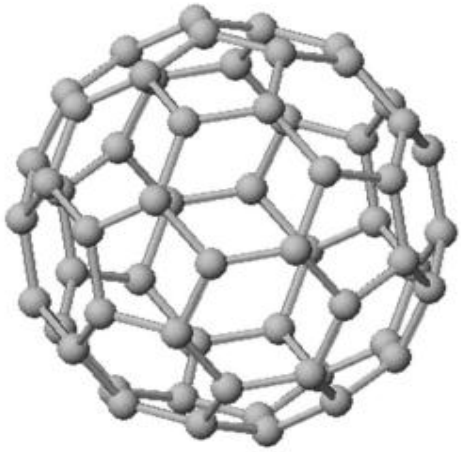

Figure 2: The structure of C60 "Buckminsterfullerene"

I.3. Carbon nanotube

During the experiment of the production of evaporation of graphite by the electric arc, SumioIijimadiscovered in 1991 the one-dimensional graphitic nanostructures[2]. This new structure is named Carbon nanotube. It is a cylindrical allotrope of carbon and classified in two types: single-walled carbon nanotube (SWNT) and multi-walled carbon nanotube (MWNT). The major difference between these two types is that single-walled carbon nanotube (SWNT) consists of a single graphene enrolling for constitute a cylinder in 1 dimension, whereas a multi-walled carbon nanotube (MWNT) comprises of several concentric graphene cylinders in 1 dimension (see figure).

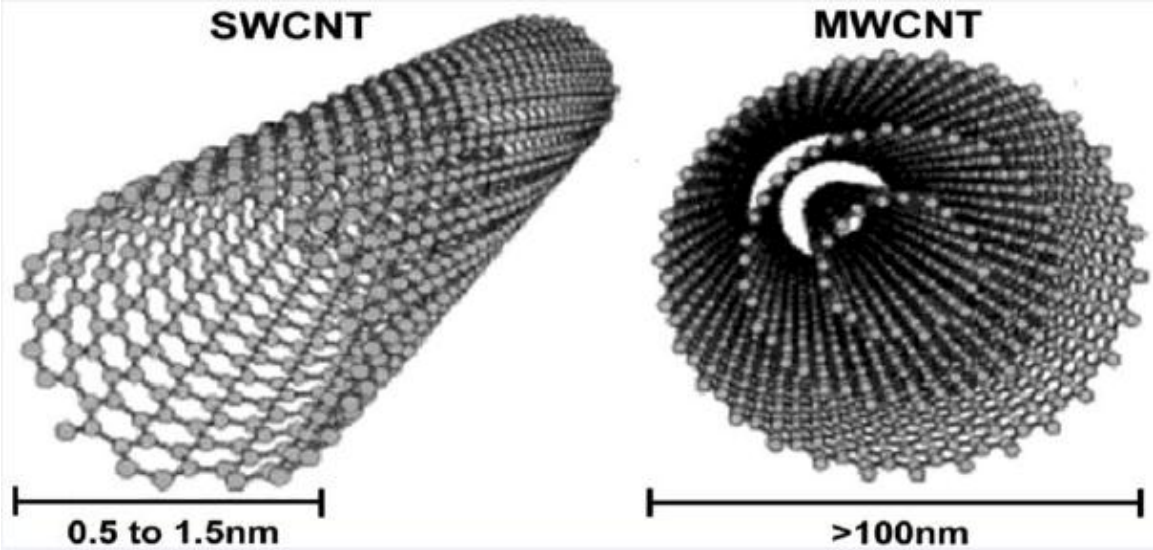

Figure 3: structures of single-walled carbon nanotube (SWNT) and multi-walled carbon nanotube (MWNT)

I.4. Graphite

Graphite exists in nature around the world with large quantities. Graphite is constructed of parallel planes of carbon atoms dispersed in regular hexagons being oneonthe other. Graphite consists of an alternate stacking of graphitic sequences of planes called graphene (ABABAB…). In this sequence, the different planes are shifted of a half-period. The nearest neighbor distance between carbon atoms is 1.42A° and the interlayer distance is 3.34A° [26]. The softness of graphite is due to a weak bonding of van der Waals force between its layers. Interactions between the covalently bonded layers are caused by van der Waals force.

Graphite under normal conditions of temperature and pressure is thermodynamically stable. Graphite has a good electrical conductivity because each atom in the plane of graphite has a free electron and also the delocalization of one of the other electrons of each atom from a π.

Graphite possesses a density of 2.267 g cm^{-3} and a low thermal conductivity from 119 to 165W $m^{-1}K^{-1}$. Its electronic properties such as band gap indicate that it is a semi-conductor material promising for technological application.

I.5. Graphene

I.5.1. Structure of graphene

The allotropes of carbon such as fullerene (C60), carbon nanotube, and graphite are constructed by graphene according to the form of graphene (fig 4).

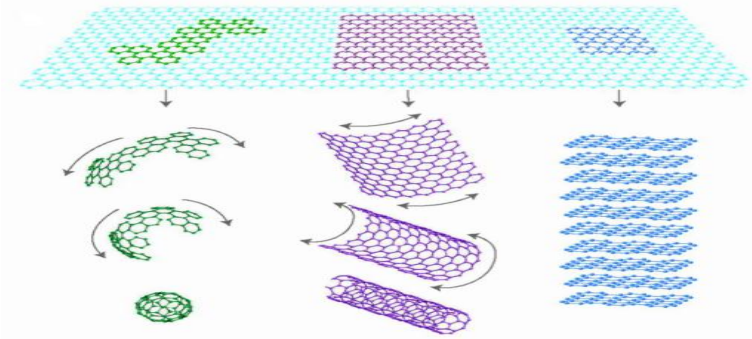

Figure 4: C 60 fullerene molecule, carbon nanotube, and graphite. Graphene, a single sheet of graphite, can be considered as a building block for all these carbon structure Geim (image produced from ref [27]).

The first synthesis of graphene was performed in 2004 by Andre Geim and Konstantin Novoselov by means of the methods of micro-mechanical cleavage of graphite [3]. The graphene structure has 2D honeycomb (hexagonal) form. The nature of bonding between two atoms of carbon is that they are covalently bonded. Graphene becomes a best material compared to diamond in the world because itis bonding between carbon-carbon atoms in 2dimentions. The hybridization of carbon atoms in graphene is sp^2. Its structure is shown in figure 2.

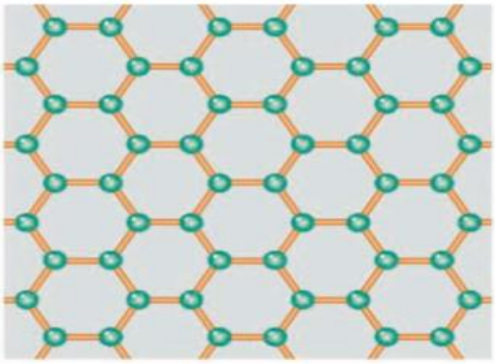

Figure 5: Honey-comb lattice structure of graphene (image produced from ref [28]).

I.5.2. Structural properties of graphene

Carbon atoms of graphene are distributed at hexagonal plan (honeycomb lattice). Figure 3 shows the structure of graphene as well as the space group of graphene structure being P6/mmm with the following lattice vectors:

$$\boldsymbol{a1} = \frac{\boldsymbol{a}}{\boldsymbol{2}}(\boldsymbol{3}, \sqrt{\boldsymbol{3}})\boldsymbol{a2} = \frac{\boldsymbol{a}}{\boldsymbol{2}}(\boldsymbol{3}, -\sqrt{\boldsymbol{3}})$$

The distance between the neighbor carbon-carbon atoms in graphene structure is in the order of 1.42A°. The lattice parameter constants of graphene is represented by triangular lattice with basis a1= a2= 2.46A°. The other three neighbor carbon atoms vectors are given by:

$$\boldsymbol{\sigma_1} = \frac{\boldsymbol{a}}{\boldsymbol{2}}\left(\boldsymbol{1}, \sqrt{\boldsymbol{3}}\right), \quad \boldsymbol{\sigma_2} = \frac{\boldsymbol{a}}{\boldsymbol{2}}\left(\boldsymbol{1}, -\sqrt{\boldsymbol{3}}\right), \quad \boldsymbol{\sigma_3} = -\boldsymbol{a}(\boldsymbol{1}, \boldsymbol{0})$$

Two possible configurations of graphene structure are called zigzag and armchair type. The difference between these structures is their orientations and the directions of the edges. In figure 3, we can obtain the armchair structure in the case of the Y direction and the zigzag structure in the case of the X direction.

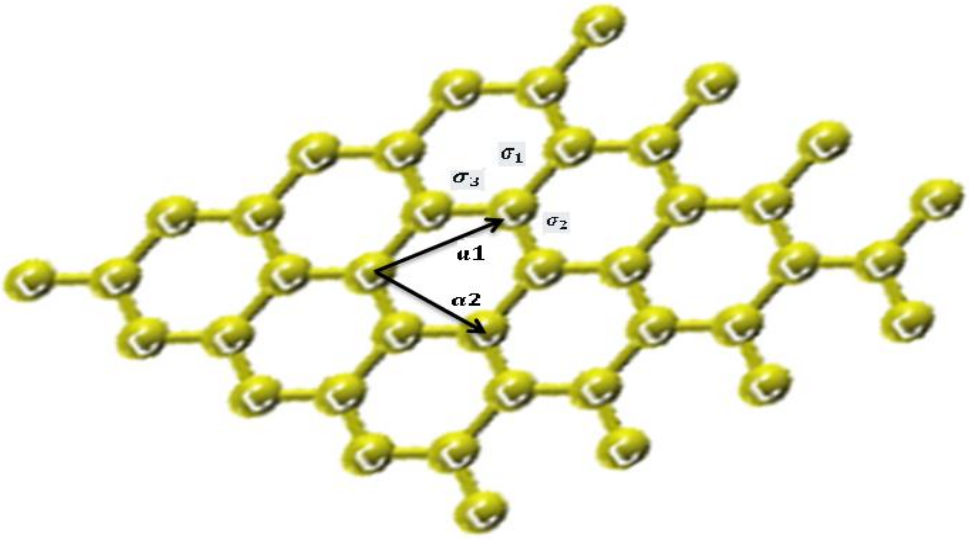

Figure 6: The lattice structure of graphene (a1 and a2 are the lattice unit vectors and are the neighbor vectors)

The type of band length in graphene is the covalent bonding formed between all atoms of carbon in hexagonal structure. The hybridization of graphene is sp2;made of by one S orbital and two P orbitals (the 2s, $2p_x$ and $2p_y$ for three valence electrons and the

fourth valence electron is in the $2p_z$ orbital which is orthogonal to the graphene plane). This hybridization sp2 forms the planar hexagonal structure. The bonding between two atoms of carbon is named sigma (σ). The distance between two carbon atoms in cubic diamond is 1.54A°, being larger than the bonding of graphene. This bonding makes graphene stronger than diamond [29]. The semi-metallic character of graphene and the linear dispersion of Dirac fermions in the band structure of graphene result from π band. This last band is formed from the overlap of half-filled $2p_z$ orbitals.

I.5.3. Electronic properties of graphene

P. R. Wallace has performed the first calculations of electronic what for one layer of graphite[30] based on simple tight-binding model. This model was carried out so as to find the low energies properties of graphite concerning itsothers layer. Furthermore, McClure in 1957[31] and Slonczewski and Weiss in 1958 [32] have developed this model. Density of states of graphene combines conduction band and valence band at Fermi level, which are formed mainly by p states. The band structure of graphene also shows valence and conduction band consisting of the bonding and anti-bonding orbitals, which touch the K-point. The connection of the two bands influences the possibility to easily excite electrons out of the valence into the conduction band independently of the wavelength. To illustrate,two bands with pz character belonging to different irreducible representations cross precisely the Fermi energy at the K point in momentum space. The linear dispersion of the bands results in quasi-particles with zero mass; called Dirac fermions[33].

$$E = \pm h\vartheta_f K$$

Where ϑ_f and K are Fermi velocity and momentum respectively.

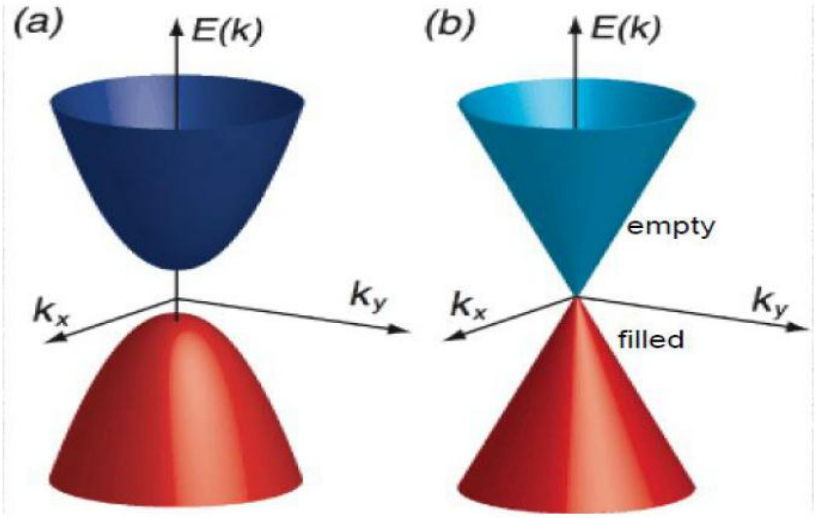

Figure 7: Band structure for (a) semiconductors (b) graphene around K-point.

I.5.4. Synthesis and experimental techniques of graphene

In the past few years, several production methods of graphene have been developingto produce high-quality graphene. The thermal chemical vapor depositions (CVD) [34], chemical synthesis[35], mechanical cleaving (exfoliation)[3] are among the famous methods which have been used for graphene synthesis. To fabricate more-layers of graphene in the experimental work, the mechanical exfoliation technique started beinglargely used because it can to produce graphene until 30-layers with a thickness of 10nm. Other techniques are microwave synthesis and unzipping nanotube are also usedin the graphene fabrication(see figure 8)[36, 37, 38].

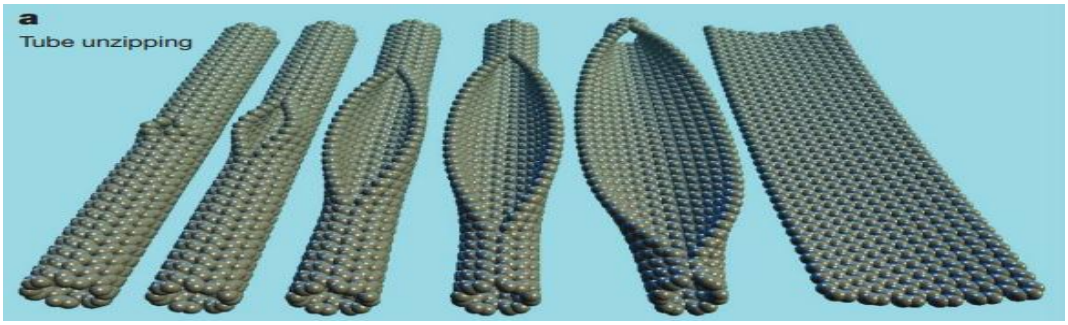

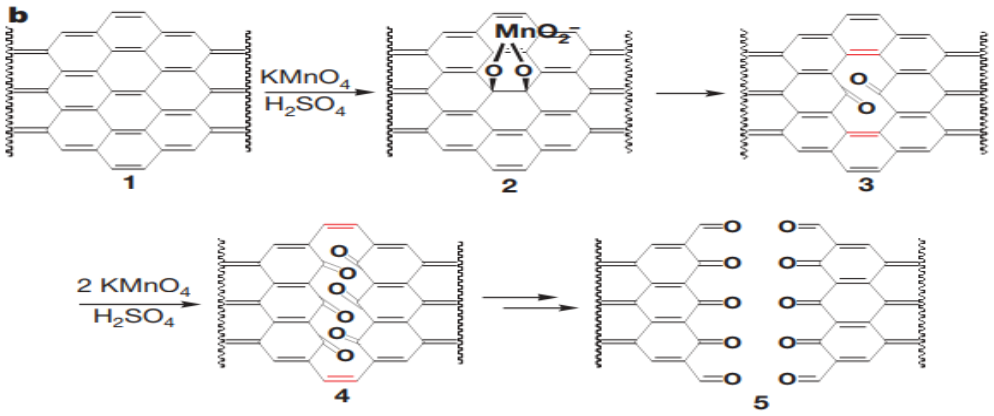

Figure 8: a) Representation of the gradual unzipping of one wall of a carbon nanotube to form a nanoribbon. Oxygenated sites are not shown. b) The proposed chemical mechanism of nanotube unzipping

a) Mechanical exfoliation

Konstantin Novoselov and Andre have used the Micromechanical cleavage to detach the graphene from graphite. The plane bonding between carbon atoms is stronger than the bonding between the different planes (van der Waals (vdW) bonding). This property facilitates the separations of the different plans of graphite for produce graphene by breaking the weak interlayer bonding. The exfoliation of graphite leading to obtain the graphene is one of the most promising ways to achieve a large-scale production at an extremely low cost (see figure 9).

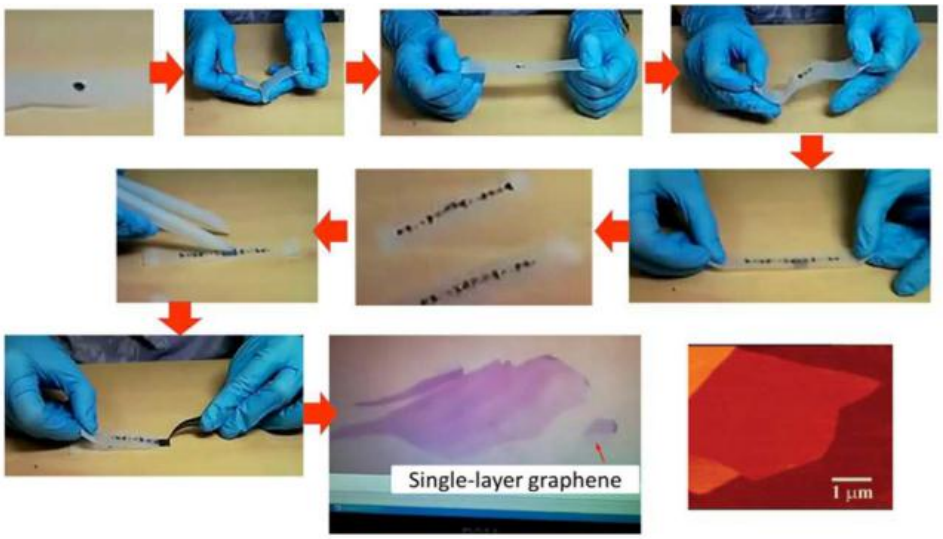

Figure 9: The illustrative procedure of scotch-tape based micromechanical cleavage of HOPG.

b) Chemical vapor Deposition

Chemical vapor deposition being a technique that deposes graphene onto transition metal substrates such as Cu [39], Ru[40]and Pb[41], is the most inexpensive and promising approach. Chemical vapor deposition is a well-known process in which a substrate is exposed to gaseous compounds. These compounds decompose on the surface in order to grow a thin film while the by-products evaporate. In this method a gaseous precursor, like methane, is supplied over a flat metallic surface. The process is based on the carbon saturation of a transition metal due to the exposure hydrocarbon gas at a high temperature[42]. While cooling the substrate, the solubility of carbon in the transition metal decreases and a thin film of carbon are thought to precipitate from the surface [43]. The high temperature, on the order of 1000°C, causes decomposition of the precursor. The metallic surface then acts like a catalyst on which a thin layer of carbon atoms deposits.

I.5.5. Applications of graphene

Nowadays, graphene becomes the most favorable material for many applications in various domains. Throughout this thesis, we have shed light on some applications of graphene such as Energy storage, Graphene-based transistors and cathode material in rechargeable lithium batteries:

a) Applications of graphene in Energy storage

A key challenge for rechargeable Lithium batteries is searching theoretically and realized experimentally a novel anode has a good performance. The research in this area has focused on developing rechargeable Lithium batteries to seek answers to increasing demands of renewable and sustainable energy sources. The Li-battery was inventing by Yazami et al. in 1983[44]. This discovery has urged intensive study on Li-battery because of unique characteristics they possess, namly large life [45], high reversible capacity[46, 47] and high energy density [48]. These properties; consequently have made this kind of batteries very commercial in many technological device. Graphite is used in commercial batteries. Lithium-ion is storage between two layers of graphite; because of their charge capacity that equal 372 mA h/g as well as acceptable reversibility.

Recent development to fabricate the lithium batteries has been using the 2D materials such as the 2D transition metal dichalcogenide. These materials have potential candidates for the anode material thanks to their charge capacity dimensionality and their flexibility. Graphene battery is similar to traditional batteries. Itis composed of an electrolyte solution of two electrodes to facilitate the transfer of ion in solution between the electrodes. Batteries based on graphene are quickly becoming more favorable than their graphite predecessors. Avariety of battery types have been developing based on graphene introduced in nanocomposites such as Li-ion batteries, Na-ion batteries, Zn-batteries and Li-S battery. The specific properties of graphene make, it an ideal candidate for producing a new generation of Lithium Batteries.

b) Applications of graphene in solar energy

For all types of conventional energy production, the solar cell is the most promising sources. It directly converts the solar energy to electrical power. Several material such as the transparent conducting oxides (TCOs) ZnO SnO2 and TiO2 have been used to convert solar energy to electrical energy. In the area of solar energy, it is necessary to increase the yield of solar cells. These are composed of two types of thin films.The first one has a high optical transmission (transparency). The graphene material has a good transparency (T = 97.7%) and a high conductance. These unique physical properties of graphene make it a material promising for uses in solar energy. Several researchers found that graphene has a gapless (semimetal). This semi-metallic character, therefore, limits its application in solar cell, which requires changing this character into a semiconductor one. So it can be applicable in photovoltaic cell.

I.6. Siligraphene

I.6.1. Structural and electronic properties of siligraphene

The effect of bonding structure and stoichiometry of the Silicon carbide monolayers, as a function of silicon and carbon concentration atoms on electronic properties of Silicon carbide, has been reported by Shi et al. [49].The super-cell of two configurations of siligraphene SiC_7 and SiC_3 are shown in Figures 10. Our calculations start by the relaxation of the structure of two types of Siligraphene. We demonstrate that the band length C-C and Si-C in SiC_7 is equal to 1.53A° and 1.79A° respectively. In addition, the value of the band length C-C and Si-C for the second type of siligraphene (SiC_3) is equal to 1.78A° and 1.42A° respectively. The vacuum space in Z axis is also relaxed as it is equal to 20A°. This value prevents the interactions between two planes of adjacent siligraphene.

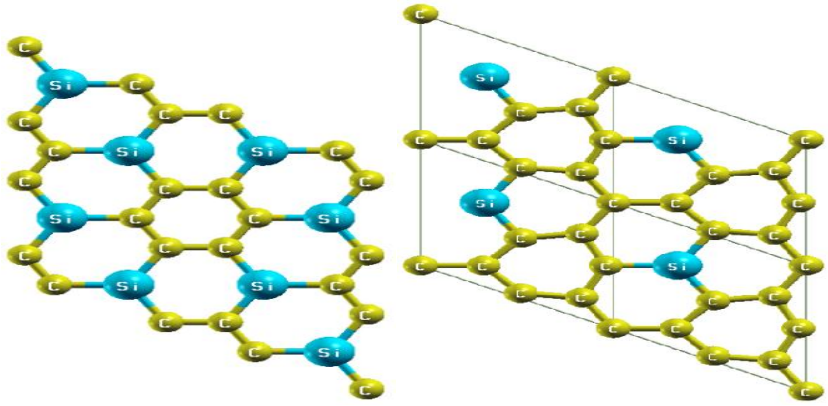

Figure 10: The crystal structures of siligraphene SiC_3 and SiC_7.

The band structure and the density of states of two types of siligraphene SiC3 and SiC7 are presented in figures 11 and 12. Our results show that the configuration of siligraphene SiC7 is a semiconductor material with a direct band gap. The valence shell of Si atom is 3s23p2 and the valence shell of C atom is 2s22p2. We calculated the band gap energy of siligraphene SiC3 and SiC7 and we found out that the band gap energies of SiC3 and SiC7 are 0.0eV and 0.79eV respectively. These values are in good agreement with refs[50, 51]. We established that the band gap is related to the concentration of silicon in hexagonal structure of graphene. We also observed that the band gap of SiC7 is directly following K wave vector.

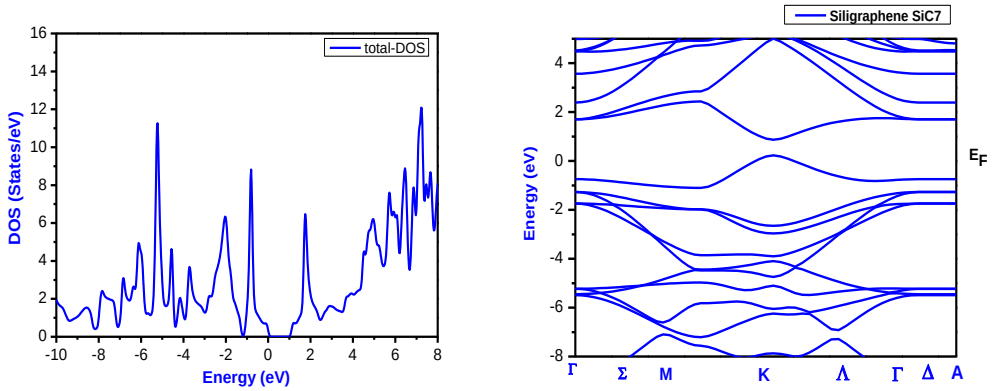

Figure 11: Band Structure and Density of states of Siligraphene SiC_7.

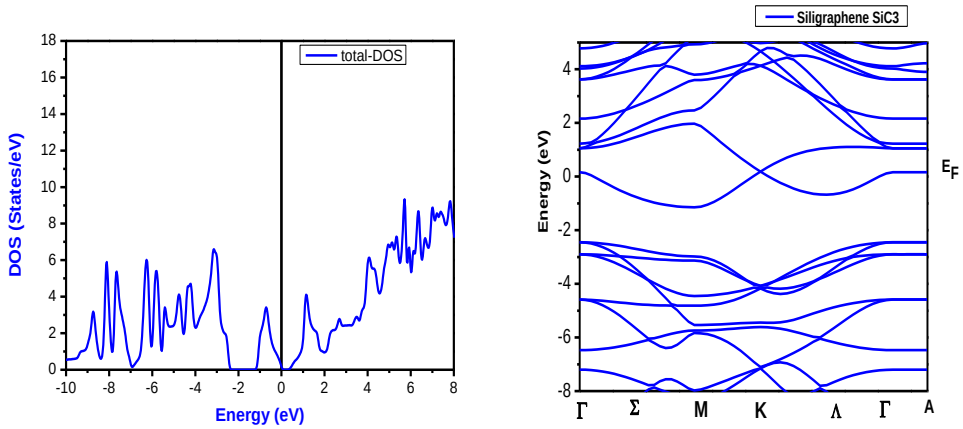

Figure 12: Band Structure and Density of states of Siligraphene SiC_3.

I.6.2. Synthesis of siligraphene

Theoretical calculations predict that we can modify the physical properties of graphene doped by silicon. According to the concentration of silicon on graphene, theoretical calculations also determine several position structures of silicon doped graphene such as siligraphene (SiC3 and SiC7) or silagraphene (SiC2). In experimental studies, it is difficult to synthesize siligraphene (SiC3 and SiC7) or silagraphene.Despite this difficulty, Wang et al. could synthesize the monolayer SiG film by means of chemical vapor deposition using triphenylsilane (C 18 H 15 Si) as the only solid source, that provides both carbon and silicon atoms. The compound of silicon doped graphene is synthetized with concentration of silicon reaching 2.63%. Silicon atoms are

incorporated into graphene lattice with pure Si-C bonds. The experimental results of synthesized SiG film indicate a typical p-type doping witha high carrier mobility about 660 cm2/Vs at room temperature [52].

II. Conclusion

In the current chapter, we have introduced some allotropes of carbon. We started by Diamond and we ended up by siligraphene,which is a new type of 2D material made of graphene doped by silicon atoms with various concentrations. The silicon atoms doped graphene change the metallic character of graphene to a semiconductor material with specifics positions and concentrations of silicon atoms in crystalline structure of graphene structure. The siligraphene is a promising material for uses in different applications.

Solar energy and energy storage are some of the graphene and siligraphene applications. Ours finding further led us to the conclusion that siligraphene SiC_3 is flexible material and that it is possible to open its band gap by strain effect. We also predict that Li-battery is a very encouraging domain of siligraphene applications to the anode of the Li-Battery device.

Part II: Methods of modeling and simulation

I. General introduction

The solid state physics an impressive rise over the last fifty years concerning the development of more rapid and precise techniques of calculation. The ultimate purpose of these new methods is to obtain the properties of many solids with a great speed. This progress has not only allowed creating a sizeable number of materials used currently in industry of new technologies, but also it has helped to better understand and organize this matter within well-formed structures of ordered atoms, on an atomic scale.

Today, fundamental research cannot do without the data-processing tools anymore to solve its problems. In solid state physics the simulation programs became essential tools. Thanks to these kind of programs, it now possible to calculate quickly the physical properties as well as we need, and to envisage the reactions of the studied systems.Therefore , the last couple of years have witnessed a significant acceleration on this area of research,namely understanding solid state physics and making new materials useful to industry, data processing etc.

These new methods of calculation, characterized by data-processing treatment, are based on two theories, strongly dependent: the theory of the functional calculus of density, on the one hand and the generation of pseudo-potential of the atom, on the other hand. During this training period, we are supposed to generate pseudo-potentials for a very new functional calculation developed recently by Tran and Blaha of the "Institute of Materials Chemistry" by the University of Vienna in Austria.

The theses works carried out in 60 years, for example, is currently now being solved in a few days thanks to data-processing simulation, which makes it possible to test many combinations, assumptions, in a very short time …

II. Ab initio methods

In order to describe the properties of such material, we need to know its Hamiltonian which is constituted of the number of nucleus and electrons. , the Ab initio methods permit to resolve approximately the Schrödinger equation so as to obtain a wave function of the systems with N-bodies:

$$H\psi = E\psi \quad (1)$$

The proper function of the equation (1) is related to the wave function which describes all the properties of the system and the proper value E, corresponding to total energy. The operator H is written with the following equation:

$$H = T_N + T_e + V_{Ne} + V_{ee} + V_{NN} \quad (2)$$

In order to describe exactly the influence of all interactions in the system, it is obligatory to calculate the Hamiltonian of the system. The equation (2) gives the general form of the Hamiltonian that is consisted of the operators T_N and T_e corresponding to the kinetic energy of the nucleus and the electrons respectively as well as the operators V_{Ne}, V_{ee} and V_{NN} being the potentials of interaction between nucleus and electrons (Ne), electrons-electrons (ee) and nucleus and nucleus (NN) respectively.

The Hamiltonian H can be expressed as the sum of a nuclear Hamiltonian HN and an electronic Hamiltonian He following these equations respectively: $H_N = T_N + V_{NN}$ and $H_e = T_e + V_{Ne} + V_{ee}$. Therefore, its total energy E of the system becomes the sum of a contribution of the energy of electrons and the energy of nucleus:

$$E = E_e + E_N \quad (3)$$

It is impossible to solve the stationary Schrödinger equation for the system that has a large number of atoms simply because its Hamiltonian becomes very complex. Therefore, itis crucial to simplify the Hamiltonian with several approximations.

a) The Born Oppenheimer approximation

To predict various properties of the matter in physics, we need to resolve the Schrödinger equation. This equation describes a periodic crystalline system composed of atomic nuclei (N) and electrons of spin σi, being very difficult. Therefore, several approximations must be made. the first approximation is called the Born Oppenheimer approximation[53].The Born-Oppenheimer approximation is based on the separation between the movement of the electrons and the movement of the nucleus because of the

difference in their masses (the mass of the proton is equal to 1836 multiplied by the mass of the electron). Moreover, this approach can separate the function of the wave to two functions:The first function of wave defines the movement of the nucleus and the second one defines the movement the electrons. Many body wave functions can be then expressed as the product of the electron wave function and the nuclear wave function.

$$\psi(ri, R_I) = \psi(ri, R)\psi_n(R_I) \quad (4)$$

The Schrödinger equation of many electrons can be written in the form:

$$H_e\psi_e = E_e\psi_e$$

$\psi_e = \psi_e(ri, R)$ Represents the function of the wave of the electrons and Ee their energies.

b) Hartree approximation

Hartree approximation was developed by Douglas Hatree in 1920[54]. This approximation defines the potential that separate it into an electron potential and an ion potential. Each electron feels in an electric filed created by all electrons of the system. Therefore, the Hartree equation is written in the following form:

$$e_i\psi_i(r) = \left[T_e + V_{ion}(r) + V_{elec}(r)\right]\psi_i(r) \quad (5)$$

For improve this approximation, the Hartree Fock approximation [55]introduces the exchange term in Hartree equation. This approach is also founded on the independent electron approximation given by the sum of a single electron Hamiltonian as follows:

$$H_{app} = \sum_{i=1}^{N}\left[T_e + V(r_i)\right] \quad (6)$$

V(ri) is the one electron potential energy in the field of all the nuclei and N is the number of electrons in the system.

The wave function is given as a product of the wave function of electrons being expressed as follows: $\psi(\vec{r}_1, \vec{r}_2, ..., \vec{r}_N) = \varphi_1(\vec{r}_1)\varphi_2(\vec{r}_2)...\varphi_N(\vec{r}_N)$

The total energy of system is: $E = \langle\psi|H|\psi\rangle = \langle\psi|T + V_{ee} + V_{en}|\psi\rangle$

III. Density Functional theory

In order to predictthe ground-state properties of electronic systems (for example semiconductors, isolators and metals), Walter Kohn has proposed Density Functional Theory approximation in the 1970's and in 1998, he was honoured the Nobel prize in chemistry. The results of electronic structure using DFT are quite comparable to experimental results. This method is one of the most important approximations in solid state physics and chemistry to calculate electronic structure. Density Functional Theory does not give a resolution for the equation (7) of the system with N electrons to obtain the function of the wave. But it is used instead to find an equation with a Hamiltonian model whose solution provides the electronic density of this system. It is a simple model because the electronic density is a unit less complex than the function of wave. The Density Functional Theory is based on Hohenberg and Kohn theorems [56]. According to the first theorem, the potential of electron-nucleus interaction V_{Ne} in the Hamiltonian equation of electrons is a function of the electronic density ρ of the system. For each system with N electrons, the potential interaction between the electron and the nucleus V_{Ne} is established by single electronic Hamiltonian. Other terms, of the electronic Hamiltonian are independent of the nucleus position. Therefore, the density ρ is determined by the H_{Ne}. The following equation represents the electronic energy at the fundamental state of a system with several electrons that function in electronic density. It can be expressed as follows:

$$E[\rho] = T[\rho] + E_{ee}[\rho] + E_{Ne}[\rho] \quad (7)$$

$E_{Ne}[\rho]$ Represents the electron-nucleus interaction

$T[\rho]$ The kinetic energy of the electrons

$E_{ee}[\rho]$ The inter-electronic interactions

The second theorem of Hohenberg [57] and Kohn shows that we can get the value of this expression by applying the variational method on the density ρ and not on the function of the wave ψ:

$$E_0 = E[\rho] = \min E[\rho] \quad (8)$$

To solve the equation (8), Kohn and Sham introduced a fictitious system in which the electrons do not interact with one another them but where the electronic density is the same as in the real system [58].

IV. Kohn-Sham equations

Nowadays, the theory of the functional calculus of the density remains the most used method in the electronic structural analyses.It owes its success to the approach suggested by Kohn and Sham (KS) N 1965.The purpose of this approach is to determine the exact properties of the system to several particles, by using methods of independent particles. In practice, this revolution on the matter has made it possible to carry out certain approximations that appeared to be very satisfactory.

The approach of Kohn and Sham replaces the system with particles interacting among each otherthat follow the Hamiltonian's (10) by an easily solved and a less complex system. This approach assumes that the density in a fundamental state of the system, in question, is equal to that of certain systems (selected) with particles not interacting with one another. This implies equations of independent particles to solve the non-interacting system(numerically handy), by gathering all the terms that are complicated and difficult to evaluate in a functional calculus of exchange-correlation Exc[n] :

$$E_{KS} = F[n] + \int d^3 r V_{ext}(r) = T_s[n] + E_{xc}[n] + \int d^3 r V_{ext}(r) \quad (10)$$

T_s: is the kinetic energy of a system of particles (electrons) independent (not interacting) drowned in an effective potential which is not other than that of the real system,

$$T_s[n] = \langle \psi | T_e | \psi \rangle = \sum_{i=1}^{Ne} \langle \varphi_i | -\frac{1}{2} \nabla^2 | \varphi_i \rangle \quad (11)$$

E_H: the energy of Hartree or the energy of interaction of Coulomb associated with the car interaction with the electronic density is defined by.

$$E_{Hartree}[n] = \frac{1}{2} \int d^3 r d^3 r' \frac{n(r) n(r')}{|r - r'|}$$

$$n(r) = \sum_{i=1}^{Ne} |\varphi_i(r)|^2$$

The solution of the auxiliary system of Kohn and Sham for the fundamental state can be seen as such problem of minimization while respecting the density

$$\frac{\partial E_{KS}}{\partial \varphi_i^*(r)} = \frac{\partial T_s}{\partial \varphi_i^*(r)} + \left[\frac{\partial E_{ext}}{\partial n(r)} + \frac{\partial E_{Hartree}}{\partial n(r)} + \frac{\partial E_{xc}}{\partial n(r)} \right] \frac{\partial n(r)}{\partial \varphi_i^*(r)} = 0 \quad (12)$$

The potential of exchange and correlation which is connected to the energy of exchange and correlation,

$$V_{xc} = \frac{\partial E_{xc}}{\partial n(r)}$$

V. Exchange-correlation potential

Fundamentally, we know that the electrons are indistinguishable (fermions).Which means that the wave–functions of the many body electron system must always be anti-symmetric? The electronic contributions in the Kohn-Sham equation are treated with a term called exchange-correlation. The correlation energy is produced by the small diminution in coulomb energy due to the small separation of the electrons of different spin affected by their charges. The correlation energy helps in defining the strength and the length of interatomic bonds. The correlation energy affects both potential and kinetic energy of the system. It is difficult toexactly calculate the correlation energy;therefore, is approximate should be use instead. In detailed form,the exchange correlation energy is a combination of both correlation and exchange energy.

$$E_{xc}(\rho) = E_x(\rho) + E_c(\rho) \quad (13)$$

Many approaches such as molecular dynamic, Monte Carlo Methods successfully calculate the exchange correlation energy that can be expressed as the function of the charge density $\rho(r)$. The exchange correlation energy of two electrons of opposite spins is written as follows:

$$E_{xc}\left[\rho(r)\right] = \frac{1}{2}\iint \rho(r_1)\rho(r_2)V(r_1 - r_2)d^3r_1 d^3r_2 \quad (14)$$

The exchange–correlation potential can be expressed as a function of the exchange correlation energy and it is written as follows:

$$V_{xc}(\rho) = \frac{\partial E_{xc}}{\partial \rho(r)} \quad (15)$$

Density functional Kohn sham equations is based on this exchange correlation potential Vxc. .

a) Local Density Approximation (LDA)

Kohn and Sham proposed the local density approximation (LDA),which considers the electronic density of solids similar to gas of electrons. Therefore, they deduced that the exchange-correlation effects are local.

This term of exchange-correlation $E_{xc}[n(r)]$ is just an integral on to space for gas of electrons that are homogeneous with n density. This can be expressed as follows:

$$E_{xc}^{LDA}[n] = \int n(r)\varepsilon_{xc}^{\text{hom}}[n(r)]d^3r = \int n(r)\left\{\varepsilon_x^{\text{hom}}[n(r)] + \varepsilon_c^{\text{hom}}[n(r)]d^3r \quad (16)\right.$$

The determination of the electronic structures of solid material has become a possible theoretically with Local density Approximation.This success gives much insights to researchers to thinkabout how to improving this approximation in order to estimate the band gap of different materials. These materials are small systems with vibration frequencies which are generally overestimated. The Local spin density approximation (LSDA) has been proposed by John C Slater [59] taking in into the electron spin at Local density Approximation so as to solve in particular the problems opposite to LDA to treat the material magnetic.

The enhancement of local density approximation has been realized by Kohn et Sham. They took into account not only the local electronic density but also a local gradient in this density (which accounts for the heterogeneity of the density).They called it approximation (GGA) Generalized Gradient Approximation[60].

b) Generalized Gradient Approximation

GGA is introduced by Kohn and Sham. It aimsat solving the false results found by the approximation local density. the Generalized Gradient Approximation concerns the term of exchange-correlation either as only a function of density or in a more general way like a function of density n and of its local variation $|\nabla_n|$.

The expression of the exchange-correlation term is written in its general form [61].

$$E_{xc}^{GGA}\left[n_\alpha, n_\beta\right] = \int n(\vec{r})\varepsilon_{xc}\left[n_\alpha, n_\beta \nabla n_\alpha, \nabla n_\beta\right] d^3r \quad (17)$$

The potential of correlation exchange is calculated from:

$$V_{XC}^{LDA}(x) = \frac{\delta E_{XC}}{\delta \rho(\vec{r})} = \varepsilon_{XC}(\rho_\uparrow, \rho_\downarrow) + \frac{\delta \varepsilon_{XC}(\rho_\uparrow, \rho_\downarrow)}{\delta \rho_\sigma(\vec{r})} \rho(\vec{r}) \quad (18)$$

Where $\varepsilon_x^{\hom}(n)$ is the energy of exchange of a no-polarized system of density n(r).

VI. Solution of the Kohn Sham equation: the self-consistency iteration procedure

When constructing the Kohn Sham equations of the system firstly the wavefunction that construct the electronic charge ρ(r) must be known. These wavefunction are the solution of the Kohn Sham equation. In other words, the estimated solution of the Kohn-Sham problem must be known before it can be solved. It can be solved interactively through following several steps.

The geometries of the system of density functional calculation are established trough following using experimental bulk lattice, constant atomic positions and cell angles. Sometimes even the results from the previous principle calculations are used. the electronic density is formed by the wavefunction. Even in the case of a spin polarized wavefunction, involving structural geometries is a fundamental requirement in defining the Kohn-Sham equation of the complete system. The Poisson's equation is constructed and solved in order to obtain the electrostatic coulomb potential.

The exchange correlation potential is used to construct the exchange correlation operator. Taking into consideration this variational basis set {ϕj}, the Hamiltonian Hij and overlap matrix Sij elements are calculated. Subsequently, the matrix H-$_{eS}$ is diagonalized. The diagonalization equation involves unknown coefficients as follows, (H –eS) cij = 0 Which result in a set of one particle eigenvalues with their corresponding coefficients Cij of expansion? The coefficients of expansion produce arelated wavefunction as follows:

$$\psi_i(r) = \sum_j c_{ij}\phi_i(r) \quad (19)$$

These coefficients are then used to construct the electron density ρ(r). The constructed electron density is called the output electron density. If the output electron density is not equal to the input one, it will be used as an input. The procedure explained above is self-consistent and repeats itself until the output density is the same as the input. This is known as the self-field cycle (scf). The resulting electron density is used in calculating the total energy of the system depending on the electron density of that system. The forces Fr=$\frac{\partial E}{\partial r}$ of the atom in the system can also be calculated using the output charge density.

a) The Plane wave Formalism

In a solid or crystal, the wave functions of the free electrons can be extended in terms of the plane waves. By ignoring the potentials caused by ions, the plane waves become exact solutions of Kohn Sham equations. An atom possessing one electron has a potential which is relatively smooth and is treated as a perturbation. Taking the example of the hydrogen atom that has the potential $\frac{-1}{r}$, its wavefunction diverges at the origin and decays exponentially with increasing distance. However, in systems containing more than one atom their wavefunctions in the core states are highly complicated and the potential is not smooth. Because of such complications, the plane waves become difficult to implement. This happens due to the requirements of the plane wave components. Two types of plane waves are used then, namely the augmented and orthogonalised types.

The augmented plane wave is based on the solution of the Schrodinger equation for the atom with a spherical region around it. This solution to the atomic problem was implemented in 1937 by slater. The augmentation solution of the augmented plane wave solution assumes the potential to be symmetric inside the spheres and to be zero outside. The construction of the augmented plane wave makes it identical to the original plane wave outside the sphere. The augmented plane wave solution is constructed so that its wavefunction is continuous at the radius r=R where by $\phi_i(r) = e^{ik.r}$ Since the wave-function is continuous at r= R, the requirements of the Schrodinger equation of the system are not clearly met and its wavefunction do not join smoothly.

The expansion of the augmented plan waves gives the correct approximation of the system's Schrodinger equation. The wave-function of the expanded augmented plane waves can be written in terms of the reciprocal lattice vectors G.

$$\psi_i(r) = \sum_G c_G \psi_{k+G}(r) \qquad (20)$$

It is noting that this plane wave is applicable in most computational calculations nowadays as it is highly accurate in terms of energy values. The second type of plane wave is the orthogonal plane wave which was introduced by herring in 1940. This method is not used in the materials, especially in sp-bonded metals.

b)The Full Potential APW methods

Recently, the development of the Augmented Plane Wave (APW) methods starting from Slater's APW, to LAPW up to the new APW+lo was described by [62]. The linearized augmented plane wave (LAPW) method is one of the most accurate methods for performing electronic structure calculations for crystals. It is based on Density Functional Theory for the treatment of exchange-correlation and uses such as the local spin density approximation (LSDA). Several forms of LSDA potentials exist in the literature. However, recent improvements using the generalized gradient approximation (GGA)[60] are available, too (see sec.2.1). Valence states relativistic effects can be included either in a scalar relativistic treatment [63]or with the second variational method including spin-orbit coupling [64, 65]. Core states are treated in a fully relativistic[66]. Like most "energy-band methods", the LAPW method is a procedure used to solve the Kohn-Sham equations such as the ground state density, total energy, and (Kohn-Sham) eigenvalues (energy bands) of many-electron systems. It mainly introduces a basis set adapted to solve the problem.

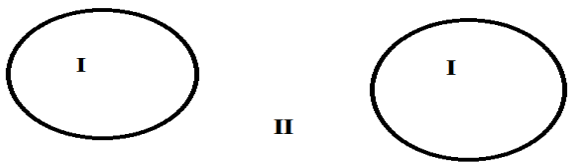

Figure 13: Partitioning of the unit cell into atomic spheres (I) and an interstitial region (II).

This adaptation is achieved by dividing the unit cell into (I) non-overlapping atomic spheres (centered at the atomic sites). (II) Represents an interstitial region. Different basissets are used in both types regions.

VII. Atomic Pseudopotential approximations (Plane wave)

As we stated previously, the objective is to reduce to the maximum the number of variables to be taken into account at the time of the resolution of the problem.We already extracted with the approximation of Born-Oppenheimer[53] all variables associated with the cores of the atoms. Still, this leads to treat a significant number of electrons.

A way possible to simplify the problem, in particular when one wants to use a base plane wave, which makes it possible to exploit the translational symmetry of the crystal, is then to consider two groups of electrons. The electrons of core are chemically inert. And the electrons of valence are the principal actors of the chemical reactions. Up on this separation, one can establishthe following model: the electrons of the heart and the core form an effective potential acting on the electrons of valence. The pseudo potential includes all the existing interactions between the core and the electrons of valence, just like between the electrons of core and the electrons of valence.

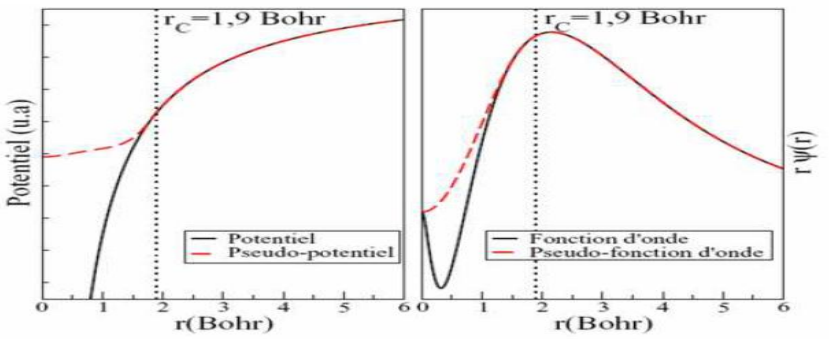

Figure 14: Diagram illustrating the replacement function of the wave and a potential of the core by pseudopotential and a pseudo function[67].

This approximation reduces the number of equations to be largely solved if one "reduces" the number of electrons in our system. This helps (and especially) to be freedfrom the most localized results which require the greatest number of plane waves. This solution was for the first time imagined by Fermi in 1934, and Hellmann proposed a pseudopotential for the potassium in 1935 in the following form [68, 69]:

$$\omega(r) = -\frac{1}{r} + \frac{2.74}{r} e^{-1.16\, r} (21)$$

Nerveless, pseudo potential started actually being used only since the fifties on and was developed later by Phillips and Kleinmann work.

VIII. Corrective Approaches

a) mBJ (modified version of the Becke and Johnson functional)

This part is chiefly based on the article of Tran and Blaha published on June 3, 2009 in Physical Review Letters [70]. The functional calculus of Tran and Blaha noted (mBJ) is a modified version of the Becke and Johnson functional.

This latter quickly proved its effectiveness compared to the modes of calculations generally used such as Local Density Approximation [71]or PBE (the version of the GGA for the solids)[72]. Tran and Blaha propose in their article a modified version of the functional calculus of Becke and Johnson[73], in the following form:

$$U_{\chi,\sigma}^{mBJ}(r) = cU_{\chi,\sigma}^{BR}(r) + (3c-2)\frac{1}{\pi}\sqrt{\frac{5}{12}}\sqrt{\frac{2t_\sigma(r)}{\rho_\sigma(r)}} \quad (22)$$

With :

$\rho_\sigma(r) = \sum_{i=1}^{N_\sigma} |\psi_{i,\sigma}|^2$ Electronic density

$t_\sigma(r) = \frac{1}{2}\sum_{i=1}^{N_\sigma} |\psi^*_{i,\sigma} \nabla \psi_{i,\sigma}|^2$ Density of kinetic energy

The potential of Becke-Roussel proposed here is approximately an equivalent to the potential of Slater used in Becke and Johnson. For the atoms, they are almost identical.

b) Approach GW

The major goal of condensed matter physics isto calculate the ground state and the excited state properties of materials. For several decades, the ground state properties of solids have been calculated within the density functional theory. Tostudy the excited state properties of the matter, it is more suitable to use Green function method. The Green function calculation requires a self-energy operator, which is non-local and energy

dependent. The GW approximation may be regarded as a generalization of the Hartree-Fock approximation (HFA), but with a dynamically screened Coulomb interaction. Thanks to the parameter J of exchange-correlation potential discontinuities, GW approximation can calculate the excited electronic states. All observables of the system have been extractedby the Green function G. Approximation. Although GW necessitates more demanding means of calculation, it provides band gap's results that are to the experiment results.

IX. Numerical protocol

In this project we used two Types of codes: Win2k and Quantum espresso (PW). These codes are based on the optimized structure: Self-consistent calculation; then are applied to extract the energy total, the gap, the moment total …

Here, we propose a diagram which summarizes the resolution of the equation of Schrödinger with various approaches.

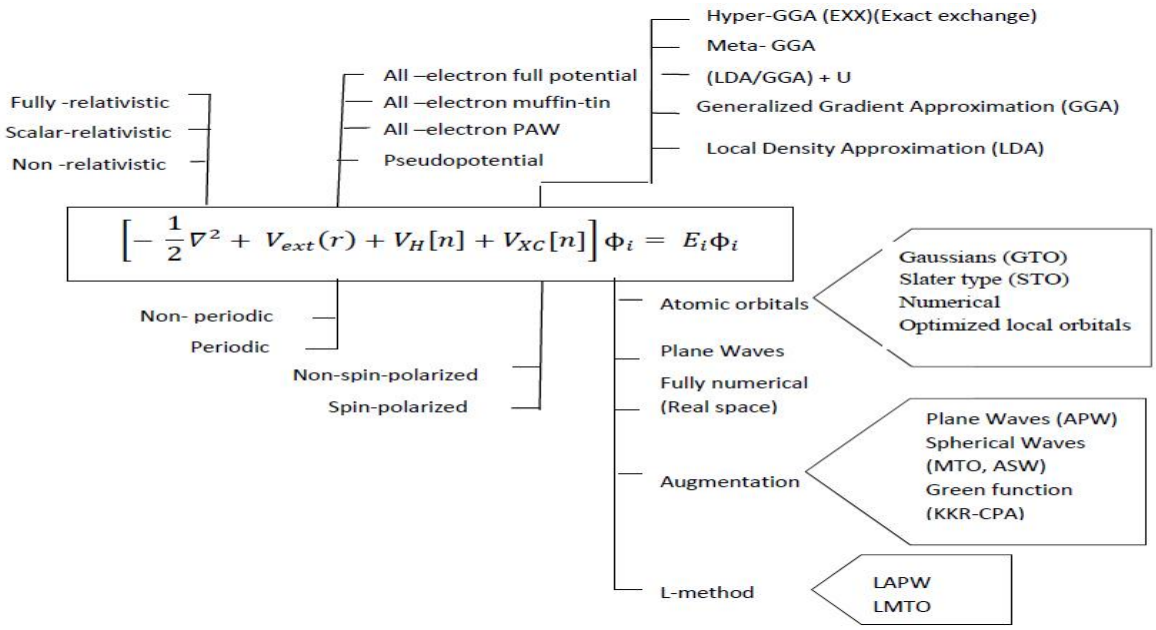

Figure 15: Diagrammatic representation of various methods based on the Density Functional Theory.

X. Conclusion

The theory of the functional calculus of density and pseudopotential, are two tools of powerful calculation in solid state physics.

They allow obtaining the physical properties of various materials in a quick and easy method using simulations data processing unlike other methods (Hartree-Fock for example) using simulations data processing. These methods are still from certain defects, which the physicists try to remove.

It is the goal of the functional calculus of Tran and Blaha, which, without reaching that point completely, made it possible to approach the experimental results. Indeed,it gives better results than the LDA (functional more currently used) while preserving a reasonable computing time.

Moreover, one better electronic simulation of the gaps of the solids makes it possible to improve the physical models, to imagine, and to easily create more new semiconductors. In the current context of seeking to find new means of storing and producing energy, the study of this kind of materials is fundamental since they are an essential element of photovoltaic materials. But the applications of the semiconductors are much used only in the photovoltaic device. They are; in addition used in computer screens for example as well asin data-processing industry and electronics (the world large-scale consumer). It is; thus, essential to optimize these materials and to improve the methods of calculation ab-initio with the aim of quickly and easily creating new solids. Throughout this training course, we could discover work in the research laboratory, as well could do fundamental research as such. Our great interest in the field of physics enabled us to see realities of the world of the research task. Relating theory to real discovery and concrete practice during this practicum period has greatly renewed and increased our attachment and passion for this discipline.

Part III:Physical properties of Siligraphene and its derivatives for different applications

Chapter 1: Optical proprieties of SiC nanosheet

I. Introduction

The main silicon carbide polytypes are 3C-SiC, 4H-SiC and 6H-SiC which have wide band gaps of 2.4 eV, 3.29 eV and 2.9 eV respectively. The shortcoming of Silicon Carbide polytypes is that they are indirect band gap semi-conductor with a weak light-emitting. The different types of bulk silicon carbide are a good material to use in optical application [74, 75, 76]. It also has an absorption edge in the ultraviolet area as poor absorber of photons in the visible light region. It presents at high temperatures this material has a good thermal conductivity and stability [77, 78, 79].

Later on, the discovery of graphene in 2004 by Geim et al.[80, 81], has mainly paved the way to study the different properties such as electronic, mechanical magnetic and optical properties[82, 83, 84, 85, 86]. The structure of graphene has a monolayer with two-dimensions of carbon atomic sheet arranged in a honeycomb lattice. The theoretical and experimental studies have led to understand all the properties such as thermal conductivity, magnetic properties[15, 16].

Recently, several studies have predicted that the silicon carbide in two dimensions has a honeycomb structure monolayer similar to graphene and silicene structure [87, 88, 89, 90].

Our work primarily relies on using first principal calculation based on density functional theory within GGA approximation[60, 91]. This approximation has given a lower band gap compared to the experimental one. That is why,is necessary to correct this difference.The correction of this difference is given by the Modified Becke Johnson approximate[73]. Thisapproximate is called GGAmBJ; the value of band gap, which is calculatedwith GGAmBJis in good argument with experimental for example we get the band gap for 3C-SiC equal 2.5eV with GGAmBJ similar to the experimental 2.41eV and for 4H-SiC. We obtained 3.58 With GGAmBJ similar to the experimental 3.29eV[92, 93].

The aim of this review is to summarize recent development in research on optical properties of SiC nanosheet. We calculated the electronic structure and the optical properties of SiC nanosheet such as the dielectric function, reflectivity, absorption

coefficient and optical conductivity are calculated for both perpendicular and parallel electric field polarizations.

II. Computational Method

The optical and electronic properties of SiC nanosheet were calculated within a self-consistent scheme by solving the Kohen-sham equation based on first principles, using DFT with the generalized gradient approximation GGA method [60, 91]and the exchange–correlation function realized by Perdew Burke Ernzerhof PBE and with mBJ approximation (Modified Becke Johnson)[73, 61]derived by Perdew and Wang [94],in wien2k package[62].The space in FP-LAPW method is presented into two regions, a spherical "muffin-tin" around the nucleus ,the radial solutions of Schrödinger Equation and their energy derivatives are used as basic functions, and an interstitial region between the muffin tins (MT) in which the basis set consists of plane waves, the complex dielectric and optical properties are calculated, in this code, using the well-known relation, $\varepsilon(\omega)=\varepsilon 1(\omega)+i\varepsilon 2(\omega)$ (1) It describe the optical response of the medium at all phonon energies $E = h\omega$, The real part of the dielectric function follows from the Kramers-Kronig relation

$$\varepsilon_1(\omega) = \mathrm{Re}\left(\varepsilon(\omega)\right) = 1 + \frac{2}{\pi} P \int_0^{\infty} \frac{\omega' \varepsilon_2(\omega')}{\omega'^2 - \omega^2} d\omega' \quad (2)$$

Where P implies the principal value of the integral

The imaginary part of the $\varepsilon 2(\omega)$ in the long wavelength limit has been obtained directly from the electronic structure calculation [95].

$$\varepsilon_2(\omega) = \frac{e^2\hbar}{\pi m^2 \omega^2} \sum_{v,c} \int_{BZ} |M_{cv}(k)|^2 \delta[\omega_{cv}(k) - \omega] \, d^3k \quad (3)$$

$M_{cv}(k)$ The transition moments elements

The absorption coefficient is obtained with following relation [96]

$$\alpha(\omega) = \frac{\sqrt{2}}{c} \omega \sqrt{-\varepsilon_1(\omega) + \sqrt{\varepsilon_1(\omega)^2 + \varepsilon_2(\omega)^2}} \quad (4)$$

The optical conductivity is given by [97]:

$$\mathrm{Re}\,\sigma_{\alpha\beta}(\omega) = \frac{\omega}{4\pi} Im\,\varepsilon_{\alpha\beta}(\omega) \quad (5)$$

The reflectivity calculation is useful to evaluate the optical properties of materials, it makes it easy to obtain the behavior of transparency, and based on the reflectivity

transmittance has been drawn. The reflectivity R(ω) follows directly from Fresnels formula[97].

$$R(\omega)=\left|\frac{\sqrt{\varepsilon(\omega)-1}}{\sqrt{\varepsilon(\omega)+1}}\right|^2 \quad (6)$$

The variation of the refractive indexn(ω) versus the energy or wavelengths may be calculated using the formula:

$$\mathrm{n}(\omega)=\sqrt{\frac{\sqrt{\varepsilon_1(\omega)^2+\varepsilon_2(\omega)^2}+\varepsilon_1(\omega)}{2}} \quad (7)$$

III. Electronic properties

In figure 16, we draw the unit cell of SiC nano-sheet the optimized lattice is equal 3.09A° and bond length between Si and C is relaxed we get the value 1.79A° is good agreement when compared with theoretical and experimental [98] the bonding between Silicon and Carbon atoms is formed by combination of Si-pz and C-pz. SiC is modeled in supercell with vacuum space in Z-axis is equal 20 A° this value it avoid the interactions between two nano-sheet adjacent.

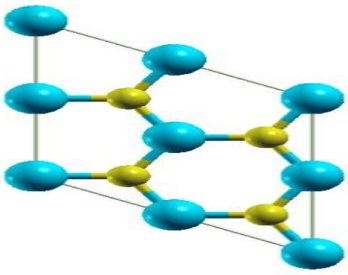

Figure 16:The crystal structures of monolayer SiC nanosheet

The calculated electronic band structure and total DOS for SiC are shown in Fig2. We found that SiC nanosheet has a band gap equal 2.51eV which calculated with GGA approximation therefore this material is a semiconductor, this results is a good argument with [99]. Also, the band gaps of SiC nanosheet calculate with GGAmBJ is equal 3.74eV. The figure 17 show that band gap is a direct followsK wave vector this result for SiC nanosheet has different compared with type of band gap for SiC bulk (3C-,4H- and 6H-SiC).

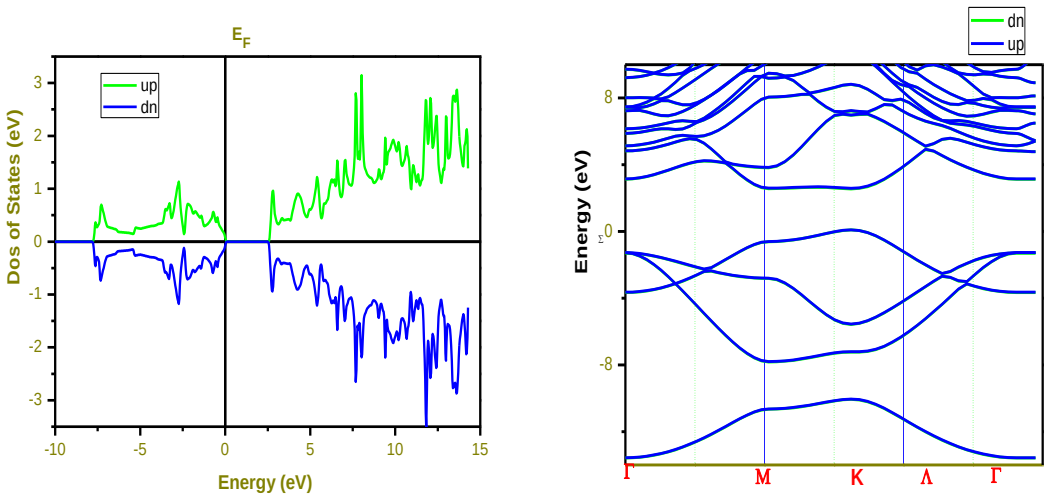

Figure 17: Band Structure and Density of states of SiC nanosheet.

IV. Optical properties

a) Dielectric function ε(ω)

Figure 18 shows the real and imaginary parts of the dielectric function, the real parts $\varepsilon_1(\omega)$ is related to the electronic polarizability of the materials studied and $\varepsilon_2(\omega)$ is calculated all transitions of all electrons between states occupied to states unoccupied. In each figure of dielectric function, the imaginary parts of dielectric function has different than the real parts in the left the figure show the imaginary parts of dielectric function the green line plot the evolution of imaginary parts according to xx direction at electric field champ its observe two peaks the big peaks at and line blue plot the evolution according zz direction at electric field champ.

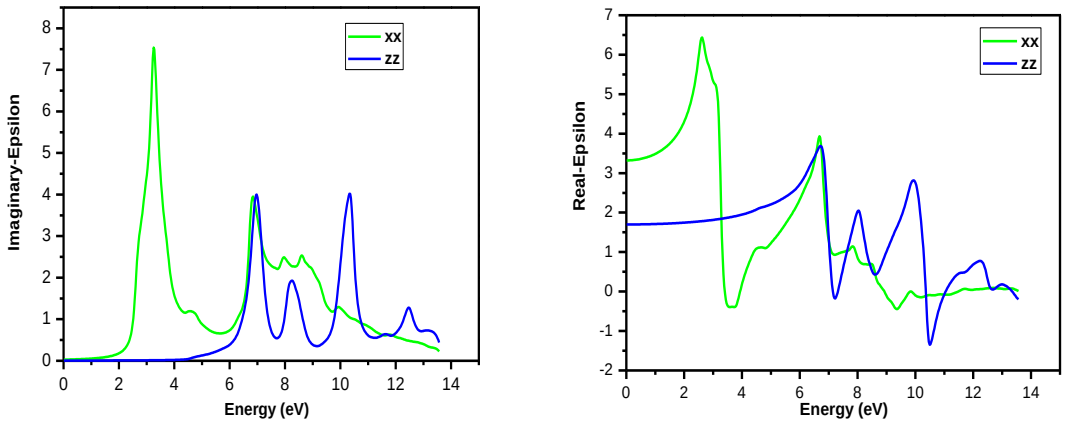

Figure 18: The real and imaginary parts of dielectric function for the electric field parallel and perpendicular to the SiC nano-sheet.

b) Reflectivity spectrum R(ω)

The reflectivity calculation is useful to evaluate the optical properties of materials, it makes it easy to obtain the behavior of transparency, and based on the reflectivity transmittance has been drawn. The reflectivity R(ω)follows directly from Fresnel's formula.

$$R(\omega) = \left| \frac{\sqrt{\varepsilon(\omega)} - 1}{\sqrt{\varepsilon(\omega)} + 1} \right|^2$$

Figure 19 plot the reflectivity of SiC nanosheet as function photon energy (eV) at two directions according to XX and ZZ , the figure show that the reflectivity according zz is equal 2.59 % at wavelength 398nm and 2.23 % at wavelength 790nm this value similar than reflectivity obtained with graphene value one 2.3% [33]. In the next step the evolution of reflectivity according xx direction has decreased as functions wavelength we get 32% of the low value of wavelength 398 nm and 10% at biggest value of wavelength 790 nm.

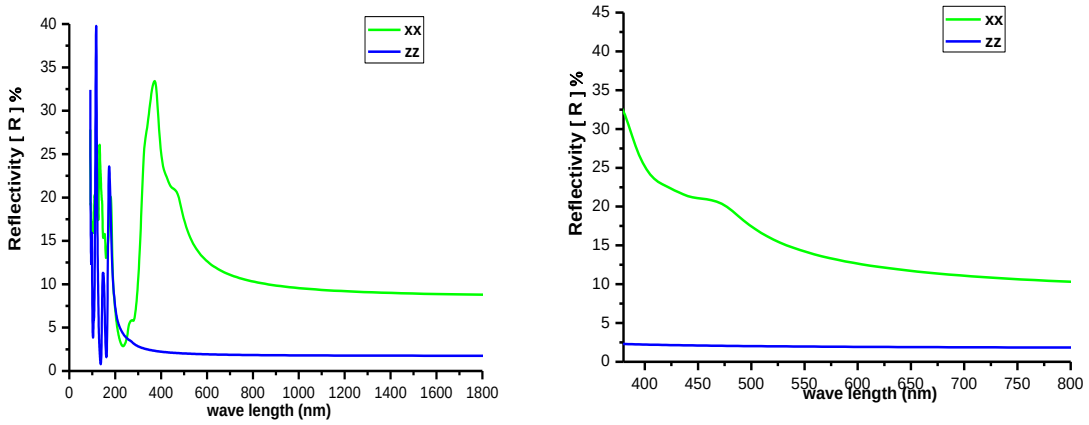

Figure 19: The reflectivity of SiC nano-sheet as function wavelength for the electric field parallel and perpendicular to the SiC nano-sheet.

c) Absorption Coefficient

The absorption coefficient of SiC nanosheet for the electric field parallel (E||xx) and perpendicular (E||zz) to the SiC nanosheet is given in figure 19. It found that absorption coefficient is started with Energy equal 2eV for axis xx and for axis zz equal 4.5eV. The first peak is getting at energy equal for (E||xx) 3.33eV and four (E||zz) 7.12eV the second peak for axis xx equal and for axis zz equal and the biggest peaks for xx and zz are obtained for higher energy at 9.36 eV the absorption coefficient equal 99.42 (104/cm) and at 10.45eV the absorption coefficient equal 159 (104/cm) respectively.

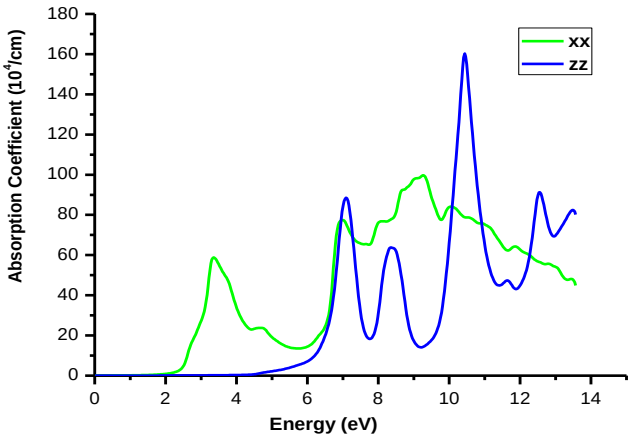

Figure 20: The absorption coefficient of SiC nanosheet for the electric field parallel and perpendicular to the SiC nanosheet

d) Optical Conductivity

The following equation is described the real conductivity

$$Re\ \sigma(\omega) = \frac{\omega}{4\pi} Im\ \varepsilon\ (\omega)$$

The real parts of optical conductivity are shown in Fig. 20 for SiC nanosheet. It is observed that optical conduction as function E (Energy) in the XX direction starts with energy equal 2.20eV, we observe 3 peaks of real–conductivity, the first peaks have obtained in points 3.31eV, the second in 6.87eV, and in points 9.20eV bat in the ZZ direction has started with energy equal 4.72eV and the first peaks is obtained in points 7.1eV, the second in 8.4eV, and in points 10.42eV.

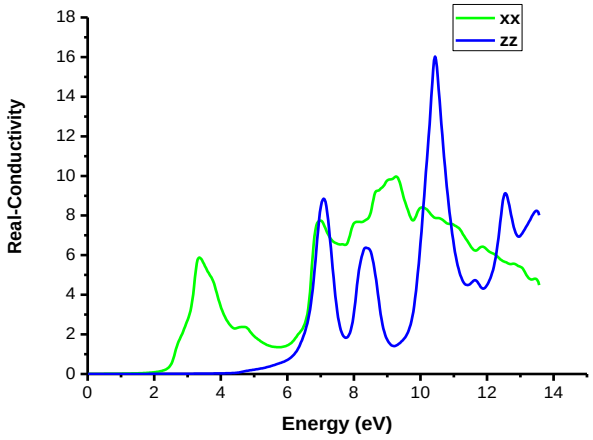

Figure 21: The real part of optical conductivity of SiC nanosheet for the electric field parallel and perpendicular to the SiC nanosheet

e) Refractive index

In this figure we observe that refraction index has varied as function electric field polarized in two perpendicular and parallel directions. The static refraction index in parallel (xx) direction equal's 1.80 is higher compared with the perpendicular direction (zz) 1.30. For direction flow xx the evolution of index refraction has different than obtained for direction of zz. The evolution index refraction for direction xx in region of energy lower than 3eV, the figure show an increase of refraction index up to a maximum value equal 2.55 at point 2.54 after that decrease up to 0.94 at point, for the second region between 4 eV and 6 eV the refraction index has become increasing as function photo

energy up to maxima lower the first maxima following this maxima the figure show the decrease of therefraction of index. The refraction index according zz direction has plotted in the figure 21; we observe three peaks at 1.99, 1.49 and 1.79 at points 6.74, 8.07 and 10.27 respectively.

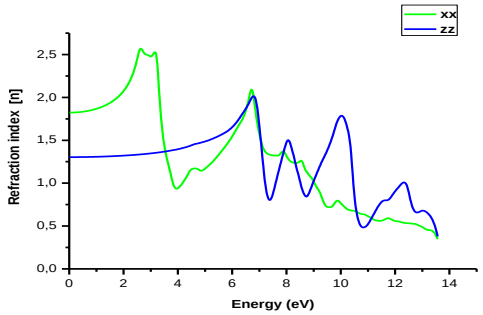

Figure 22: Refractive index of nanosheet SiC for perpendicular (zz) and parallel (xx) direction

f) Energy Loss Function

The figure 22 show the energy loss function as function photo energy with intra-band transition and without intra-band, in the first peaks has obtained with inter-band at points 4 eV after that we get tree peaks for without inter-band transition at 7.41eV, 8.73eV and 11.07eV respectively.

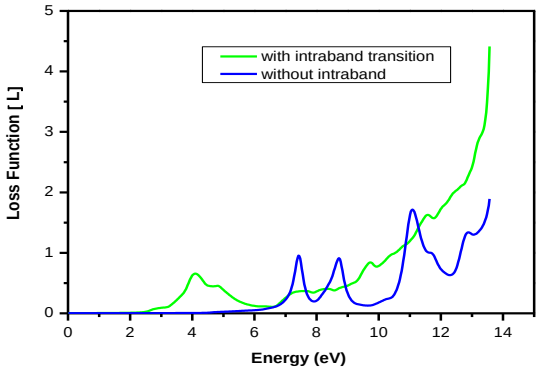

Figure 23: Energy Loss Function

V. Conclusion

In summary we have present the optical properties of silicon carbide nanosheet we calculate the dielectric function, reflectivity spectrum, absorption coefficient, optical conductivity and refraction index for both perpendicular and parallel electric field polarizations. We obtained the all result of optical properties are in good argument with result obtained with graphene. For that the silicon carbide nanosheet can be replace graphene because has higher chemical stability. After our full-course SiC nanosheet study can be employed to describe in devices nano-optoelectronics.

Chapter 2: Optical Conductivity enhancement and band gap opening With Silicon doped graphene

I. Introduction

Graphite is composed of several series of layers which are arranged in a honeycomb (hexagonal) lattice of a hexagonal arrangement of carbon atoms; each atom is related to three close carbons in a planar network. To separate these layers in full-course, of which the thickness is the order of the nanometer, makes it possible to obtain the layers of the graphene. This last was first discovered in 2004, by micro-mechanical cleavage of graphite, at the Centre for Mesoscopic and Nanotechnology of Manchester University, UK, directed by Geimet al. [3, 4, 100]. The name of graphene is given to a flat monolayer of carbon atoms which are placed in hexagonal structure into a two-dimensional (2D) (which takes the form of planar honeycomb lattice sp^2 bonded carbon atoms). The production of isolated graphene was realized by several experimental groups [101, 102]. The bonding of carbon graphene is very strong and thus it is highly stable and has high electron mobility[103]. The graphene has also high thermal properties [10-12]. Several researchers have studied the electronic, magnetic [15, 16], optical[19, 104] and mechanical properties[105] of graphene. The applications of graphene are currently considered covering the field of the flexible electronic components. Recent research has revealed many possible applications of carbon graphene in the domain of nano-electronic devices, for example, the fabrication of nano-sized transistors [106], and in solar cell technology [107].

To address chemical and mechanical instability of currently used indium tin oxide (ITO), graphene has been suggested as a promising flexible transparent electrode but challenges remain in achieving high efficiency of graphene-based polymer solar cells (PSCs) compared to their ITO-based counterparts. It has been demonstrated that graphene anode- and cathode-based flexible PSCs with record-high power conversion efficiencies of 6.1 and 7.1%, respectively. The high efficiencies were achieved via thermal treatment of MoO3 electron blocking layer and direct deposition of ZnO electron transporting layer on graphene [24, 108].

To date, graphene electrodes have been applied for different types of solar cells, namely, solid-state solar cells, electrochemical solar cells, quantum dot solar cells (QDSCs), and polymer solar cells. The main advantages of applying graphene in different solar cells are: (i) it creates a window for inducing wide ranges (from UV to far IR regions) of photon energy inside the solar cells, (ii) it exhibits higher charge transfer (CT) kinetics at the interface of electrochemical hybrid cells, (ii) it manufactures a flexible device with robust architecture, (iv) it provides greater heat dissipation.

On the other hand, electro-catalytic activities of graphene play a key role in enhancing the efficiency of electrochemical solar cells like dye-sensitized solar cells (DSSCs), where the liquid/solid interface acts as a pathway for transferring electrons.

Due to their physical properties such as a high transmittance, optical conductivity and thermal conductivity, the graphene has been extensively studied as a potential material for application in solar cell. It has been shown that the optical performance of graphene may be improved when it is functionalized with organic molecules[109]. The deposition of graphene on textured silicon surfaces has decreased the reflectance value, it became lower than 5%, these results have been reported by Rakesh Kumar et al. [110], the reflectivity decreases also in boron and Nitrogen co-doped graphene nanosheet [111]. Graphene, a single-monolayer of sp2 -hybridized carbon, has been predicted to exhibit a particularly simple optical absorption spectrum. In the infrared-to-visible spectral range, the expected absorbance has been calculated to be independent of frequency. Many of the electronic properties of graphene, with its linear dispersion near the Fermi energy, can be modeled in terms of massless Dirac Fermions. In this context, the predicted conductivity can be viewed as an intrinsic property of two-dimensional massless Fermions. The optical conductivity of graphene has been measured by Nair et al. [112] and Stauber et al.[113].

The objective of this paper, is to study the optical properties of carbon graphene that are intrinsic and doped by silicon with various concentrations (1/2=50%, 1/4=25%, 1/8 =12.5 % and 1/12= 8.33%), we show that the optical carbon graphene intrinsic properties are determined by the direct inter-band electron transitions. The idea of our calculation is concentrated on improving the transmittance and optical conductivity in visible region.

We will study the effect of silicon doped carbon graphene on transmittance and optical conductivity.

II. Calculation Method

To properly describe the band gap of material we must introduce the excitonic effect, which is a two-particle entities, we need a two-particle theory at least. DFT is a one particle theory, thus it is not suited to properly describe the excitonic effect. For solids we must use the Bethe Salpeter Equation (BSE) or GW[28-29] which are implemented in other codes than WIEN2K, they are very expensive in terms of computational time and memory. So, in order to provide a more reliable estimate of the effect of silicon on the electronic properties of graphene we performed G_0W_0 and TB-mBJ calculations. The $G_oW_o$runlevel solves the Dyson equationusing the GW approximation for the self-energy operator. This approximation is currently one of the most successful approximationsfor self-energy operator and hasyielded remarkably accurate band structures for many materials. The GW approximation is obtained as first term in the expansion of Hedin equations in the expansion in the screened interaction [29].We used the PWscf code (quantum espresso) [30] for the DFT calculations and Yambo code [31] for GW calculations. The calculations were carried out using the Perdew-Burke Emzerhof pseudo-potential (PBE), with non-relativistic calculation. The plane-wave basis sets up to a kinetic energy cut-off equal to 120 Ry. The GW calculations are very expensive in CPU time, and takes time to test it on a number of parameters, thus we have chosen to do the calculation in the direction gamma Γ-Γ, to get an idea of the correction in band-gap valu**e.**

Electrical and optical properties of graphene doped with and without Si were calculated within a self-consistent scheme by solving the Kohen-sham equation based on first principles DFT using the Generalized Gradient Approximation GGA method [32-33] and TB-mBJ approximation (Modified Becke Johnson)[34,36] derived by Perdew and Wang [37,38],in wien2k package [39].

$$\upsilon_{\chi,\sigma}^{mBJ}(r) = c\upsilon_{\chi,\sigma}^{BR}(r) + (3c-2)\frac{1}{\pi}\sqrt{\frac{5}{12}}\sqrt{\frac{2t_\sigma(r)}{\rho_\sigma(r)}}$$

Where $\upsilon_{\chi,\sigma}^{BR}(r)$ is the BeckeRoussel potential [40] and c parameter proposed with the following equation

$$c = \alpha + \beta\left(\frac{1}{V_{cell}}\int_{cell}\frac{\left|\nabla_n(r')\right|}{n(r')}\,\mathrm{d}^3r'\right)^{1/2}$$

Where$t_\sigma(r)$, is the spin-dependent kinetic-energy density, and $\rho_\sigma(r)$ is the spin-dependent electron density.In the FP-LAPW [40] method, the space is divided into two regions, a spherical "muffin-tin" around the nucleus in which radial solutions of Schrödinger Equation and their energy derivatives are used as basic functions, and an interstitial region between the muffin tins (MT) in which the basis set consists of plane waves. The complex dielectric and optical properties are calculated, in this code, using the well-known relation:

$$\varepsilon(\omega) = \varepsilon_1(\omega) + i\varepsilon_2(\omega)(1)$$

It describes the optical response of the medium at all photon energies $E = \hbar\omega$.

The real part of the dielectric function follows from the Kramers-Kronig relation

$$\varepsilon_1(\omega) = 1 + \frac{2}{\pi}P\int_0^\infty \frac{\varepsilon_2(\alpha)\alpha d\alpha}{\alpha^2-\omega^2} \quad (2)$$

Where P implies the principal value of the integral

The imaginary part, $\varepsilon_2(\omega)$, in the long wavelength limit, has been obtained directly from the electronic structural calculation [41].

$$\varepsilon_2(\omega) = \frac{e^2\hbar}{\pi m^2\,\omega^2}\sum_{v,c}\int_{BZ}|M_{cv}(k)|^2\delta[\omega_{cv}(k)-\omega]\,d^3k(3)$$

$M_{cv}(k)$: The transition moments elements

The absorption coefficient is obtained with the following relation [41]

$$\alpha(\omega) = \frac{\sqrt{2}}{c}\omega\sqrt{-\varepsilon_1(\omega)+\sqrt{\varepsilon_1(\omega)^2+\varepsilon_2(\omega)^2}} \quad (4)$$

The optical conductivity is given by [41]:

$$\mathrm{Re}\,\sigma_{\alpha\beta}(\omega) = \frac{\omega}{4\pi}\mathrm{Im}\,\varepsilon_{\alpha\beta}(\omega) \quad (4)$$

The calculation of reflectivity is very important to evaluate the optical properties of materials; it makes it easy to understand the status and behavior of transparency, based on

the reflectivity that we can draw from the transmittance. The reflectivity R(ω)follows directly from the Fresnel's formula [41].

$$R(\omega) = \left|\frac{\sqrt{\varepsilon(\omega)}-1}{\sqrt{\varepsilon(\omega)}+1}\right|^2 \quad (5)$$

The variation of the refractive index is also recommended to calculate the energy versus the wavelengths, it gives how the material can behave and canal.To confirm the results found by the optical absorption and the transmittance, the refractive index is given as followsn(ω):

$$n(\omega) = \sqrt{\frac{\sqrt{\varepsilon_1(\omega)^2+\varepsilon_2(\omega)^2}+\varepsilon_1(\omega)}{2}} \quad (6)$$

III. Results and discussions

III.1. Electronic properties

The primitive cell of monolayer graphene is shown in Figures 23 and 24. We started our calculation by the relaxation of graphene parameter, the obtained value is equal to a=2.46Å and the band length C-C is equal to1.42Å, this value is in good agreement with ref [114]. To avoid the interactions between two adjacent monolayer graphene, a vacuum space in Z axis of 20Å is chosen.

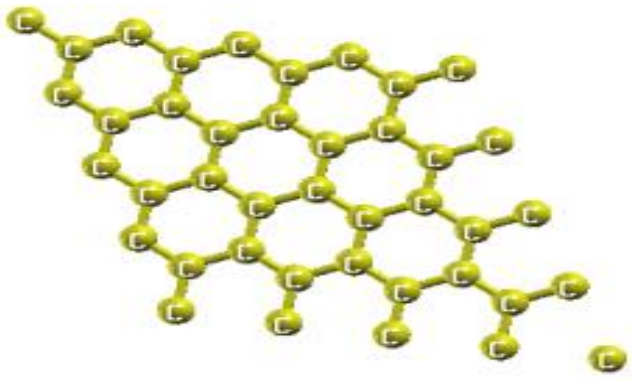

Figure 24: The crystal structures of monolayer graphene

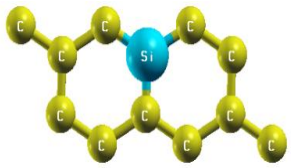		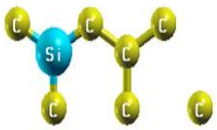	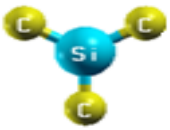
Supercell 3x2x1 (8.33%)	**Supercell 2x2x1 (12.5%)**	**Supercell 2x1x1 (25%)**	**Supercell 1x1x1 (50%)**

Figure 25: The crystal structures of monolayer graphene doped with Silicon.

Figure 25 shows the calculated electronic band structure and total DOS for graphene using GGA. The density of states combines conduction band and valence band at Fermi level, which are formed mainly by p states.

The band structure of graphene reveals valence and conduction band, consisting of the bonding and anti-bonding orbitals, which touch at the K-point. The connection of the two bands influences the possibility to easily excite electrons out of the valence into conduction band independent of the wavelength.

A graphene sheet has a honeycomb structure with two crystallographic equivalent atoms in its primitive unit cell. Two bands with pz character belonging to different irreducible representations cross precisely at the Fermi energy at the K point in momentum space. As a result graphene is a zero-gap semiconductor. The linear dispersion of the bands results in quasi-particles with zero mass, so called Dirac fermions. At energies close to the degeneracy point, the electronic states form perfect Dirac cones.

Using the TB-mBJ approach (Figure 26), the band gap of graphene is nearly zero, this result shows that the gapless observed in graphene is an intrinsic property.

.

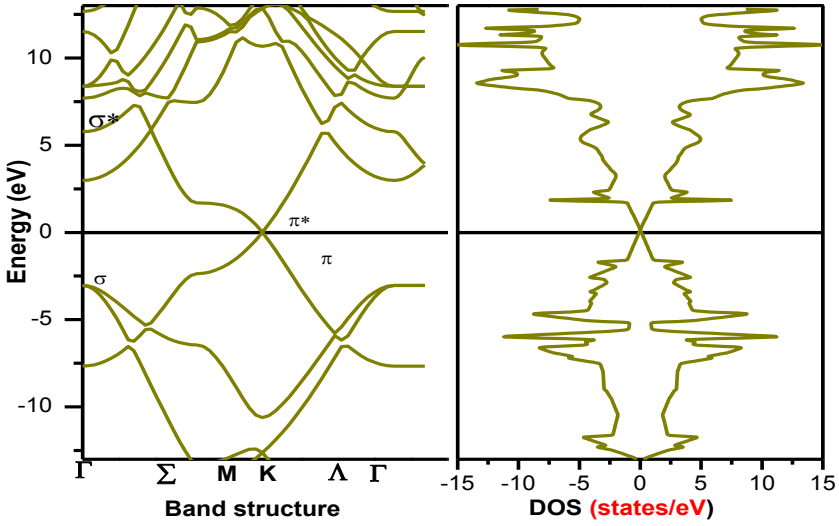

Figure 26: Band Structure and Density of states of graphene.

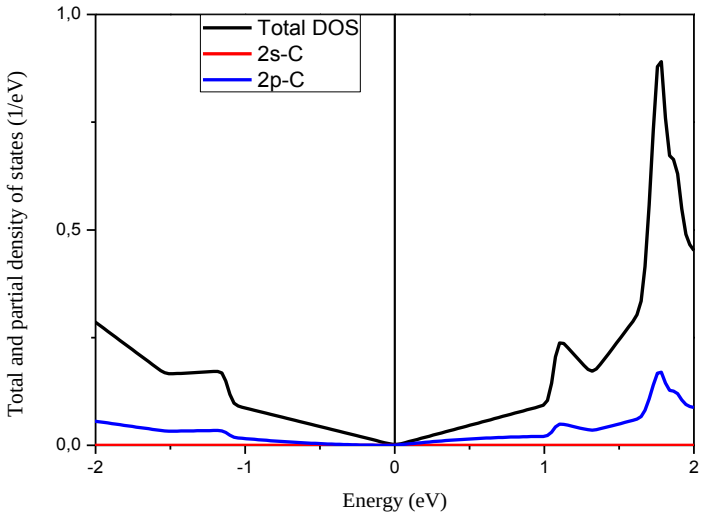

Figure 27: Total and partial density of states for graphene using the TB-mBJ approach

The total and partial density of states, displayed in Figure 27 and 28 for Silicon doped Graphene with 12.5% and 8.3% of silicon respectively, show the opening of band gap.

In Dirac points the effective mass is equal to zero, usually bandgap opening leads to increase the effective mass and decrease the mobility.

Silicon has a larger atomic radius than carbon, the intensity of the interaction increased, therefore there will be a repulsion force which involves opening of the band-gap, and we

also note hybridization between the p orbital for both Si and C, thus the σ band remains unchanged contrary to π band (Figure 28).

For the lower concentration of Si there is no change in the electronic structure. It can be predicted that silicon doping in graphene structure, has less destructive effect on graphene mobility due to resemblance of Si and C atoms. When we increased the concentration (8.3%; 12.5 ...) the semiconductor behavior dominates over that of the gapless, so the gap increased (Figure 29).

In order to have a correct band gap values, the TB-mBJ and GW approaches are used, both these two approaches give good results as represented in Table1 for different concentration, except for the value of 50%.Although we can see a global behavior of the band gap as function of Si doping.

As mentioned above, the GW calculation shows that the band-gap is indirect between Γ and K for 12.5%, the result is in agreement with[21]. Since the top of valence band is under Fermi energy level, this material has semi-conducting behavior.

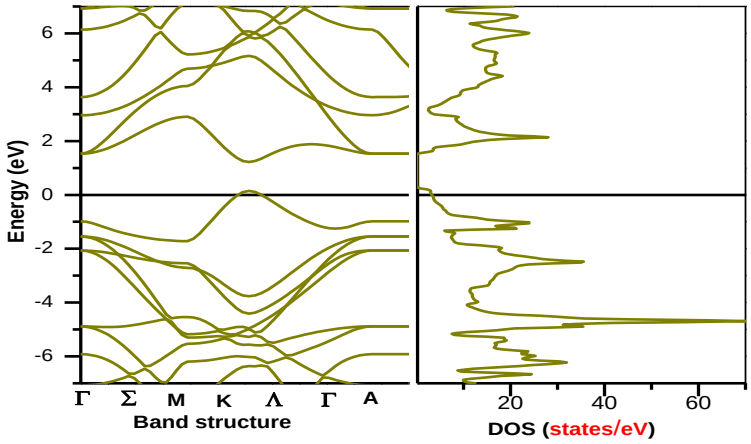

Figure 28: Band Structure and Density of states of Si doped graphene with 12.5%.

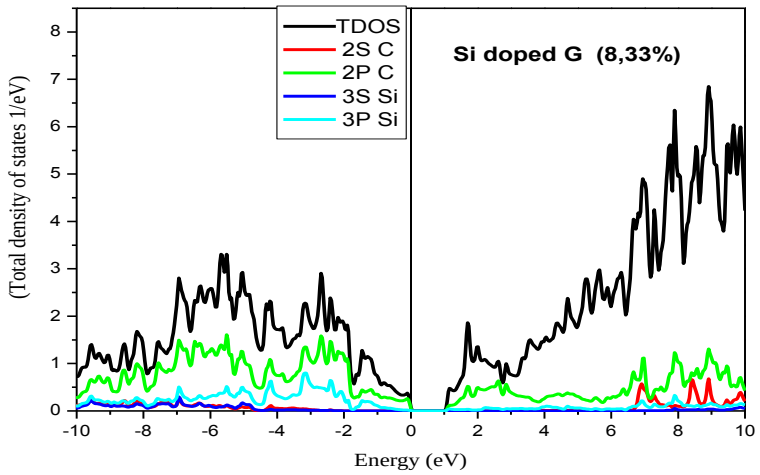

Figure 29: Total and partial DOS of Si doped graphene (8.33%)

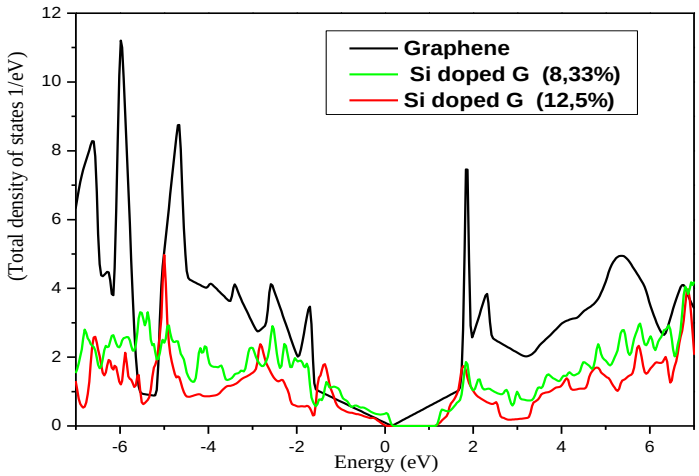

Figure 30: The total DOS for Si doped graphene for different concentration; 8.33% and 12.5%.

Table 1: band gap values of graphene as a function of silicon concentration

Concentration of Silicon	0%	8.33%	12.5%	25%	50%
Band gap of graphene (eV)					
(Wien2k)	0.0	1.022	1.357	1.955	2.51
Pwscf (pbe)	0.0	****	1.062	1.96	2.65
mBJ	0.054	1.434	1.966	2.49	3.43
GW(G0W0)	0.094	***	2.13	2.35	2.78

In summary, we proved that the theoretically subjected silicon-doped graphene sheet shows semiconducting behavior. The bandgap has dependency on Si concentration. The observed bandgap in Dirac points is direct and its value can be tuned by dopant proportion in unit cell.

Silicon is the least effective atom to open a band gap in graphene, inducing very few changes on its band structure, probably because it has the same number of valence electrons, and thus the occupation of the bands may not be changed, for more than 8.33%, it has an effect and the band gap is increased.

III.2. Optical properties

Graphene is characterizedby good transparency, good thermal and mechanical properties. In this section we will study the effect of silicon doping on the graphene optical properties, such as reflectivity and optical conductivity.

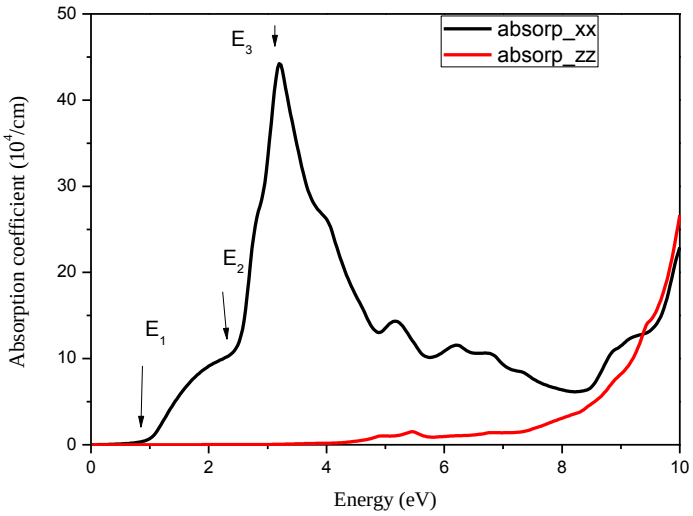

Figure 31: the absorption coefficient of Silicon doped graphene (8.33%) as function of photon energy in both direction xx and zz

Due to hexagonal symmetry the optical properties are different for both direction xx and zz, we will interested in the following results only at the direction xx. The critical point represented in Figure 30, indicate the optical transition which correspond to:

$E_1 : \pi \rightarrow \pi^* 1.4eV$, $E_2 : \sigma \rightarrow \pi^* 2.4eV$, $E_3 : \sigma \rightarrow \sigma^* 3.4eV$

III.2.1. Reflectivity spectrum R(ω)

As we mentioned before, graphene is semi-metal, so it was interesting to study the reflectivity and the effect of doping Si on these optical properties

Figure 31 and 32 show the reflectivity with and without silicon doping in (xx direction) as function of Energy and wavelength respectively. For energies less than 5eV, the reflectivity increases as a function of energy. However, the reflectivity of the silicon doped graphene is higher than graphene undoped. In the energy domain 5eV<hv< 8eV the reflectivity decreases. For energy values higher than 8eV, the reflectivity increases as a function of energy, although, the reflectivity of the silicon doped graphene is higher from 200nm to 400nm (UV).

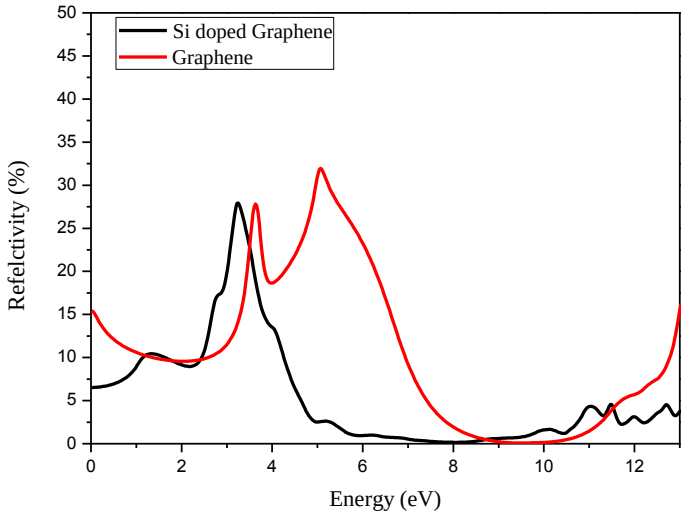

Figure 32: The reflectivity of silicon doped graphene (8.33%), and graphene undoped as function of energy

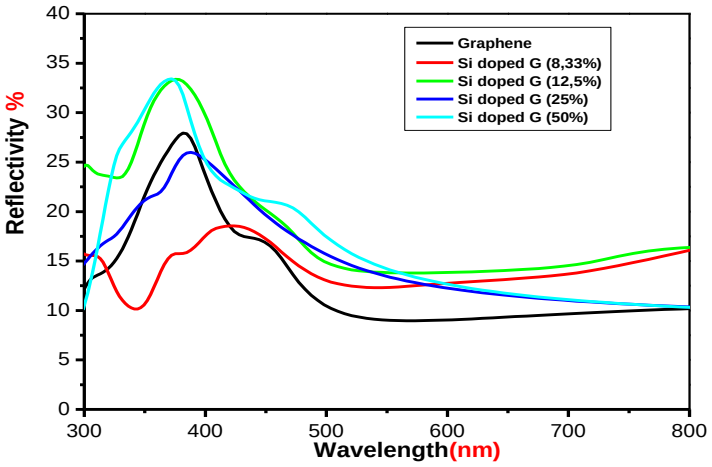

Figure 33: The reflectivity of silicon doped graphene as a function of wavelength for different silicon concentrations.

In Figure 33, the reflectivity starts at 15% however the Si doped graphene starts at 7%, the mainly peak located at 3.8 eV correspond to the Plasmon energy for graphene, where the real part of dielectric function becomes negatives (see Figure 10).

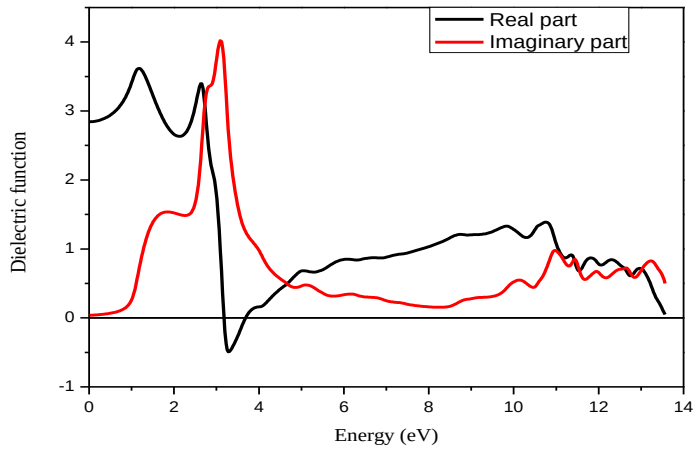

Figure 34: real and imaginary part of dielectric function for Si doped graphene (8.33%)

III.2.2. Optical Conductivity

Graphene is a good conductor due to the absence of band gap; its optical conductivity is calculated by Yao et al.[115]. Doping with silicon is motivated by the improvement of the optical conductivity of graphene, compared with doping by others materials, like B, Mn[21, 22, 116, 117]. Wang SJ et al. have been fabrication the graphene films with highly conducting and transparent [118].

Figure 34 shows the conductivity of graphene with and without silicon doping, in this case the conductivity of graphene starts at 0 eV because graphene is gapless and for silicon doped graphene the conductivity starts at 0.84 eV. The optical conductivity of silicon doped graphene is higher than that of pure graphene and the maxima of the peak for silicon doped graphene is at 2.66eV, while that of graphene is at 3.78eV.

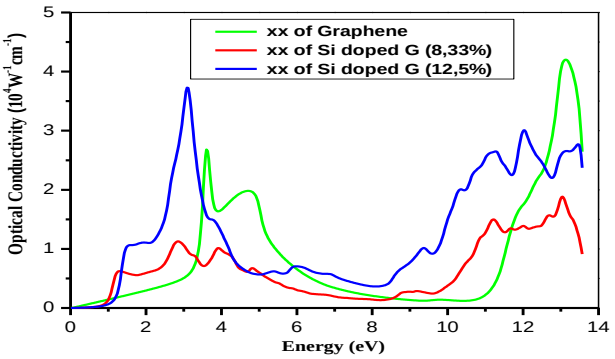

Figure 35: The optical conductivity of silicon doped graphene (8.33%, 12.5%) and undoped as function of energy (eV).

Figure 35 show that optical conductivity increases as a function of silicon concentration. Its highest value in visible, at 3.78eV (>400nm), is obtained for 12.5% of silicon.

The optical conductivity is related to the absorption spectra, thus the main edge observed in Figure 12 is related to the optical transitions cited previously

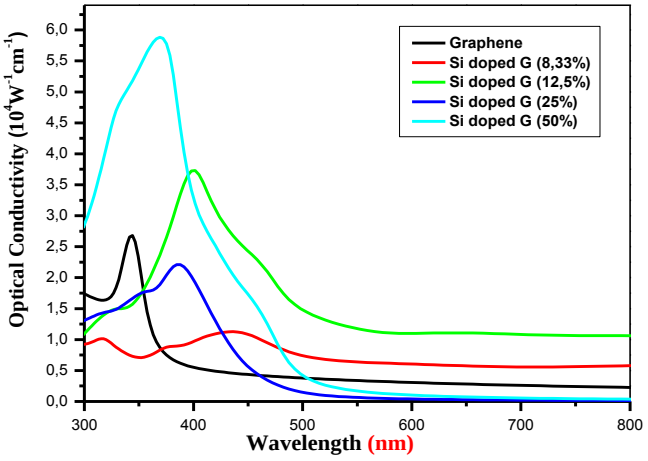

Figure 36: The optical conductivity of silicon doped graphene as function of wavelength for different silicon concentrations.

III.2.3. Refractive index

Figure 36 shows the refractive index of pure and Si-doped graphene, as a function of energy, with parallel and perpendicular electric field. The static refraction index is equal to 1.17 for graphene according to z direction and 2.3for x direction. While, for silicon doped graphene, it is equal to 1.25 for x direction and 2.48 for z direction. Figure 13 shows that the refractive index for silicon doped graphene is lower than graphene for energy between 3.12 eV and 5.29 eV. In the complex refractive index, the imaginary part accounts for the losses of energy of the wave when it crosses the medium. Therefore, this imaginary part comes from all the effects in which the photons transmit a part of their energy. If the index of refraction is lower than one in semiconductors due to the presence of electronic gas and the frequency of plasma. The medium becomes optically "dispersive ", which means that there is deterioration of the frequency of the signal.

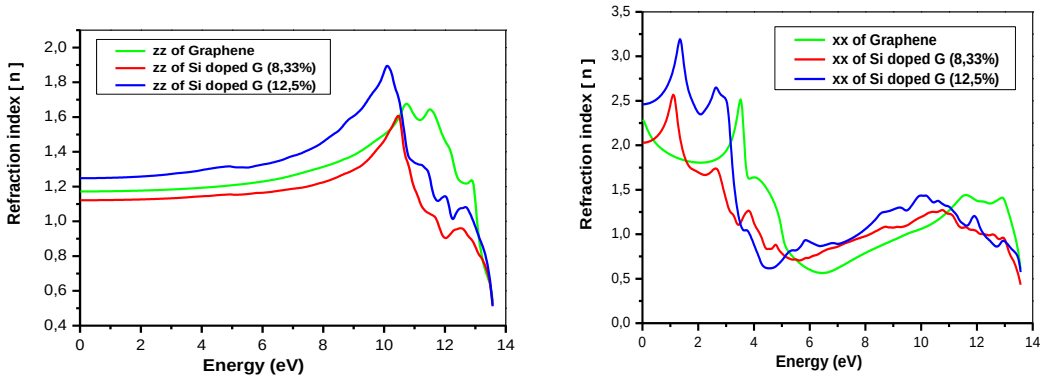

Figure 37: Refractive index of graphene with and without silicon doping (8.33%, 12.5%)in parallel (z) and perpendicular (x) electric field

IV. Conclusion

We have studied the electronic structure of pure and silicon-doped graphene, within three approaches GGA, TB-mBJ and GW. Due to the hexagonal symmetries, all the optical properties are different in parallel and perpendicular electric field direction then the graphene is anisotropic material, in addition we can control the value of band gap as function of Si concentration, therefore all the optical properties are changed (absorption, transmission).The optical conductivity is related to the absorption, according to the band gap cited in Table 1, graphene is gapless therefore, its optical conductivity starts at very low energy while it has an enhancement, for Si doped graphene in the visible region.

Finally, we conclude that silicon doping increases the optical conductivity of graphene in visible region and it allows the graphene to be used in photovoltaic cells.

Chapter 3: Magnetic behavior of Mn doped silicon carbide nanosheet

I. Introduction

Due to higher physical properties graphene has attached several groups of researches for inventing and development many applications of graphene in solar cell technology[19]. Graphene is also used to construct the nano-sized transistors[119]. This material was discovered by using micro-mechanical cleavage of graphite by Geim et al. in 2004[3][4], many research groups have been extensively studying grapheneby using different methods [120, 121][6-13]. This discovery has motivated the researchers to explore other material have 2D dimensional similar to graphene such as silicene germanene AlN, SiC monolayer. Ghosh S. et al. and chen S. et al. calculated the thermal property of graphene. Also, the optical and magnetic properties of graphene were studied in ref[122, 123]. In this context, the idea of doping graphene with transition metals is a good idea for improving the properties of graphene such as magnetic or optical properties. Naji S. et al. has predicted the magnetic properties induced with a transition metals case of Fe , Ni and Co adsorption on graphene[15, 16]. Leibo Hu et al.[124]has studied the effect of adsorption of transition metals on graphene on the density of states and on the magnetic moments of transition metals using Density Functional Theory (DFT). In addition, they calculated the stable geometry, adsorption energy, density of state, and magnetic moment of each atom adsorbed on graphene system. Houmad M. et al have investigated the effect of silicon doped graphene on optical conductivity. They are predicting that the optical conductivity of graphene increases as a function of silicon concentration doped graphene[23]. Here, we focus our studies in Silicon carbide nanosheet that has a structure similar to those of graphene. However, the band gap of silicon carbide nanosheet is equal 2.51eV totally different from to graphene (gapless). This result is confirmed in ref[125].

The idea of this paper is to study the effect of the Manganese atom (Mn) doped Silicon carbide nanosheet on magnetic and optical properties. We found that the compounds of Mn doped SiC nanosheet exhibit a half metallic ferromagnetic property

with a higher polarization at the Fermi level, and the Mn increases the absorption coefficient. Our theoretical calculations are done with First principal calculation using FPLW approximation.

II. Computational model and method

DFT Density functional theory based calculations were performed using the wien2k code [21]. The (GGA) generalized gradient approximation [22-23], parameterized by PBE Perdew Burke Ernzerhof [24]. In this study the plane waves were determined using FP-LAPW [25] method, the space is divided into regions a spherical "muffin-tin" around the nucleus in which radial solutions of Schrödinger Equation and their energy derivatives are used as the basic functions, and an interstitial region between the muffin tins (MT).

III. Results and discussion

III.1.The Electronic properties of SiC nanosheet pure

In this paper, we study the electronic properties of pure SiC nanosheet and doped with Mn. The structure of SiC nanosheet doped with Mn is shown in figure 37, a supercell equal 4x2x1 is chosen. The structure of SiC nanosheet is located plane (x-y) we used the vacuum space equal 20A° in the (z) direction to avoid the interaction between two layers adjacent of SiC nanosheet. We begin our calculations by the total density of states of SiC nanosheet pure, we observed in figure 38, the total density of states of majority spin and minority one is symmetrical, this result shown that SiC nanosheet pure has any magnetic property, and this one have a large band gap equal 2.51eV so SiC nanosheet is a semi-conductor.

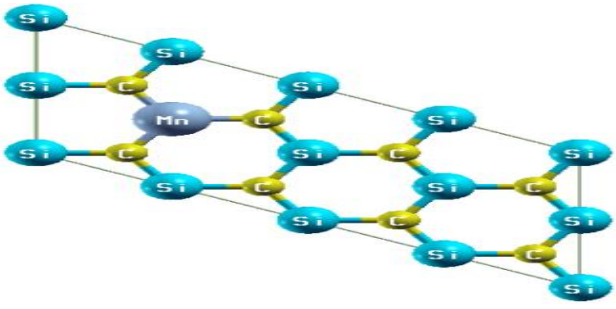

Figure 38: The crystal structures of monolayer SiC (supercell 4x2x1) nanosheet doped with Mn.

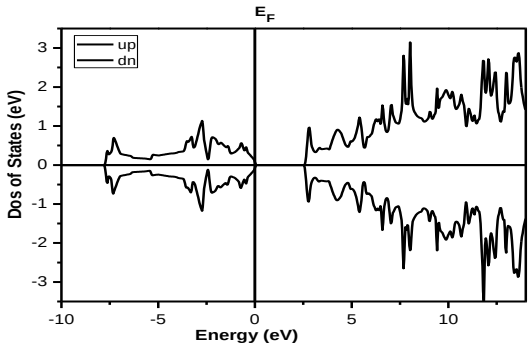

Figure 39: Density of states of SiC nanosheet pure.

III.2 Electronic and Magnetic properties of Mn doped SiC nanosheet

The result obtained by M. Wu et al., are predicted the magnetic induced with (manganese) Mn–doped graphene when substituted one atom of carbon by manganese [126]. The total density of states of Mn doped Silicon carbide nanosheet is calculated in Figure 39 , we observed that 3d states of Mn is localized in level of Fermi energy this result found that this compounds has a half metallic ferromagnetic states.

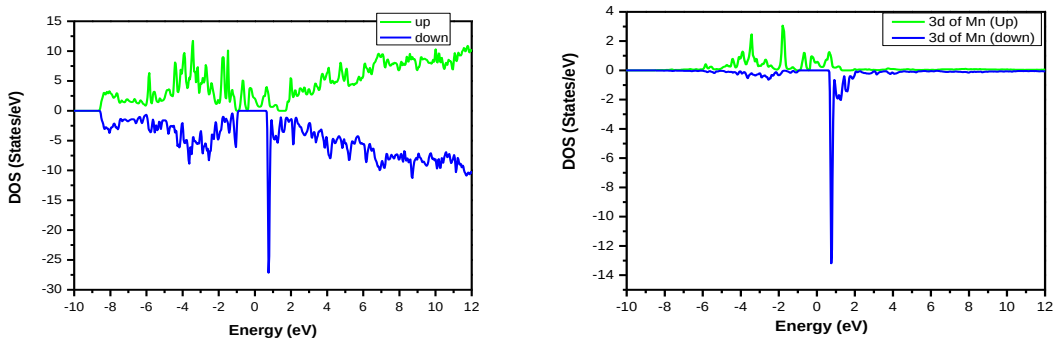

Figure 39: Total and 3d-Mn density of states of Mn doped SiC nanosheet (4*2*1).

III.3 Optical properties of Mn doped SiC nanosheet

The study of optical properties is very interesting for predicting that one material can be used in solar cell applications, for that we calculate the optical properties of compound Mn doped SiC nanosheet. In this paper, we calculated the dielectric function using the following relation is the summation between real parts and imaginary one of functions dielectric $\varepsilon(\omega) = \varepsilon_1(\omega) + i\varepsilon_2(\omega)$ (1), it describes the optical response of the

medium at all photon energies $E = \hbar\omega$. The real part $\varepsilon_1(\omega)$ and the imaginary part $\varepsilon_2(\omega)$ of the dielectric function were followed from the Kramers-Kronig relation[127].

$$\varepsilon_1(\omega) = 1 + \frac{2}{\pi} P \int_0^{\infty} \frac{\varepsilon_2(\acute{\omega})\acute{\omega} d\acute{\omega}}{\acute{\omega}^2 - \omega^2} \quad (2)$$

$$\varepsilon_2(\omega) = \frac{e^2\hbar}{\pi m^2 \omega^2} \sum_{v,c} \int_{BZ} |M_{cv}(k)|^2 \delta[\omega_{cv}(k) - \omega] \, d^3k \quad (3)$$

Where P implies the principal value of the integral an$M_{cv}(k)$: The transition moments elements

In figure 39, we observe comparative results of imaginary-Epsilon and absorption coefficient between 4H-SiC bulk and SiC nanosheet with and without Mn doped. We obtained the peak of imaginary-Epsilon has localized at 3.24eV for SiC nanosheet different than the bulk 4H-SiC at 6.71eV. And when we doped SiC nanosheet with Mn we observe that the peak of SiC NS doped with Mn became at points 2.30eV. In the next step we calculate the coefficient of absorption as function Energy (eV) we obtained that manganese doped SiC NS increase the coefficient of absorption at visible region compared with coefficient absorption of SiC NS (figure 40).

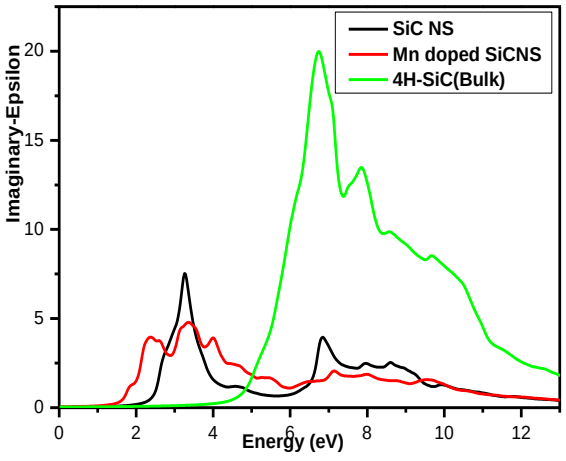

Figure 40: Imaginary part of dielectric function of Mn-doped SiC Nanosheet.

The absorption coefficient is obtained with following relation[96]

$$\alpha(\omega) = \frac{\sqrt{2}}{c} \omega \sqrt{-\varepsilon_1(\omega) + \sqrt{\varepsilon_1(\omega)^2 + \varepsilon_2(\omega)^2}} \quad (4)$$

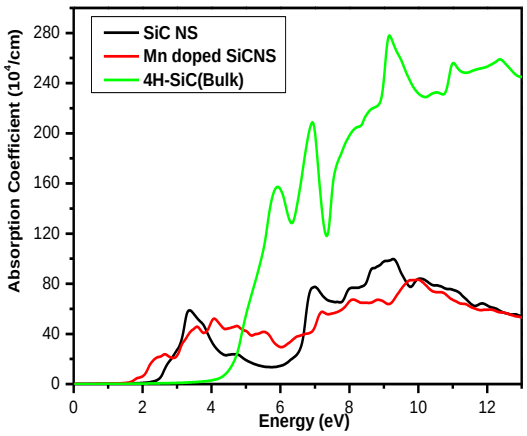

Figure 41: Absorption coefficient of Mn-doped SiC Nanosheet.

IV. Conclusion

We have studied the electronic structure, optical and magnetic properties of Silicon carbide nanosheet pure and doped by Mn. The silicon carbide nanosheet is a semiconductor with a wide band gap equal 2.51eV. The effects of Manganese doped SiC nanosheet on magnetic and optical properties (absorption coefficient, optical conductivity) are studied. We obtained that Mn induced the magnetic in SiC nanosheet and increases the absorption coefficient of Silicon carbide nanosheet in the visible light region.

Chapter 4: Electrical property of siligraphene and its derivatives

I. Introduction

The monolayer of graphene is one plan of graphite. Before 2004, the vision in science has synthesized experimentally new materials that have structure with two dimensional and deduced their physical properties. This objective has been realized in the Centre of Mesoscopic and Nanotechnology of Manchester University, UK by A. Geim et al. [3, 4]. This group used the micro-mechanical cleavage of graphite to produce graphene. Graphene has better physical properties compared to graphite due to its hexagonal structure which is bi-dimensional. Unlike graphite (3 dimensional), a carbon atom in graphene is surrounded by three other atoms of carbon in planar sheet which make just three connection. The bond length between two carbon atoms (sp^2 bonded carbon atoms) has measured by Geim et al. using the transmission electron microscope (TEM).Its equal to 0.14nm.HC. Schniepp et al. and C. Berger et al. these two groupsexperimentally produced the isolate graphene[101, 128]. The recent research confirmed that graphene has high electron mobility [129, 130, 131]. The mechanical, electronic, optical and magnetic properties of graphene have been studied in these refs [15, 16]. 2D materials emerge as potential systems for different applications such as nanoelectronics, [132, 133, 134, 135] solar energy[136, 137] and energy storage [138, 139, 140]. These 2D materials have both high mobility and a gap intrinsic charge carriers which makes them more efficient than silicon which is the basis of the current electronics industry. To date graphene (2D equivalent of graphite) are two-dimensional materials experiencing the greatest interest. While graphene suffers from a zero energy gap, our idea is to look for graphene-like materials that may possess both properties (mobility and gap). In this work, we propose a new 2D material emerge that can replace silicon in several industrial applications.

Pablo A. Denis to demonstrate that the band gap of graphene (monolayer or bilayer) can be opened with silicon, aluminium, phosphorus and sulfur doping; they also studied the mono and dual Doped Monolayer Graphene[20, 141], the formation of the band gap

in graphene with silicon doped has been analyzed by MCS Escaño et al. MSS Azadeh et al.[21, 22].Additionally, they used doping technics by density functional calculation. Houmad et al. has demonstrated that it is possible to open the band gap of graphene with silicon doped; they found that the optical conductivity increased as a function of silicon concentration [23, 142]. Likewise, other methods to open the band gap of graphene are proposed like the functionalization of graphene with hydrogen or molecule adsorptions [24, 143, 144][32,33,35]. The optical properties of graphene can also be improved when it is functionalized with organic molecules [109].

Recently, until the siligraphene has one derivatives of graphene, it is formed with the graphene doped (or contained)by silicon(g-SiC7 or g-SiC3) . The new 2D Silicon-Carbon has been fabricated experimental with single layer and bilayer by Lin [145]. The aim of this paper is to predict the optical properties and the electrical property of siligraphene. We used density functional theory and semi-classical Boltzmann equation implanted in WIEN2K code, we showed that siligraphene is a semiconductor with a small band gap and the electrical conductivity increased as function silicon concentration (g-SiC7; g-SiC3).

We show that siligraphene is a very promising 2D material with great impact that can lead to exceptional results in the field of solar energy and other application. Consequently, we pushed the experimental researches to discover this new 2D material (siligraphene) for using in solar cell application.

II. Computational details

Our calculations are based on Density functional theory (DFT) implanted in wien2k code [38] using generalized gradient approximation (GGA) [39], parameterized by PBE Perdew Burke Ernzerhof [40]. In this study the plane waves were determined using FP-LAPW [41] method, the space is divided into regions a spherical “muffin-tin” around the nucleus in which radial solutions of Schrödinger Equation and their energy derivatives are used as the basic functions, and an interstitial region between the muffin tins (MT). To study the electrical propriety of Siligraphene we used Boltzmann theory implanted in Boltztrap package [42] it’s calculated as function of Temperature based on following equation:

$$\sigma_{\alpha\beta}(T;\mu) = \frac{1}{\Omega}\int \sigma_{\alpha\beta}(\varepsilon)\left[-\frac{\partial f_{\mu}(T;\ \mu)}{\partial \varepsilon}\right]\partial\varepsilon$$

The electrical conductivity$\sigma_{\alpha\beta}$ is obtained with $\sigma_{\alpha\beta}(\varepsilon) = \frac{1}{N}\sum_{i,k}\sigma_{\alpha\beta}(i,K)\frac{\delta(\varepsilon-\varepsilon_{i,K})}{d\varepsilon}$

αandβ are the tensor indice $E_{i,j}$ is band structure and Ω is the number of k points that are sampled in the Brillouin zone . ϑ(k)is the band velocity, τ(k) is the relaxation time and f is Fermi function.

III. Results and discussions

III.1. Electronic properties

The effect of bonding structure and stoichiometry of the Silicon carbide monolayers as function of silicon and carbon concentration atoms on electronic properties of Silicon carbide has been reported by Z. Shi et al. [146].The super-cell of two configurations of siligraphene SiC_7 and SiC3 are shown in Fig.41. We are beginning our calculations by the relaxation of the structure of two type of Siligraphene, we show that the band length C-C and Si-C in SiC_7 is equal to 1.53A° and 1.7939A° respectively, and the value the band length C-C and Si-C for the second type of siligraphene (SiC_3) is equal to 1.7843A° and 1.4177A° respectively. The vacuum space in Z axis is also relaxed is equal 20A° this value avoid the interactions between two plans adjacent siligraphene.

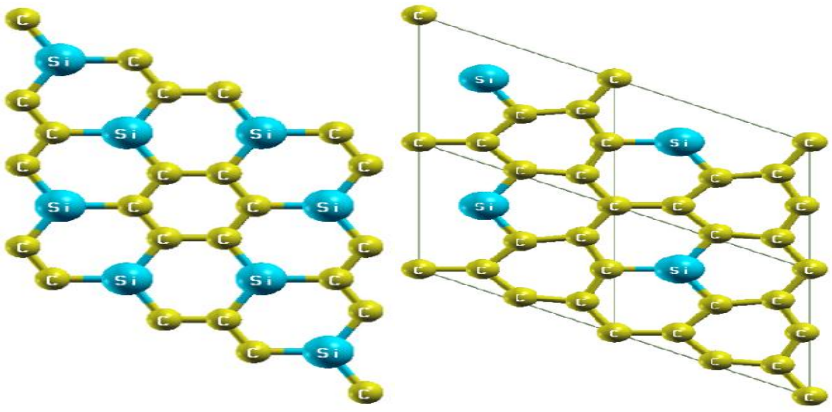

Figure 42: The crystal structures of siligraphene SiC_3 and SiC_7.

The band structure and density of states of two types of siligraphene SiC_3 and SiC_7 are presented in figure 42 and 43, our results show that these two configurations are semiconductor materials with direct band gap. The valence shell of Si atom is $3s^2 3p^2$ and

the valence shell of C atom is $2s^2 2p^2$. We calculated the band gap energy of siligraphene SiC_3 and SiC_7, we obtained that the band gap energy of SiC_3 and SiC_7 are 0.0eV and 0.79eV respectively these values is in good argument with [147, 148]. We established that the band gap is related to the concentration of silicon in hexagonal structure of graphene. We observed also the band gap of SiC_3 and SiC_7 is direct following K wave vector.

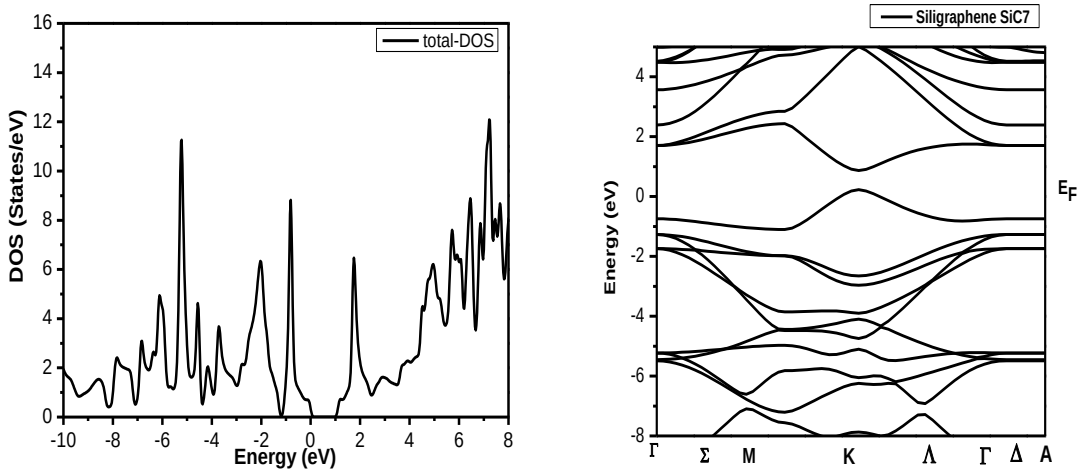

Figure 43: Band Structure and Density of states of Siligraphene SiC7.

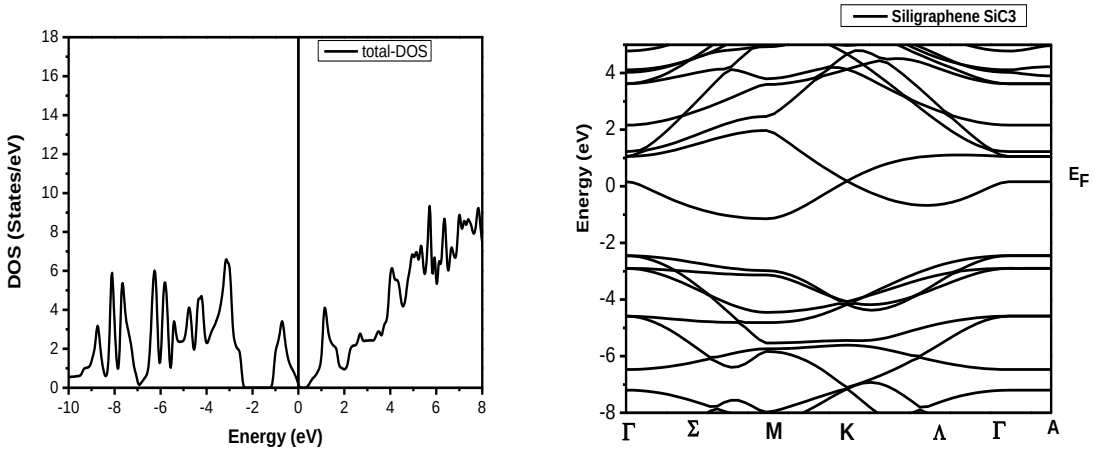

Figure 44: Band Structure and Density of states of Siligraphene SiC_3.

III.2. Optical properties

The character semi-metals of graphene has been limited to the directly application of graphene in solar cell application, this difficulty pause the scientists to resolute this problem's many idea has been established for example the functionalization of graphene with molecular or doping with atoms such as Silicon or germanium[149], the optical properties of graphene has been studied by Nair et al. [150], in particular the optical conductivity of graphene has been measured by Stauber et al. [151], The two groups established that graphene has a higher optical conductivity. The absorption coefficient is obtained with the following relation.

$$\alpha(\omega)=\frac{\sqrt{2}}{c}\omega\sqrt{-\varepsilon_1(\omega)+\sqrt{\varepsilon_1(\omega)^2+\varepsilon_2(\omega)^2}} \quad (4)$$

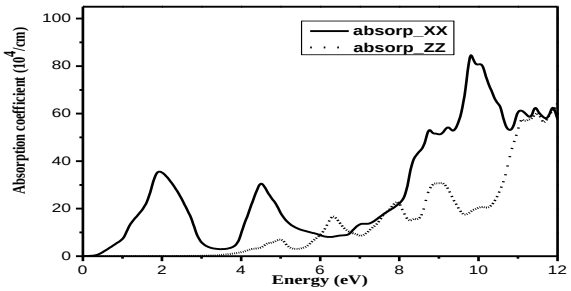

Figure 45: the absorption coefficient of Siligraphene (SiC7) as function of photon energy in both direction xx and zz.

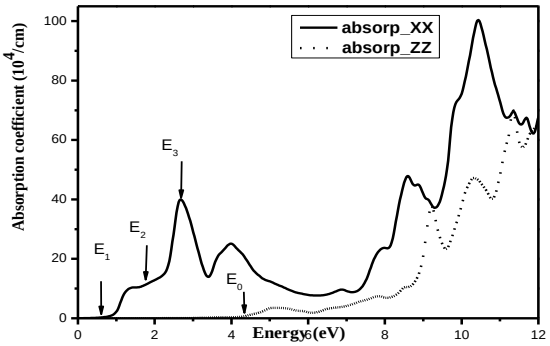

Figure 46: the absorption coefficient of Siligraphene (SiC3) as function of photon energy in both direction xx and zz

The absorption coefficient of two siligraphene is shown Figure 44 and 45, we observe that the absorption coefficient for xx direction is different to zz direction this difference is due to anisotropy of siligraphene, we observe also that the absorption coefficient started firstly for SiC7 compared with SiC3 for two direction xx and zz because the band gap of SiC7 is lower than the band gap SiC3 therefore the first transition is in siligraphene SiC7 following K wave vector. The absorption coefficient of SiC7 started at energy equal 0.39eV for xx direction and 3.55eV for zz direction, but for siligraphene SiC3 is started at 0.511eV for xx direction and 4.34eV for zz direction.

III.2.1. Reflectivity spectrum R(ω)

The reflectivity of material plays an important role in a solar cell material application; the measurement of reflectivity of graphene has given 2.3%. Other experiment results obtained that reflectance of silicon surface decreased when the deposition of graphene on textured silicon surfaces, also it's possible the decreasing the reflectivity used the doping of graphene with boron and Nitrogen [152]. The reflectivity R(ω) is calculated with the Fresnel's formula:

$$R(\omega) = \left|\frac{\sqrt{\varepsilon(\omega)}-1}{\sqrt{\varepsilon(\omega)}+1}\right|^2 \quad (5)$$

In figure 46, we plot the reflectivity of siligraphene for two direction xx and zz we observe that reflectivity of siligraphene type SiC_7 is lower than SiC_3 we analyzed this result ofthe different concentration of silicon in two types.

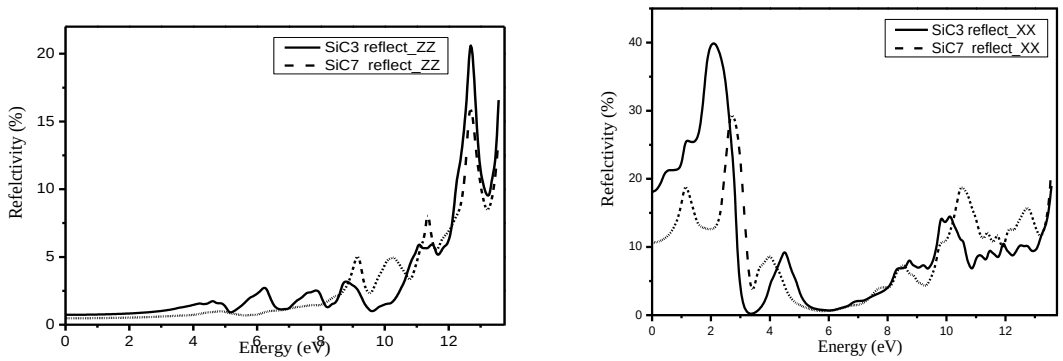

Figure 47: The reflectivity of siligraphene SiC7 and SiC3 as function of photon energy in both direction xx and zz

III.2.2. Electrical conductivity

The developments of solar cell material application are limited to yield of physical properties of absorbed material used in the cell l. The transport properties of graphene monolayer and bilayer are studied [153]; also the improving of the electrical conductivity of graphene with chemical doping (Potassium nitrate) is studied by khan et al.[154]. The platinum (Pt) metal adsorbates affect the properties of graphene and increasing their electrical conductivity [155]. At this time; we studied the electrical conductivity of siligraphene ($\boldsymbol{\sigma/\tau}$is conductivity divided by time relaxations) based on the Boltzmann equation implanted in bolztrap package. We observe the difference between the electrical conductivity of siligraphene g-SiC3 and g-SiC7, the figure 47, show that the electrical conductivity of g-SiC3 is better than the electrical conductivity g-SiC7 this difference is due to the difference of silicon concentration in siligraphene structure. We find also that the electrical conductivity of siligraphene decreases as function the temperature for g-SiC_3 and increasing for SiC_7 these results confirmed that g-SiC_7 is a semiconductor materials but g-SiC_3 is a conductors.

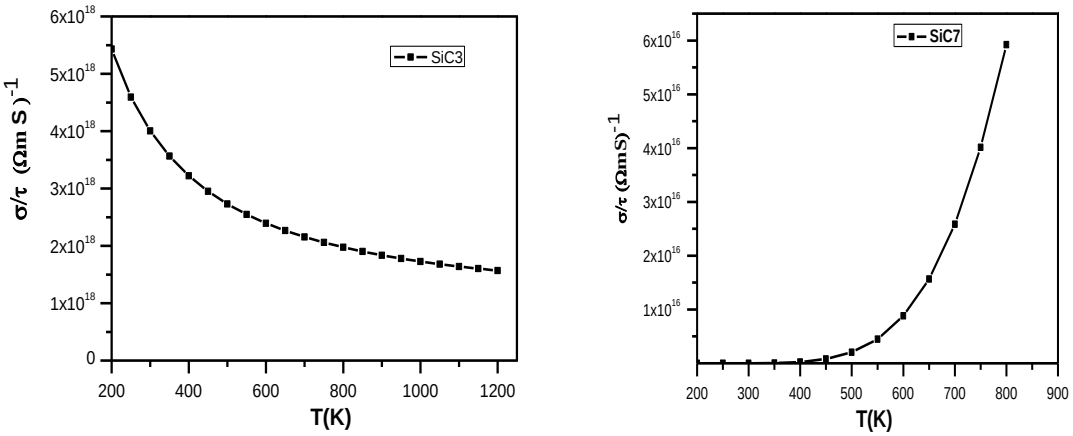

Figure 48: The electrical conductivity of siligraphene g-SiC_7 and g-SiC_3 as function temperature.

III.2.3. Thermal property of siligraphene

The figure 48 show the thermal property of siligraphene SiC3 and SiC7 we observe that the siligraphene g-SiC3 has a better thermal property compared with siligraphene g-SiC7; also we obtained that thermal properties of g-SiC7 is increasing as

function temperature but for g-SiC3 the thermal properties decreased as function temperature lower than 450 °K and become increasing for high temperature than 450 °K.

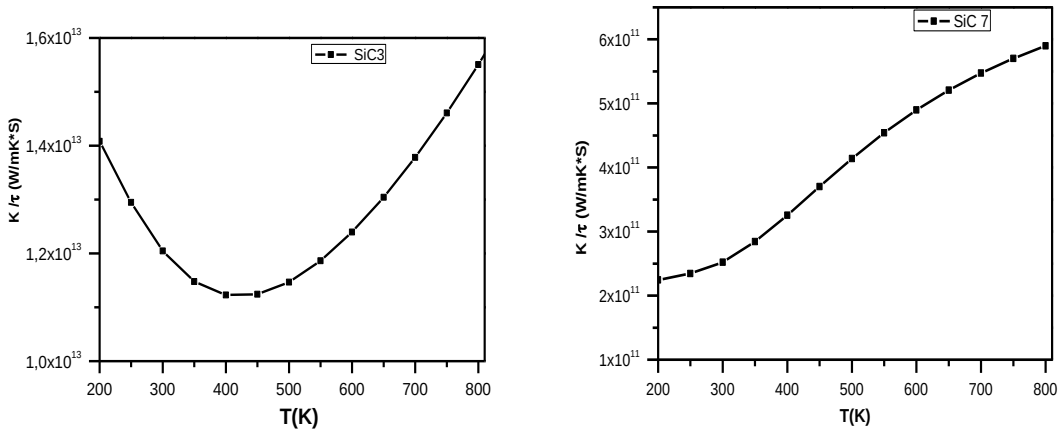

Figure 49: The thermal property of siligraphene g-SiC_7 and g-SiC_3 as function temperature.

IV. Conclusion

The thermal, electrical property and optical properties of two structures of siligraphene are calculated within wien2kand Boltztrappackages. Our results predict that these two siligraphene have a direct band gap. We concluded that the optical properties are depending to silicon concentration in siligraphene, and the reflectivity of SiC_7 is lower than the reflectivity of SiC_3 following xx and zz direction. Finally, we can observe that the electrical conductivity of g-SiC_3 is better than the electrical conductivity of g-SiC_7. We predict that siligraphene have the potential to use in solar cell application.

Chapter 5: Electronic and Electrical properties of Siligraphene (g-SiC3) in The Presence of Various Strain

I. Introduction

Nowadays, 2-D nanomaterials are very significant to utilize in various applications, such as using graphene to create or control various properties of the nanoelectronics materials[156, 157], solar cells[158, 159], and energy storage[160, 161]. In fact, these 2-D nanomaterials that are consisted of carbon atoms are more efficient in the current electronics industry than the ones consisted of silicon due to these 2-D nanomaterials, which have both high mobility charge carriers and an intrinsic bond. To date, some scientists are focusing on using graphene (2-D nanomaterial) in the scientific limelight for the past few years due to a range of interesting properties, that display the various nanoelectronics, spin-tronic and optoelectronics[162, 163]. However, graphene is suffering from a zero-electronic band gap[164, 165, 166], which limits its use in various application, such as in solar cell for Photovoltaic (PV) application like as absorber material in solar cell.

There are various methods (theoretically and experimentally), such as chemical doping, adsorption to open and control the electronic band gap of graphene, which makes it very interesting in different applications. Recently, Denis, P. A[20, 167] demonstrated that the band gap of graphene (monolayer or bilayer) can be opened with silicon, aluminum, phosphorus and sulfur doping. By using chemical doping, the electronic properties, such as electronic band gap is very sensitive to the phosphorus atoms. So, it is dependent on the concentrations and sites of the phosphorus atoms. For adsorption method, Mohammed, M. H. et al. found out that graphene can be utilized as gas sensor due to the electronic properties, such as electronic band gap, total energy, and dipole moment which are affected by these gas molecules. Other studies have focused to study the physical properties of Single and bilayer graphene with various impurities, such as silicon, which leads to open an electronic band gap by using DFT method[23, 168, 169]. Other significant properties are the optical properties of graphene. The optical properties of

graphene can be developed when they are functionalized with organic molecules or using graphene to construct the inorganic nano-materials[109, 170, 171].

This study aims at gaining insight into the influence strain on the electronic and optical properties of 2-D nanomaterial (siligraphene) by using density functional theory (DFT). The DFT calculations have been carried out to investigate and find out various electronic and electrical properties with and without various percentages of strain (-1% to -10%). By engineering the strain in the electronic and electrical properties of g-SiC_3, this 2-D martial will be useful to explore unusual electronic and electrical properties effects and exotic electronic and photovoltaic cell applications based on g-SiC_3. Then, this phenomenon is assumed to be particularly significant for different applications in the future nanoelectronics and solar cell applications by applying different percentages of strain on the siligraphene (g-SiC_3).

II. Computational details

In this work, all these examinations, containing the geometry optimizations and electronic structure computations are carried out via using the plane-wave projector-augmented wave method, as implemented in the density functional theory (DFT), which is performed in the Quantum Espresso package [30]. To simulate the mono layer of g-SiC_3 in this study, we utilized the 3×3 supercell of the g-SiC_3, which is comprised from 31 atoms (23 carbon and 8 silicon atoms). Electron–ion interactions are described by using ultra soft pseudo potentials with a kinetic energy cut-off 38 Ry and the convergence criteria for energy are assumed 10-8 Ry. A 10 × 10 × 2Monkhorst-Pack grids was utilized to perform the Brillouin-zone. In order to avoid the interaction between images, we separated them by putting 20Å a distance between them. The first step of our calculations is started with relaxation our structure. So, we utilized Perdew Burke Ernzerhof (PBE) [31, 32]to achieve the electronic band gap, lattice constants and atomic coordinates. The above process is used to investigate the electronic properties of the g-SiC_3, such as electronic structure, electronic band gap, total energy. To study the electrical conductivity of the g-SiC_3, we have used Boltzmann theory, which is implanted in the Boltztrap package [33]. It's calculated as a function of the temperature based on the following equation:

$$\sigma_{\alpha\beta}(T;\mu) = \frac{1}{\Omega}\int \sigma_{\alpha\beta}(\varepsilon)\left[-\frac{\partial f_{\mu}(T;\ \mu)}{\partial \varepsilon}\right]\partial\varepsilon$$

The electrical conductivity $\sigma_{\alpha\beta}$ is obtained with $\sigma_{\alpha\beta}(\varepsilon) = \frac{1}{N}\sum_{i,k}\sigma_{\alpha\beta}(i,K)\frac{\delta(\varepsilon-\varepsilon_{i,K})}{d\varepsilon}$.

The α and β are the tensor indices, and $(E_{i,j}, \Omega, \vartheta(k), \tau(k), \text{and } f)$ are the band structure, and the number of k points that are sampled in t, Brillouin zone, the band velocity,the relaxation time, and Fermi function, respectively.

III. Results and discussions

III.1. Electronic properties

First of all, we perfectly optimized a pristine 3×3 supercell of the g-SiC_3, as displayed in the Fig.49. We found out that the bond length between (C-Si and C-C) are (1.784 and 1.417) Å, respectively, which is agreement with previous studies[34, 35]. With free strain, we calculate the electronic band structure of Sci3. Our results are very interesting results. This structure has zero electronic band gap is zero, which is an agreement with the electronic band gap value of graphene and another study[172].

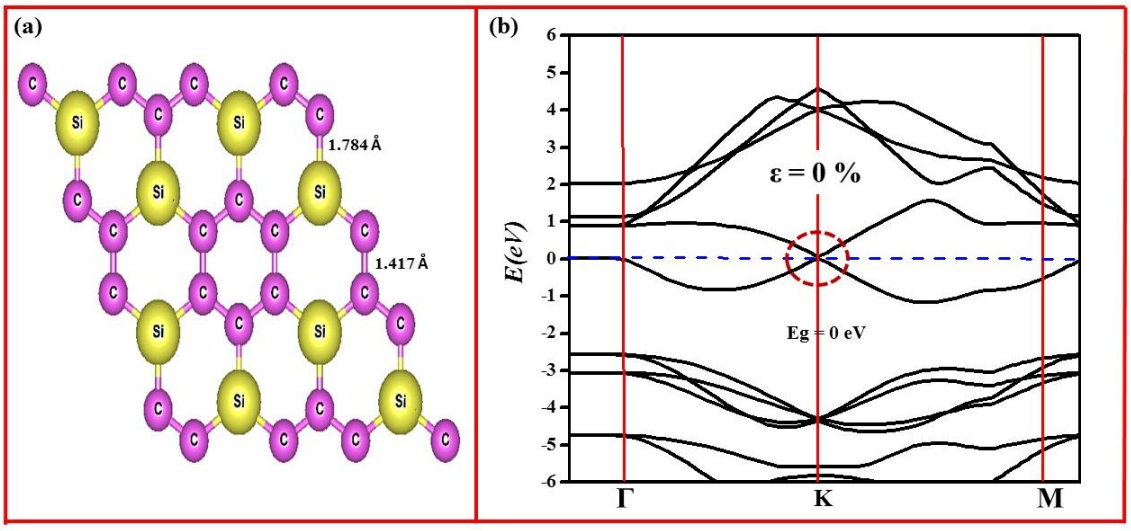

Figure 50: The crystal structures and electronic band Structure of siligraphene g-SiC_3 in free Strain.

By applying a range of biaxial strain values from (0 to -9) % along the ab plane. The geometrical structure is affected due to the bond lengths are altered. Comparing the bond length between atoms with and without various percentages of strain, we observed

that there is small increasing in the bond length between C-C atoms under (-1 and -9) % strain and it is reduced under other strain (-2 to -8) %. The same behavior we found out when we applied these percentages of the strain In or Out the plane. They have the same value of the altering Si-C bond length (In or Out the plane) under all strain values, except in the 9% strain is different, as demonstrated in the Fig.50.

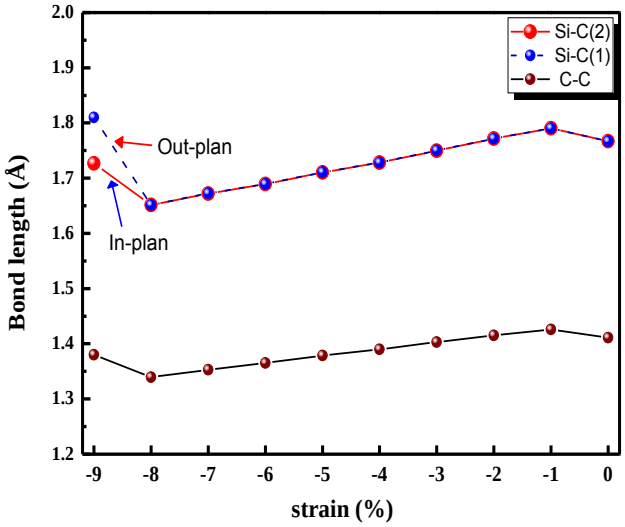

Figure 51: Variation of bond lengths with various percentage of strain

The electronic properties, such as electronic band gap, total energy also calculated with various percentages of the strain (-2, -4, -6, -8, -9, and -10) %. There is not affected on the electronic band structure under small value of strain (-2, -4, -6, -8) %. So, this 2-D nanomaterial is still having semimetal behavior due to the electronic band gap is not altered (zero electronic band gap). However, the electronic band gap is opened at the K point when we increased the strain to -9 % and -10 %. There are various types of electronic band gap, direct (1.26 eV) with -9 % strain and indirect (1.43 eV) with -10% strain, as represented in Figs.51 and 52 and summarized in Table 1. Also, we observed that the geometrical structure of the SiC_3 is changed under -9 % and -10 % strain. It's becoming buckled due to the bond length between C and Si atoms is increased under these values of strain (see Fig.53).

Strain %	**0**	**-2**	**-4**	**-6**	**-8**	**-9**	**-10**
Gap(eV)	0	0	0	0	0	1.62 direct	1.43 indirect

Table 1: The electronic band gap value with various train %

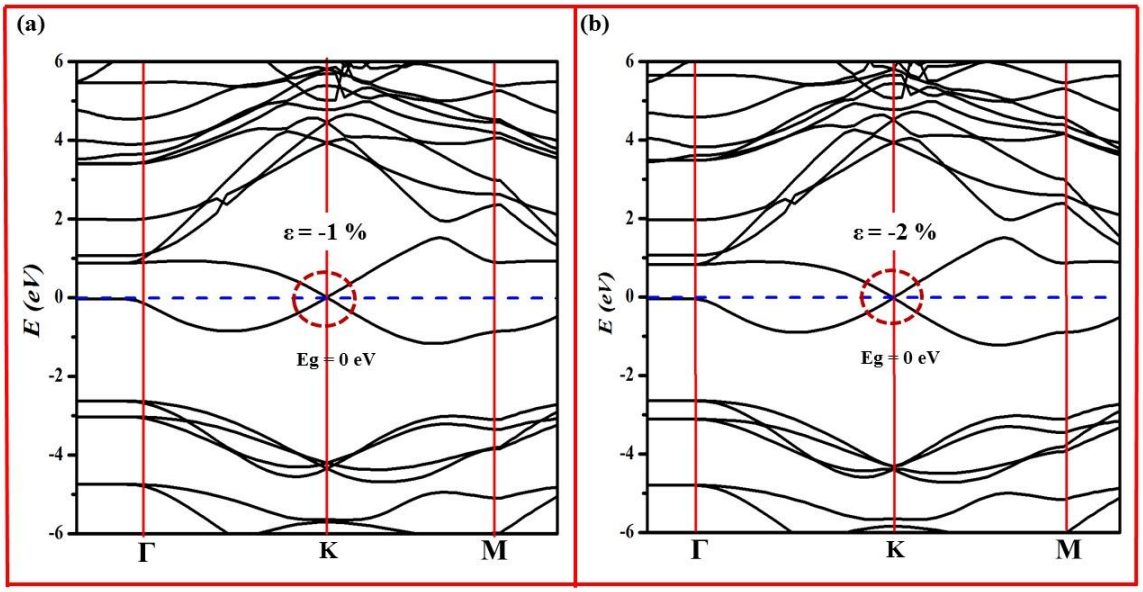

Figure 52: The electronic band structure of Siligraphene (g-SiC_3) under (-1 and -2) % strain compressions.

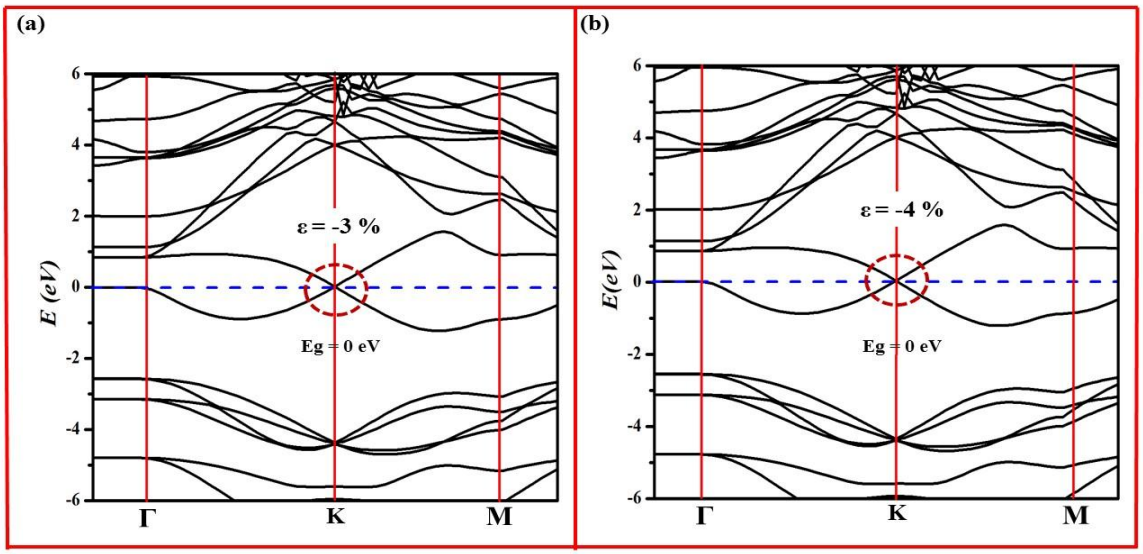

Figure 53: The electronic band structure of Siligraphene (g-SiC_3) under (-3 and -4) % strain compressions.

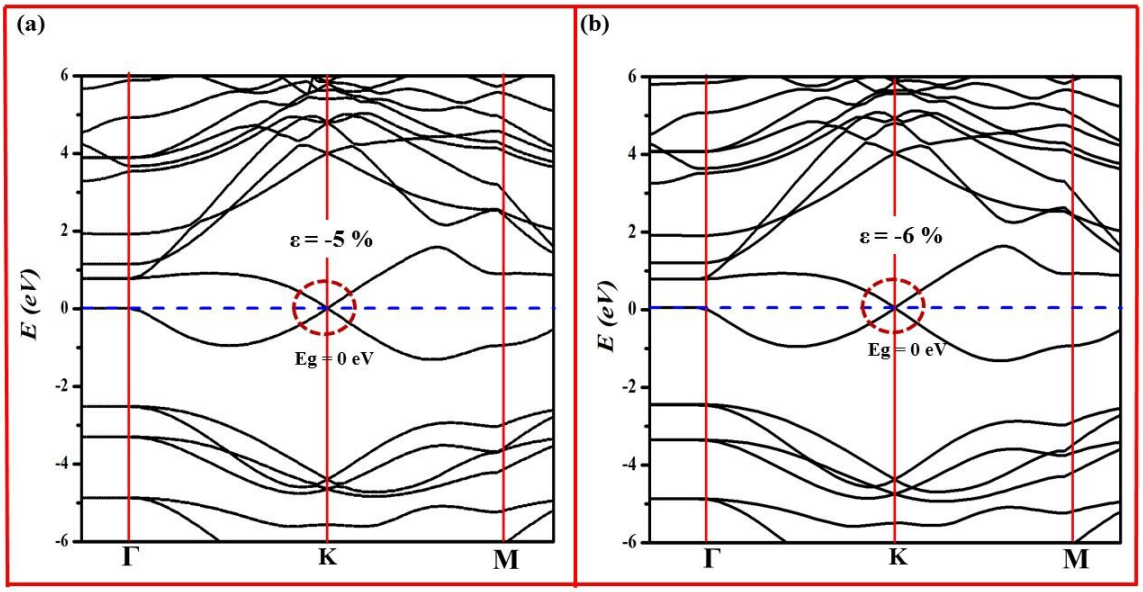

Figure 54: The electronic band structure of Siligraphene (g-SiC_3) under (-5 and -6) % strain compressions.

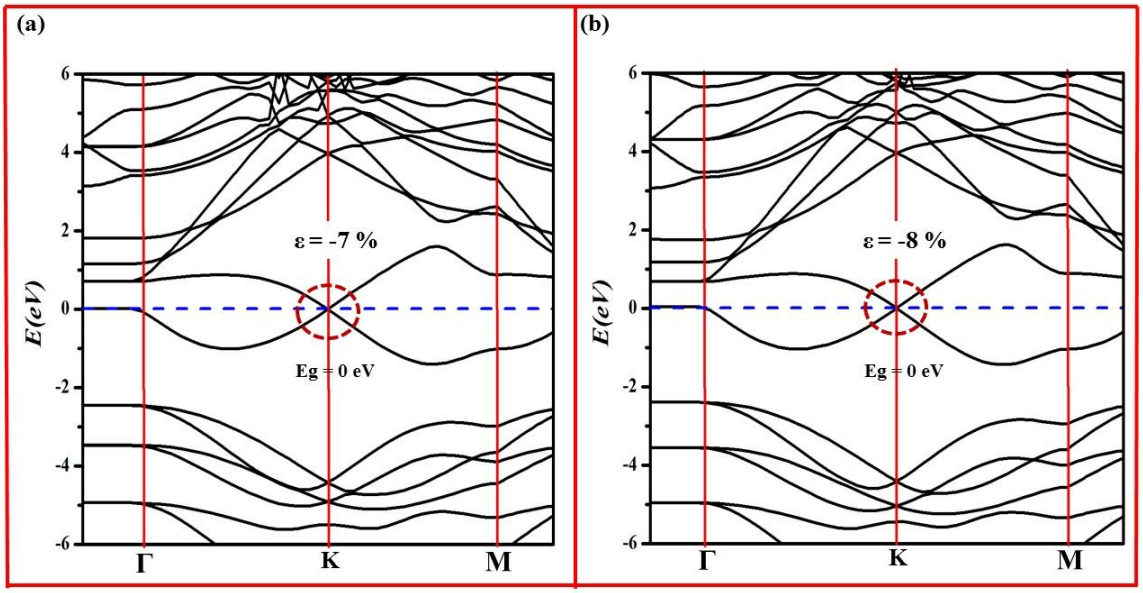

Figure 55: The electronic band structure of Siligraphene (g-SiC_3) under (-7 and -8) % strain compressions.

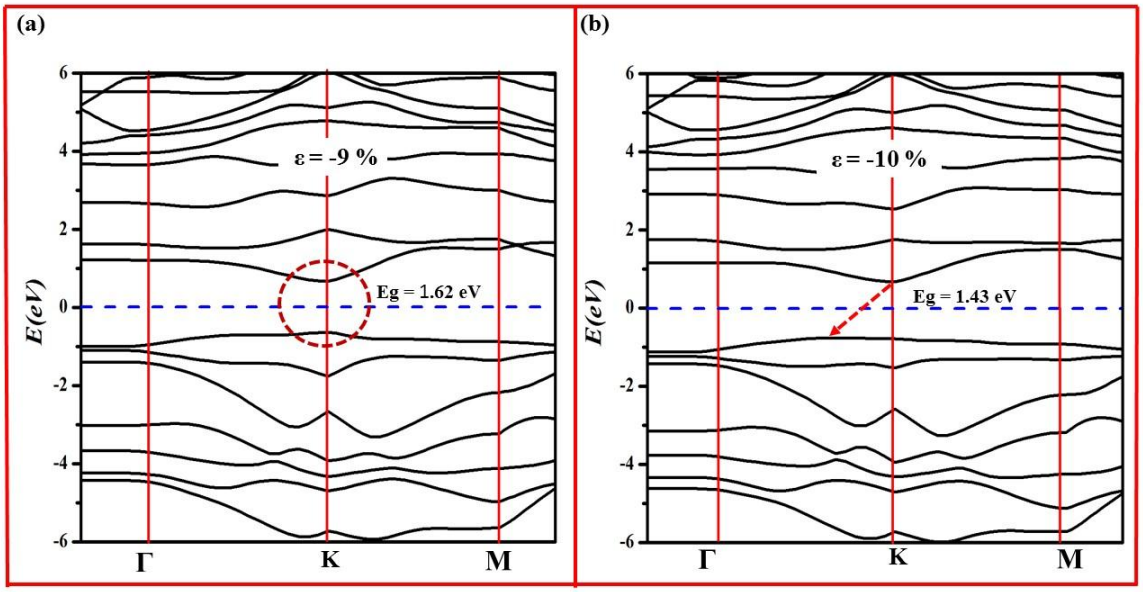

Figure 56: The electronic band structure of Siligraphene (g-SiC_3) under (-9 and -10) % strain compressions.

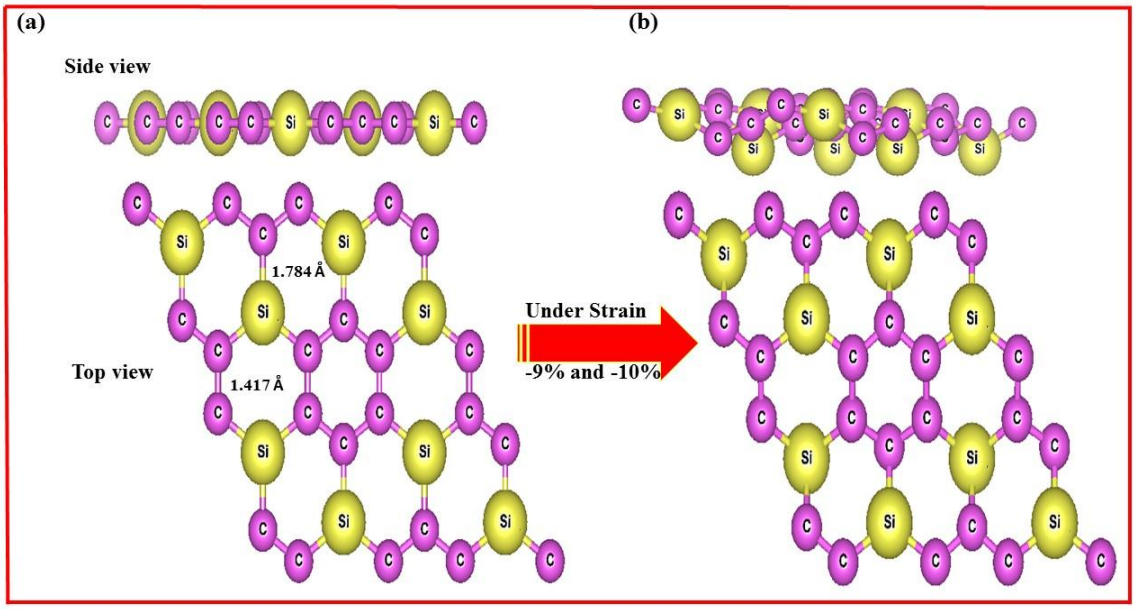

Figure 57: The geometry Structure of Siligraphene (g-SiC_3); (a) without strain. (b) with -9% strain

Another significant property is the total energy. We computed the total energy of the SiC_3 with imposing a range of biaxial strain values from (-10 to 10) % along the ab plane. The negative strain values represent a compressive strain while the positive ones

represent a tensile strain. Fig.57 demonstrated that the total energy is increased under the strain effect from 0% to -8% (for compressive strain) and 0% to 10% (for tensile). However, after compressive strain equal to -8% the total energy decreasing.

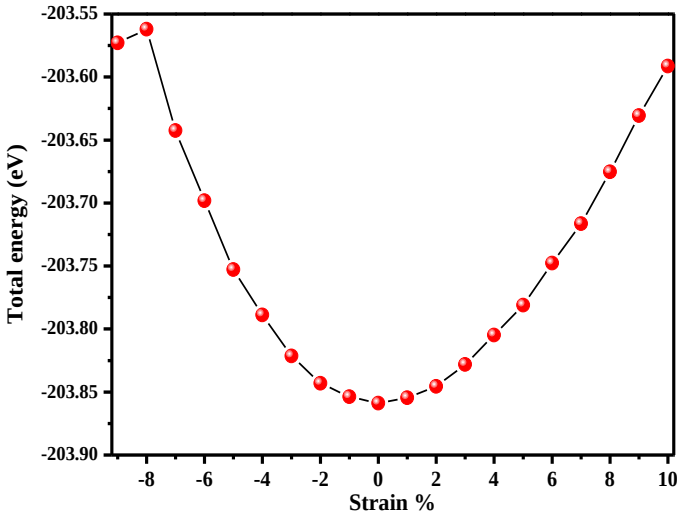

Figure 58: Total energy of siligraphene SiC_3 as function of Strain (%).

III.2 Electrical conductivity of the g-SiC_3 with and without strain

In this section of our paper, we calculated the electrical conductivity of the g-SiC_3 in the pristine and with -9% strain cases. In fact, we chose (0% and -9%) strain values due to before this value (0% until -9%) we got there is not affected on the electrical conductivity, and with -9% and -10% have the same affected on the electrical conductivity. All these calculations are done in the temperature range of (100–800) ^{0}K. We found out very fascinating results. So, the behavior of the g-SiC_3 is altered from metallic to semiconductors with strain effect due to the electrical conductivity is very sensitive to the strain values. Consequently, it is increased smoothly by increasing the temperature comparing without strain it's decreased smoothly by increasing the temperature, as exhibited in Fig. 58.

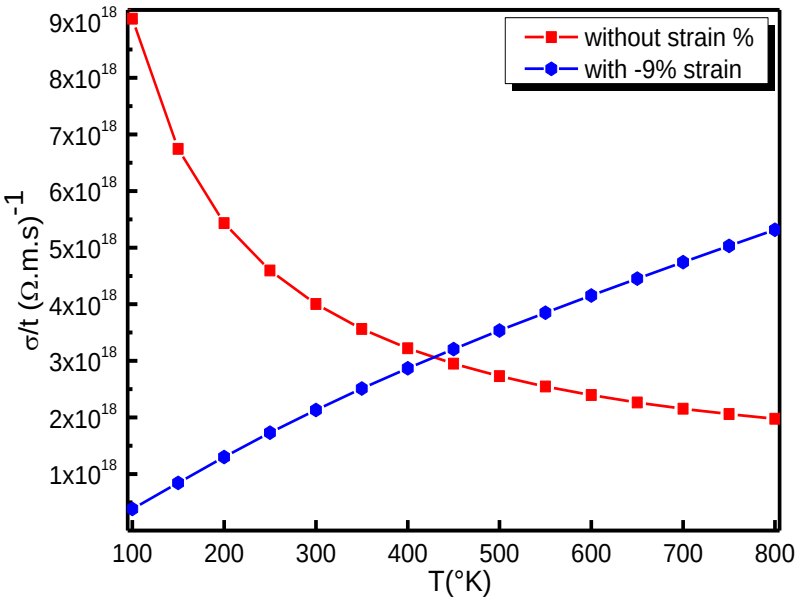

Figure 59: The electrical conductivity of siligraphene g-SiC_3 as a function temperature without and with strain -9%.

III.3 Charge density distribution with and without strain effect

We also calculated the charge density distribution of the g-SiC_3 in the pristine and with -8% strain. As we explained that the g-SiC_3 is consisted from Si and C atoms. So, there are two hexagonal regions in this structure. First hexagonal is consisted from C_6 atoms, and from C_4 and Si_2 atoms for the second hexagonal. In the pristine case, we observed that there is not charge density accumulation between these hexagonal. However, the electronic density is highly presented between C atoms due to their nature covalent band its equal to +0.2556 electron/$(Å)^3$ along the bonding directions, and the electronic density value is lowered between Si-C atoms along the bonding directions (+0.3195 and +0.1278) electron/$(Å)^3$ around C and Si atoms, as represented in Fig. 59. Now, when we applied -8% strain, we observed that the charge density distribution of valence electrons is changed compared with the pristine case. We obtained that the higher charge density is decreased to +0.12 electron/$(Å)^3$ between C-C atoms, and it's varied from +0.12 to +0.3 electron/$(A°)^3$ between Si-C atoms. We also detected that the charge density shared with two hollows, which is constituted from two hexagonal shapes (C-C and Si-C)

atoms. Then, they are become occupied by charge density when we applied -8% strain compared with the pristine case (0% strain).

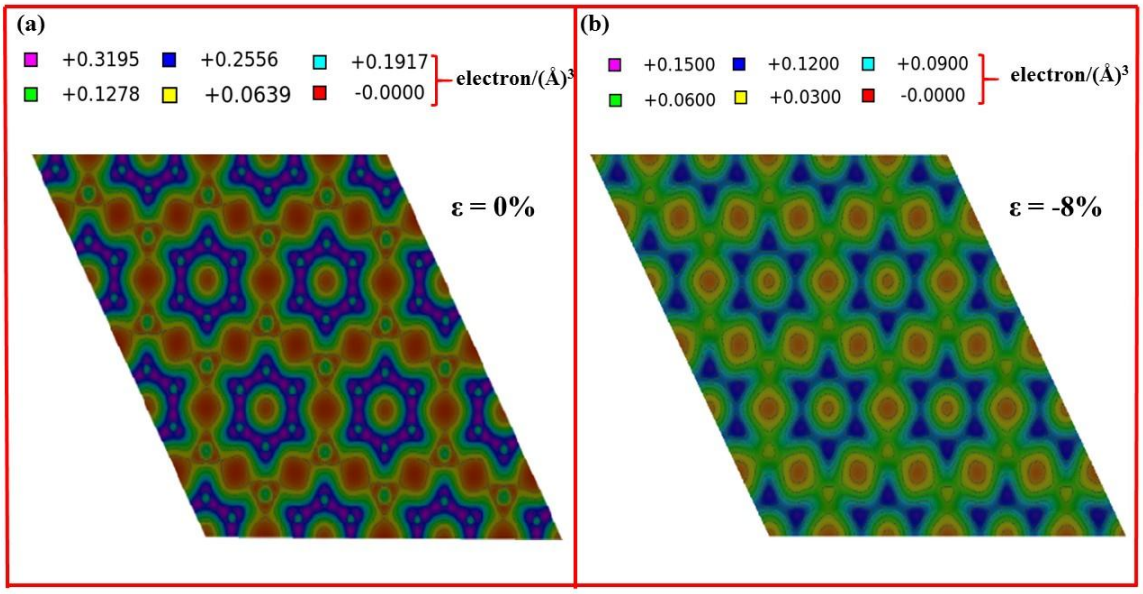

Figure 60: The charge density distribution of Siligraphene (g-SiC_3); (a) without strain (0%). (b) under (-8%) strain.

IV. Conclusion

We have studied the electronic properties and electrical conductivityof the siligraphene (g-SiC_3) by using quantum espressoand Boltztrappackages. Our results show that various percentages of strain effected on the electronic properties. So, the electronic band gap is opened under -9% and -10% strain. Additionally, the geometry structure also altered. We observed that the bond length between C-Si atoms is increased under -9% and -10% strain, which is led to buckle geometrical structure of the g-SiC_3. Furthermore, we found out very fascinating result. The electrical conductivity of g-SiC_3 is increased when we applied various percentages of strain. So, we get a higher value for electrical conductivity at strain equal -9 % when the siligraphene (g-SiC_3) is changed their properties semimetal to semiconductor. We concluded that siligraphene (g-SiC_3) is a flexible nanomaterial can be used at smart nanomaterial such as in a smartphone.

Chapter 6: Detection various properties of two Single-layer Tetragonal Silicon Carbides

I. Introduction

Graphene is a 2-D nanomaterial, which is called the single layer of graphite. Graphene is consisted of sp^2 hybridized carbon atoms, which are arranged in the honeycomb lattice[173]. It is synthesized experimentally by using the micro-mechanical cleavage of graphite at the Centre for Mesoscopic and Nanotechnology of Manchester University, UK by A. Geim et al. in 2004[3]. Due to the bond length between C-C atoms, it has higher physical properties. Graphene has better physical properties by comparing it to graphite thanks to its hexagonal structure, which is bi-dimensional. Graphene is 2-D but graphite is 3-D. In graphene sheet, C atom is surrounded by three other C atoms in the planar sheet, which is makes just three connections. By using the transmission electron microscope (TEM), the bond length between 2C atoms is 0.14 nm, which is measured by Geim et al.. Also, there are two groups produced experimentally by the isolated graphene[174].

There are several researchers who have worked to create graphene, and studied the electronic, optical, mechanical, and magnetic properties [15, 16, 175, 176]. For instance, they found out this material has high electron mobility[177, 178]. Graphene can be used in various applications, such as solar energy[179], nanoelectronics[180], and energy storage[181].These 2D nanomaterial has both a high mobility and gap intrinsic charge carriers that make them more efficient than silicon, which is the basis of the current electronics industry. However, graphene has limited electronic applications due to zero electronic band gap. Therefore, there are many methods used to improve its properties, such as chemical doping and adsorption. For instance, Pablo A. Denis[20] demonstrated that the band gap of graphene (monolayer or bilayer) can be opened with silicon, aluminium, phosphorus and sulfur impurities. The formation of the band gap in graphene with silicon doped has been analyzed by MCS Escaño et al. MSS Azadeh et al.[21, 22]by using DFT. Houmad et al. has been demonstrated that it is possible to open the band gap

of graphene with silicon doped. They found out that the optical conductivity increased as a function of silicon concentration[23, 143, 182]. Likewise, other methods to open the band gap of graphene are proposed such as the functionalization of graphene with hydrogen or molecule adsorptions[24, 183]. The optical properties of graphene can also be improved when it is functioning with organic molecules[109].

Nowadays, there are some researchers who work to create new 2-D nanomaterials such as MoS_2, WS_2, and $MoTe_2$. Li et al.[184]studied the MoS_2 nanomaterial with the repeated square-octagon rings, and they observed that the new system has massless Dirac and heavy fermions neighboring the Fermi surface.

To the best of our insight, single-layer tetragonal silicon carbide(SiC) (2-D nanomaterials), are consisted of silicon and carbon atoms. In fact, these 2-D nanomaterials have never been studied up to date. Here, we will study how the sites of the C and Si influence the various properties such as electronic, optical, and electrical conductivity properties of the two types of the SiC, called as T1 and T2.

II. Computational details

Our calculations are based on the density functional theory (DFT), which is implemented in wien2k code [35] using generalized gradient approximation (GGA) [36], parameterized by PBE Perdew Burke Ernzerhof [37]. In this study, the plane waves were determined using FP-LAPW [38] method, and the space is divided into regions a spherical "muffin-tin" around the nucleus in which radial solutions of Schrödinger Equation and their energy derivatives are used as the basic functions, and an interstitial region between the muffin tins (MT). The electronic and optical properties are studied by the above method and the electrical propriety is studied by using Boltzmann theory, which implanted in the Boltztrap package [39]. It's calculated as a function of Temperature based on the following equation:

$$\boldsymbol{\sigma_{\alpha\beta}(T;\mu) = \frac{1}{\Omega}\int \sigma_{\alpha\beta}(\varepsilon)\left[-\frac{\partial f_{\mu}(T;\ \mu)}{\partial \varepsilon}\right]\partial\varepsilon}$$

The electrical conductivity$(\boldsymbol{\sigma_{\alpha\beta}})$ is obtained with $\boldsymbol{\sigma_{\alpha\beta}(\varepsilon) = \frac{1}{N}\sum_{i,k}\sigma_{\alpha\beta}(i,K)\frac{\delta(\varepsilon-\varepsilon_{i,K})}{d\varepsilon}}$

Here, (α, β) are the tensor indices, and ($E_{i,j}$, Ω, $\vartheta(k)$, $\tau(k), and\ f$) are the band structure, the number of k points, which sampled the Brillouin zone, the band velocity, the relaxation time, and Fermi function, respectively

III. Results and discussions

III.1. Electronic properties

In this part of study, weinvestigated that how the positions of the carbon and silicon atomsin the two structures of the single-layer tetragonal silicon carbides (SiC), which termed as(T1 and T2) effect on their electronic properties. Our calculation is started by relaxing all structures SiC (T1 and T2). After that, we found out that the bond length between Si and C atoms is (1.85 and 1.92) Å, and the angle value is α= 93.20° and β= 86.79°, in the hexagonal and cubic shapes of the T1, respectively. Additionally, it is (1.76, 1.50, and 2.22) Å for Si-C, C-C, and Si-Si bond length in the hexagonal and cubic shapes for T2, respectively, as shown in Fig. 60. The vacuum space in Z axis is equal 20Å, to avoid the interaction between two layers of the SiC.

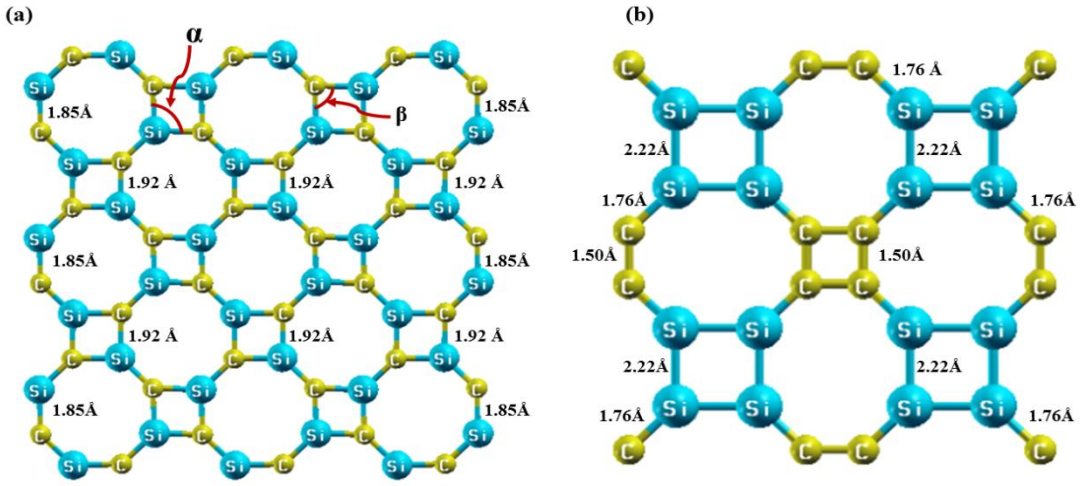

Figure 61: The atomic structures of two types single-layer tetragonal silicon carbides, (a) T1, (b) T2.

After calculating the electronic band structure of the 2-D nanomaterials (T1 and T2), we detected very interesting results. The electronic properties of these 2-D nanomaterials depending on the sites of the Si and C atoms in these structures (T1 and T2). So, we

found out that they are semiconductor and conductor nanomaterials, respectively, due to the nature of band length between atoms. The first type of our nanomaterials has only one kind of the bond length between C and Si (C-Si), but the second type has three kinds of the bond length between atoms (Si-C), (C-C), and (Si-Si). Also, it depends on the valence shell of these atoms, which is $3s^2 3p^2$ and $2s^2 2p^2$ for the Si and C atoms, respectively. We also found out the direct electronic band gap of this semiconductor material, which is 1.74 eV at X wave vector, and it is zero eV, between X and M wave vectors for conductor material. To ensure our result, we calculated the electronic density of state (DOS) of these 2-D nanomaterials. Our finding of the DOS is conformed our interesting results, as displayed in Figs. (61 and 62).

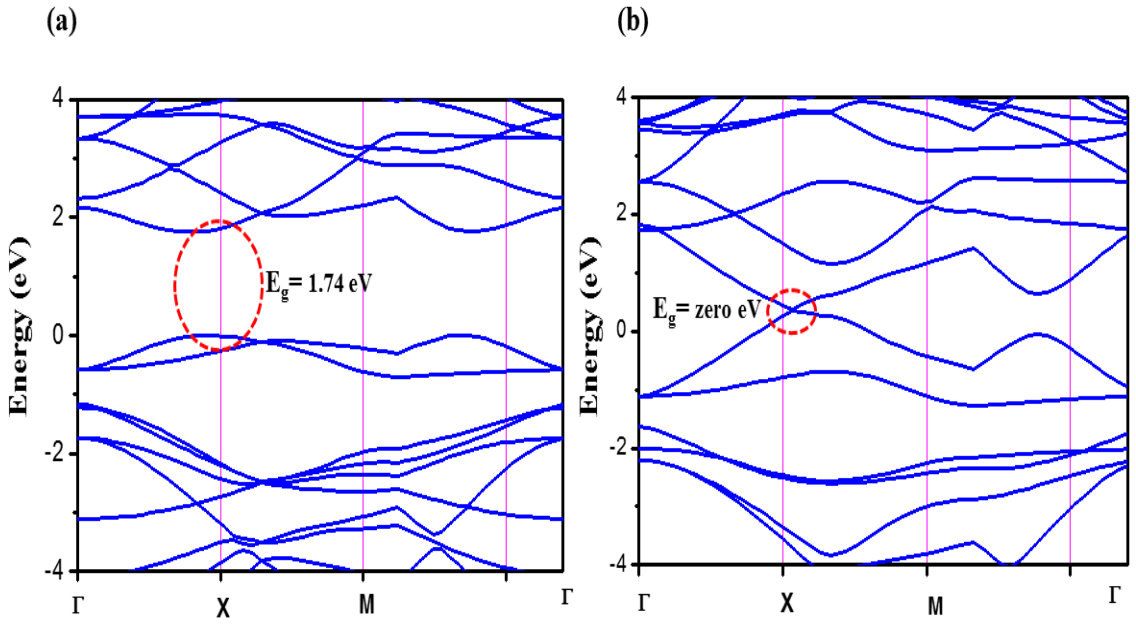

Figure 62: The electronic band structures of two types single-layer tetragonal silicon carbides, (a) for T1, (b) for T2

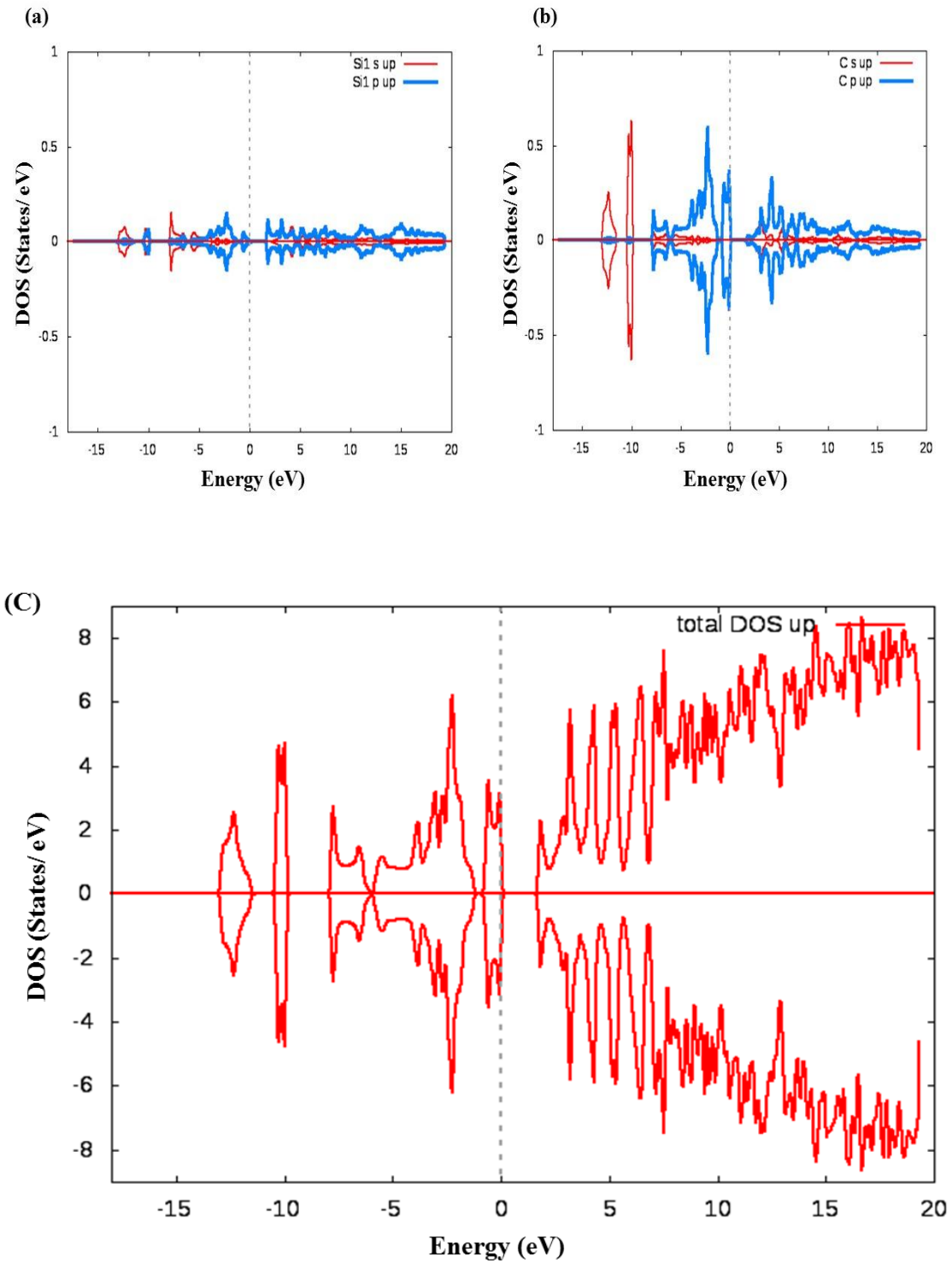

Figure 63: The electronic densityof states (DOS) of the single-layer tetragonal silicon carbides (T1) (a) for Si up, (b) for C up, and (c) the total DOS of the T1

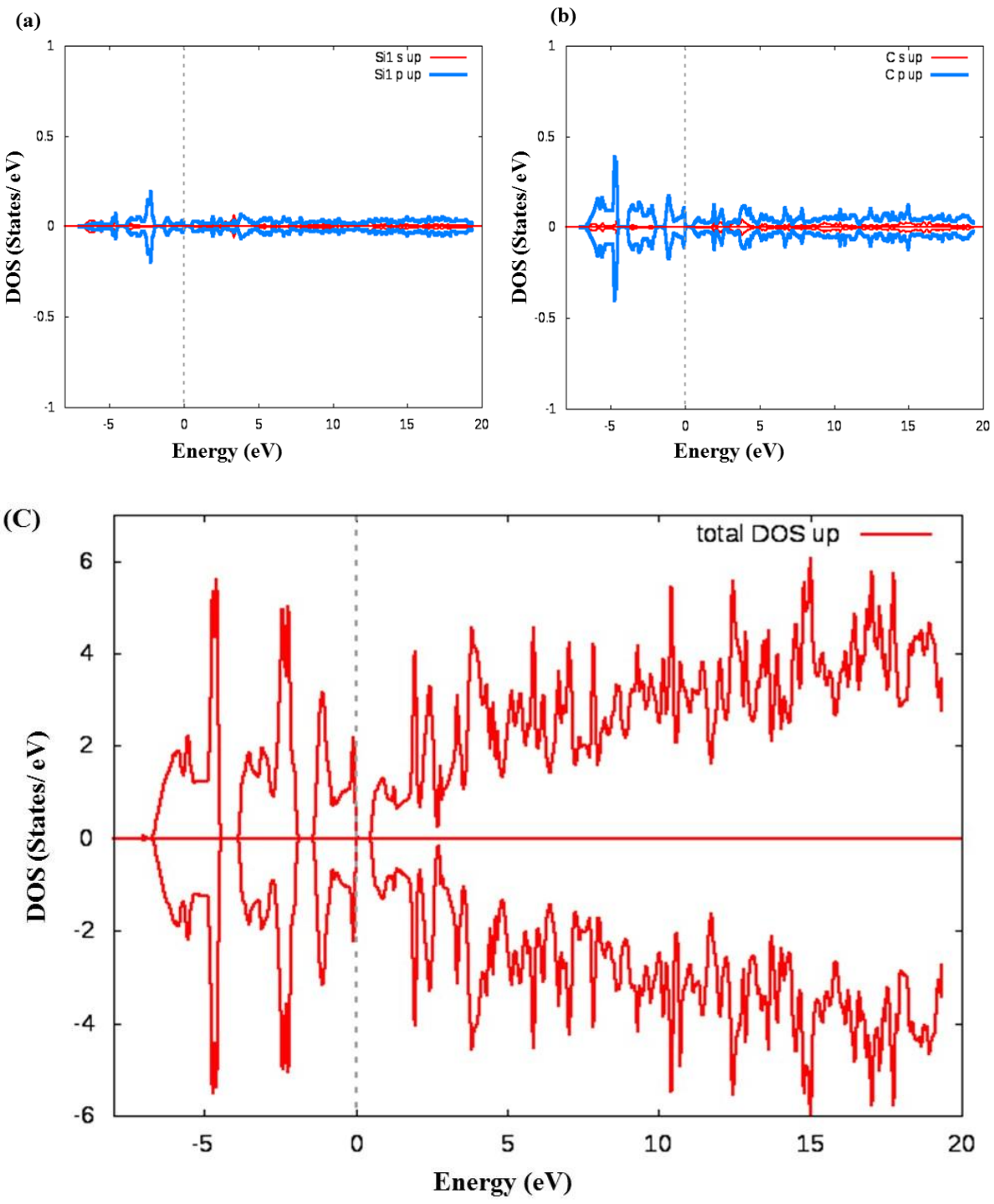

Figure 64: The electronic density of states (DOS) of the single-layer tetragonal silicon carbides(T2), (a) for Si up, (b) for C up, and (c) the total DOS of the T2.

III.2. Optical properties

After finding the interesting electronic properties results of the above 2-D Nanomaterials (T1 and T2), we carried out to compute the optical properties, especially the absorption coefficient of these Nanomaterials. By using the following, we computed the absorption coefficient of the T1 and T2.

$$\alpha(\omega)=\frac{\sqrt{2}}{c}\omega\sqrt{-\varepsilon_1(\omega)+\sqrt{\varepsilon_1(\omega)^2+\varepsilon_2(\omega)^2}} \qquad (4)$$

We observed that the absorption coefficient of the T1 and T2 in the xx direction is different in the zz direction due to the anisotropy of single-layer tetragonal silicon carbides (T1 and T2). By comparing the absorption coefficient of the T1 and T2 in the various directions (xx and zz), we detected that it is firstly started for the T2 and secondly T1 in the xx direction, but it has reversed behavior in the zz direction. In the xx direction, the absorption coefficient starts with an energy value ($E_1 = 0.95\ eV$) for T1, but it is ($E_1 = 0.25\ eV$) for T2. On the other hand, the absorption coefficient starts with an energy value ($E_0 = 2.44\ eV$) for T1, but it is ($E_0 = 2.25\ eV$) for T2 in the zz direction, as shown in Fig.64.

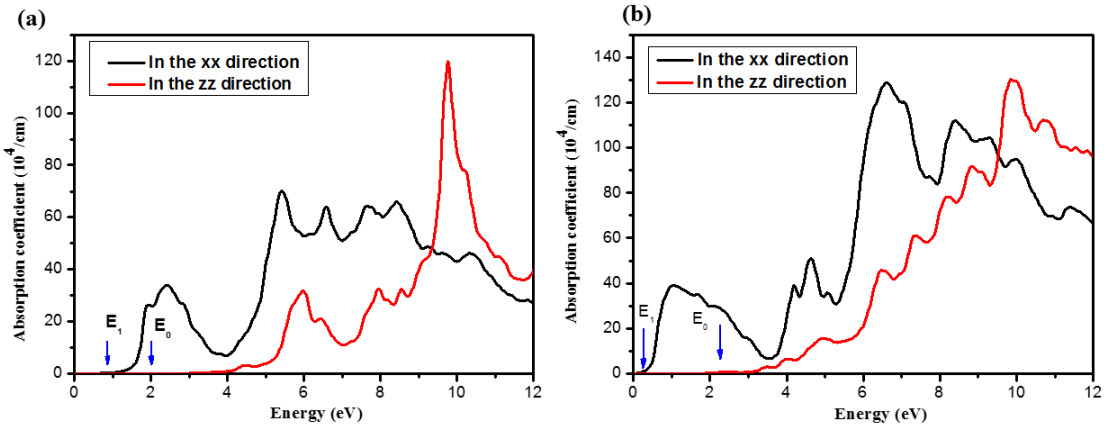

Figure 65: The absorption coefficient of two single-layer tetragonal silicon carbides, (a) for T1 and (b) for T2.

III.3. Electrical conductivity

In this section of our study, we studied the electrical conductivity of our 2-D nanomaterials (T1 and T2) by using Boltzmann equation, which is entrenched in the bolztrap package [45]. This property is calculated at the temperature range (50–800) K. Our finding shows that these 2-D nanomaterials have a difference electrical conductivity. Figure 6 (a) shows that the electrical conductivity increasesfor the nanomaterials T1 when increasing the temperature until 200 K. After this temperature, it is reduced smoothly. However, it is increased smoothly with increasing the temperature (see Fig. 65 (b)), which is very fascinating result. From our results, T2 has a fantastic electrical conductivity comparing with T1 due to the electrical conductivity is affected by the sites of the C and Si and the nature of band length between them in the T1 and T2 structures.

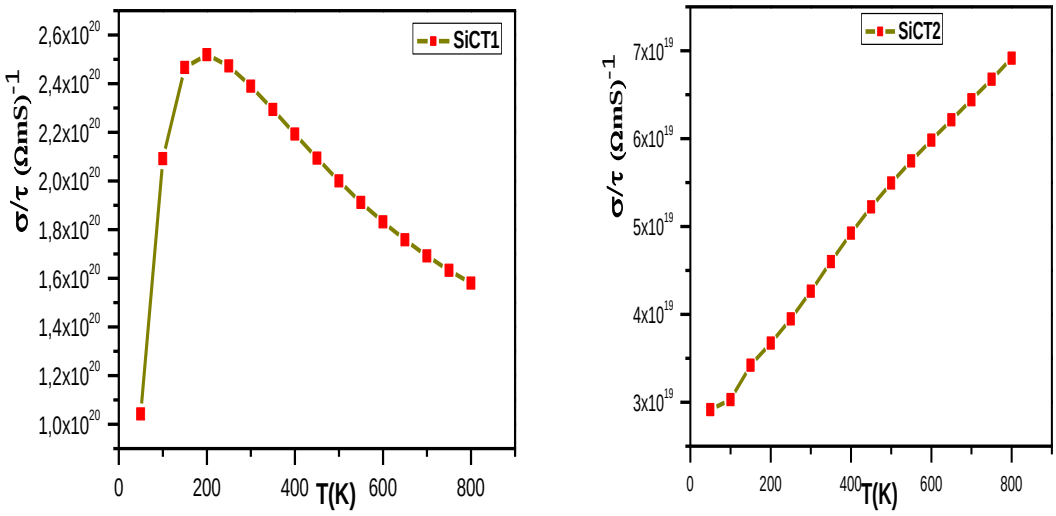

Figure 66: The relationship between the electrical conductivity of two single-layer tetragonal silicon carbides and temperature;(a) for T1 and (b) for T2.

IV. Conclusion

We have studied the electronic, optical, and electrical conductivity properties of two single- layer tetragonal silicon carbides (T1 and T2) by using DFT and Boltzmann theory, which are implemented in the wien2k code and Boltztrap package, respectively. We detected that the behaviors of these 2-D nanomaterials are affected and depended on the sites of the C and Si atoms in the SiC structures. Our results observed that T1 and T2 are a semiconductor nanomaterial with direct electronic band gap, and conductor nanomaterial, respectively. For the optical properties, we found out these properties also influenced by the positions of the C and Si atoms in the T1 and T2 structures. Another important result is electrical conductivity. So, T1 has better electrical conductivity comparing with T2.

Chapter 7: Improving the electrical conductivity of Siligraphene SiC7 by strain

I. Introduction

The radical advance in renewable energy (specifically solar energy) has increase of the factor of transforming solar energy to electrical one. For getting; this transformation is passed with specifics materials, which have a nature semi-metal, for absorbing the photon energy and transforming in to electrical conductivities [185, 186]. Several efforts have been devoted by different research groups to discover the novel materials that have higher physical properties such as electrical conductivity and transparency[187, 188]. For example: doping ZnO bulk with aluminum for increasing their transparency[189]. In 2004; the first materials which have a higher properties is called Graphene. This last become the famous materials in nanotechnology area because their successful applications in many Nano-dives[190, 191].

What is the graphene? Graphene is a one layer or one plan of graphite material. It constitutes of carbon atoms in a hexagonal structure. Their band length between two carbon atoms is the strongest banding equals 1.42 Å. It makes graphene a strong material compared with diamond. In this context, graphene have also a good transparency [192] and, their transmittance is about 97.7% for using it directly graphene in solar cell is not good because its metallic characters have gapless for realizing this aim. It is necessary to change the metallic nature of graphene to semiconductors [193, 194]. This idea has been deposited by several research groups theoretically or experimentally. We cited here the paper realized by Denis et al. and Dai et al. They are confirmed that when graphene is doped with heteroatoms has changed their physical properties[195, 196]. Also, doping graphene by different concentrations of Silicon is an effect on band gap of graphene; it's varied from zero to 2.51 eV according to functional concentration of Silicon doping[23]. This prediction are confirmed by Shi et al. [197] and realized experimentally by Wang et al. [198]. These groups measured the band gap of silicon (concentration 2.7-4.7%) doped graphene, using the ultraviolet photoelectron spectroscopy and found that the band gap of Si doped graphene (concentration 2.7-4.7%) is equal 0.13-0.25eV. Those results

experimentally confirmed the theoretical proposition posed by Houmad et al. [23]. It's possible to use graphene doping with silicon in solar cells application. Also, it's likely supervising the BG with silicon doping graphene. The changing of dopant (such as aluminum, silicon, phosphorus and sulfur) for graphene studied by Denis et al.; demonstrated that the band gap of graphene (monolayer or bilayer) opened[199]. Other groups used the chemical functionalization for open the band gap of graphene[200, 201].

Herein, our studies focalized on siligraphene SiC_7 which is formed by graphene doped with specific concentration of silicon. Their crystal cell constitutes of one atoms of silicon and seven atoms of carbon around in hexagonal structures[202, 203]. In this work, we explore the influence of biaxial tensile and compressive strains on electronic and electrical conductivity of g-SiC_7, based on first principal calculations. We note that the band gap of siligraphene reduced with strain effect but the electrical conductivity increases according biaxial tensile function and compressive strains effect.

II. Computational details

The structural and electronic properties are investigated using the plane-wave projector-augmented wave method as implemented in the QUANTUM-ESPRESSO package [46]. Electron–ion interactions are described using ultra soft pseudo potentials with a kinetic energy cut-off of 38 Ry and the convergence criteria for energy are assumed 10−8 Ry. We perform Brillouin-zone integrations using Monkhorst-Pack grids of special points with 10x10x2 meshes for the calculations of structural and electronic properties. For structural relaxation, to well estimating the band gap, lattice constants and atomic coordinates we use the PBE Perdew Burke Ernzerhof[47, 48]. Starting from the above obtained band structures; we further investigated the carrier transport properties. To study the electrical propriety of Siligraphene we use Boltzmann theory implanted in Boltztrap package [49], it's calculated as function of temperature based on following equation:

$$\boldsymbol{\sigma_{\alpha\beta}(T;\mu) = \frac{1}{\Omega}\int \sigma_{\alpha\beta}(\varepsilon)\left[-\frac{\partial f_{\mu}(T;\ \mu)}{\partial \varepsilon}\right]\partial\varepsilon}$$

The electrical conductivity $\boldsymbol{\sigma_{\alpha\beta}}$ is obtained with $\boldsymbol{\sigma_{\alpha\beta}(\varepsilon) = \frac{1}{N}\sum_{i,k}\sigma_{\alpha\beta}(i,K)\frac{\delta(\varepsilon-\varepsilon_{i,K})}{d\varepsilon}}$

αandβ are the tensor indices $E_{i,j}$ is band structure and Ω is the number of k points that are sampled in the Brillouin zone. ϑ(k), τ(k) and f present the band velocity, the relaxation time and f Fermi function respectively.

III. Results and discussions

III. 1. Stability and electronic properties

Thegeometric structural of Siligraphene g-SiC_7 are optimized for getting the stable structure of band lengths between all atoms constituted Siligraphene g-SiC_7 Carbon and silicon. As shown in Fig. 66, there is one atom of Silicon and seven atoms of Carbon which can be divided on three types according to the distance which links them to the Silicon atom. Thus, the distance between the Silicon atom and the first type of Carbon atom (Si-C, the first close neighbor) equals 1.7939 Å with the bond angle C-Si-C equals 120° and the optimization of C-C band lengths equals 1.53 Å.

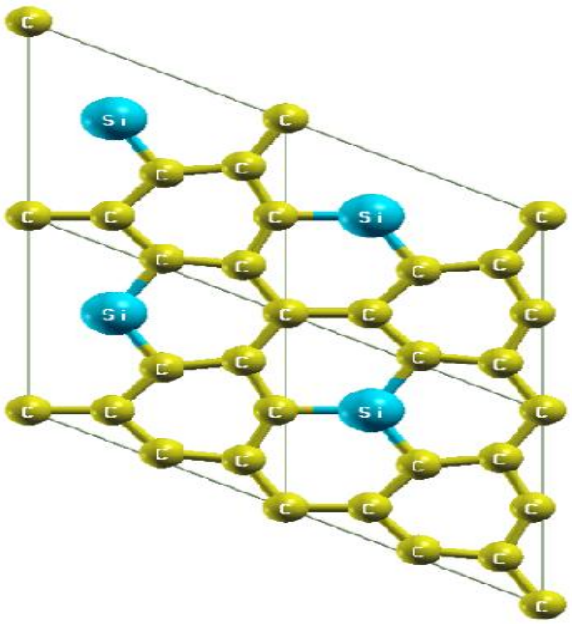

Figure 67: The crystal structures of Siligraphene g-SiC_7.

The structural stability under the strain is very important for studying the physical properties. The mechanical stability is investigated and estimated with formula (1) by applying equi-biaxial (compressive or tensile) strains.

$$Strain,\% = \frac{a1 - a}{a} \times 100\%$$

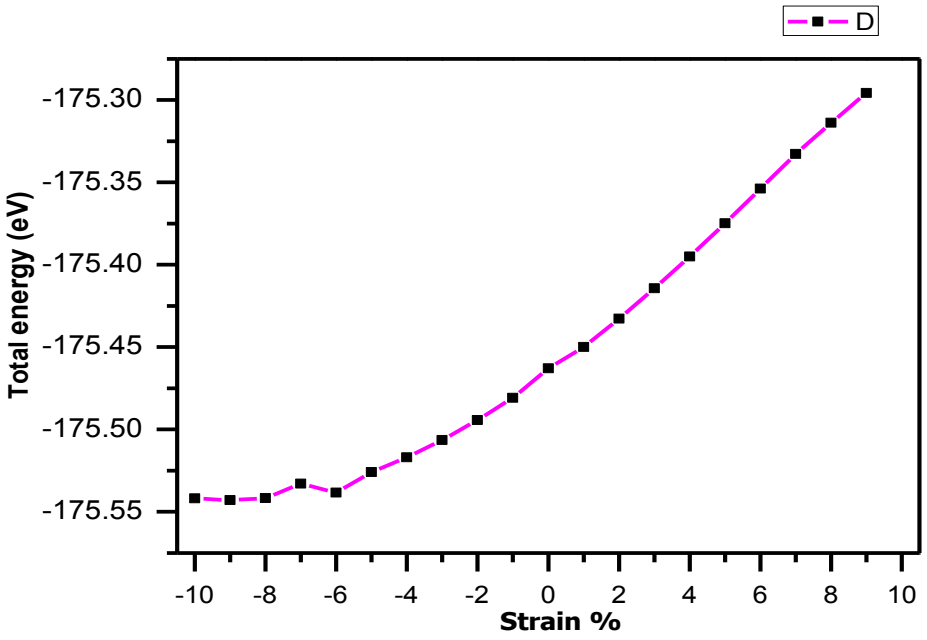

Figure 68: Total energy of Siligraphene g-SiC_7as function of Strain (%).

We imposed a range from -10% to 10% of biaxial strain values along the ab-plane, the negative values of the strain represent a compressive strain, while the positive ones represent a tensile strain. The figure 67, shows the total energy increases with tensile strain is increasing from 0 % to 10%, therefore, our systems Siligraphene g-SiC_7 become instable with tensile but for compressive strain, we observe that total energy of Siligraphene g-SiC_7 become lower. Therefore, the Siligraphene become stable with tensile strains.

Strain (tensile)	**Band gap of SiC_7 (eV)**
0%	**0.79**

1%	**0.78**
2%	**0.72**
3%	**0.66**
4%	**0.58**
5%	**0.51**
6%	**0.43**
7%	**0.34**
8%	**0.19**

Table 1: Band gap of Siligraphene g-SiC_7 as strain function.

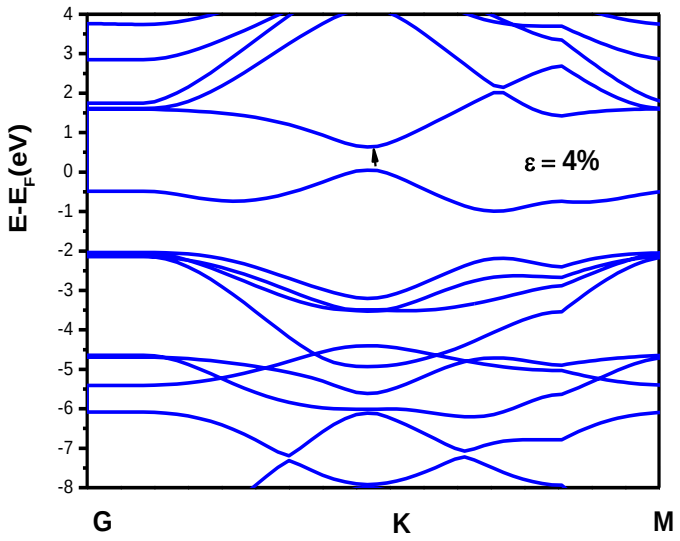

Figure 69: Band Structure of Siligraphene g-SiC7 under strain's tensile (Ɛ = 4%).

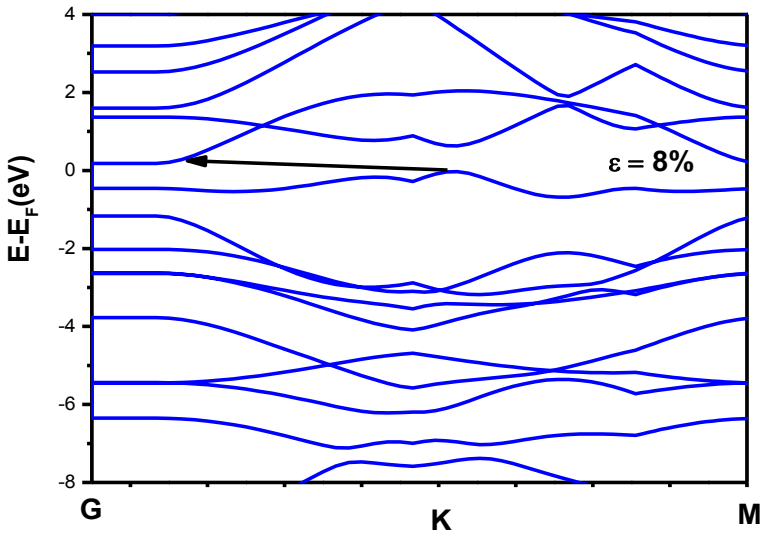

Figure 70: Band Structure of Siligraphene g-SiC7 under strain tensile (Ɛ = 8%).

The table 1, gives the variation of band gap as function of the tensile strains, we note that the band is decreasing when the tensile strain is increasing; this profile confirmed the results obtained by Dong et al. [147], also we plotted the band structure for the tensile 4% and 8% in figure 68 and 69. We observed that the band gap was decreasing and the type of band gap was changing in the direct to the indirect between 4% and 8% respectively.

III.2. Transport properties of Siligraphene g-SiC7 under strain

a) Electrical conductivity as function temperature and under tensile strains (0 to 6%).

We have investigated the transport properties of Siligraphene g-SiCusing Boltzmann transport equations implanted in BolzTrap packages[204]. Indeed, we have studied the electrical conductivity.

To complete our study, we discussed the effect of tensile strains on electrical conductivity of Siligraphene g-SiC_7.

So, in figure 70, We observe that the electrical conductivity of the system increasing as the function of temperature and under tensile strains. The higher value of 6% tensile strains equals 1.55x 10^{18} (Ω.m.S^{-1}) for temperature 800K but for 0% equals 5.86x10^{16} (Ω.m.S^{-1}) for temperature one.

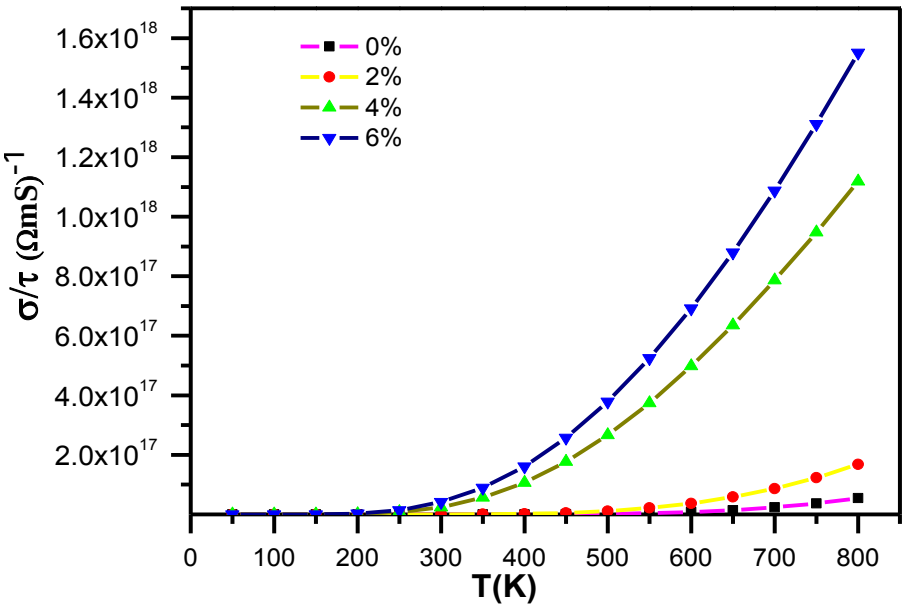

Figure 71: Electrical conductivity as function of the temperature for different value of the tensile strain.

IV. Conclusion

We have performed, in this study, our calculation to study theoretically the electrical and stability properties of the structure of Siligraphene $gSiC_7$ as function of strain effects using the Boltztrap packages and quantum espresso code. Our results shows that the band gap of Siligraphene change under biaxial (compressive and tensile) strains.

On the other hand, we have found that band gap decreases under biaxial (compressive and tensile). Therefore, the electrical conductivity of Siligraphene g-SiC_7 becomes higher under biaxial (compressive and tensile) compared with electrical conductivity of Siligraphene g-SiC_7 without strain.

Chapter 8: Siligraphene as anode novel Materials for Rechargeable Lithium Batteries

I. Introduction

A key challenge for rechargeable Lithium batteries is searching theoretically and realized experimentally for a novel anode has a good performance. The research in this area has been a focus on developed rechargeable Lithium batteries for an answer of demands increasing for renewable and sustainable energy resources. The first successful commercialization of rechargeable lithium batteries was in 1991. Great efforts have been made to develop the Lithium batteries after their first creation. Also, their development is the passage by inventing the novel material which can be possible to apply in Lithium battery. The first creation of Li-battery was in 1979 by Yazami et al.[205]. The Li-battery is intensive studies after their discovery; because of their good life [206], higher reversible capacity[207] and higher energy density [208], have used too commercialization in a much technological device. The graphite is used in commercial batteries; the lithium-ion has been storage between two layers of graphite; because it has a charge capacity equals372 mA h/g and also, has an acceptable reversibility. In addition, the demands, increasing for application the Li-batteries in different areas such as portable electronic devices and electric vehicles, pushed the search to improve the capacity of lithium-ion battery electrodes.

Motived by their excellent properties at different application such as conversion systems and advanced energy storage, the graphene anodes are used for Lithium batteries have been attaching several research groups to develop their capacity, due to their unique chemical and physical properties and the success of application of graphene have encourage the research to invent a new class of materials known as 2D materials. In this context, the discovery of graphene has been opened an innovative possibility to apply the graphene in the development of electron device. For example; the construction of the novel nano-transistors is based on graphene[209, 210]. This material has a gapless, much effort has been devoted to opens their band gap. This objective has been realized by many

research groups using various technical: the first technical is measured by Avetisyan et al. and Mak et al. , are used the electric fields for opening the band gap of graphene. Denis et al. and Dai et al. are calculated the effect of heteroatoms doped graphene on their physical properties [144]. Also, Houmad et al. has been choosing silicon for doping graphene[23]. They are predicting that silicon opening the band gap of graphene and the band gap varied between zero to 2.51 eV as function of silicon concentration this results confirmed by Z. Shi et al. [211]. This predictis realized experimentally by Wu et al. He has measured the effect of silicon doping graphene with level 2.7-4.7% on their gap. He is founding that the silicon opens the band gap of graphene based on electrical measurements using the field effect transistor and deduced from a band gap of Si-graphene equals 0.13-0.25eV used ultraviolet photoelectron spectroscopy confirmed the theoretically prediction posed by Houmad et al. it's possible to use silicon doped graphene in solar cells application. In addition, it's possible to control the band gap with silicon doping graphene. Also, they are found that silicon has increased the optical conductivity in visible light region. The changing of the dopants for graphene is studied by Denis et al.; they are demonstrated that the band gap of graphene (monolayer or bilayer) possible to be open with aluminum, silicon, phosphorus or sulfur. Other groups used the chemical functionalization [212].

Recent development for fabricating the lithium batteries is using the 2D materials such as the 2D transition metal dichalcogenide. These materials have potential candidates for the anode material because their charge capacity, dimensionality and their flexibility. Graphene battery is similar to traditional batteries. Also, it's composed by an electrolyte solution between two electrodes for facilitating the transfer of ion in solution between the electrodes. Graphene based batteries are quickly becoming more favorable than their graphite predecessors. Variety types of batteries have been developed based on graphene introduced in nanocomposites such as Li-ion batteries, Na-ion batteries, Zn-batteries and Li-S battery. The batteries are constituted of three parts: the anodes, cathodes and interface to improve the performance of batteries. It's necessary to improve all three parts. The mechanical instability and the structure changes of Li insertion in 2D materials have limited the performance of all batteries for that the research focalized to increase the life and higher reversible capacity of batteries.

Here, we Proposed the novel anode based on siligraphene for industrialized the Li-ion batteries (LIBs). Based on first principal calculations we find that this novel anode has a diffusion of li ion batteries; this important theoretical result pushes experimental research to create this anode.

II. RESULTS AND DISCUSSION

II.1. Li adsorption and diffusion on the Siligraphene

In this section, we plotted the different positions of the Lithium atom in the Siligraphene structure (thickness of a single layer). In order to examine the binding of the siligraphene surface with Li, we firstly started with by placing a single ad-atom at five different adsorption sites as shown in Figures 2a-2e. We found that the most stable configuration such as: Vertical distances between Li ad-atom and the siligraphene (SiC_3) at the distance between Li and Carbon (C) Top d_{Li-C} = 1.7115A°, between Li and Si (Si) Top d_{Li-Si} = 1.3459A°, Silicon Atom H2 d_{Li-Si} = 2.3374A°, carbon Atom H2 d_{Li-C} = 2.4604A°, carbon Atom H1 d_{Li-C} = 2.2018A°.

Vertical height (h) at the all sites and distances (dP – A) from the siligraphene to the Li ad-atom position at the different site (T1 top on Carbon atoms; T2 top on Silicon atoms; H1 hallo of Carbon hexagonal on siligraphene ; Hall of Silicon-carbon hexagonal on siligraphene H2) all results are displayed in table 1:

Relaxation (site favorable)

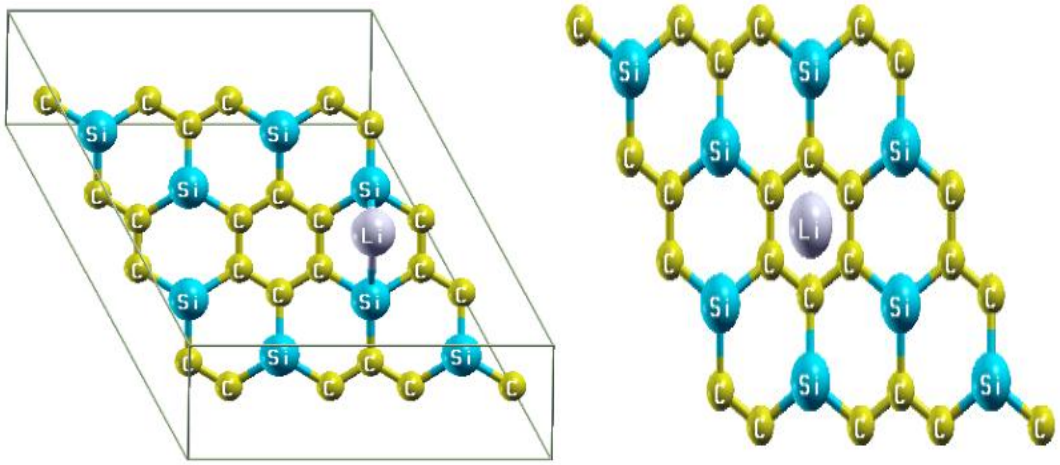

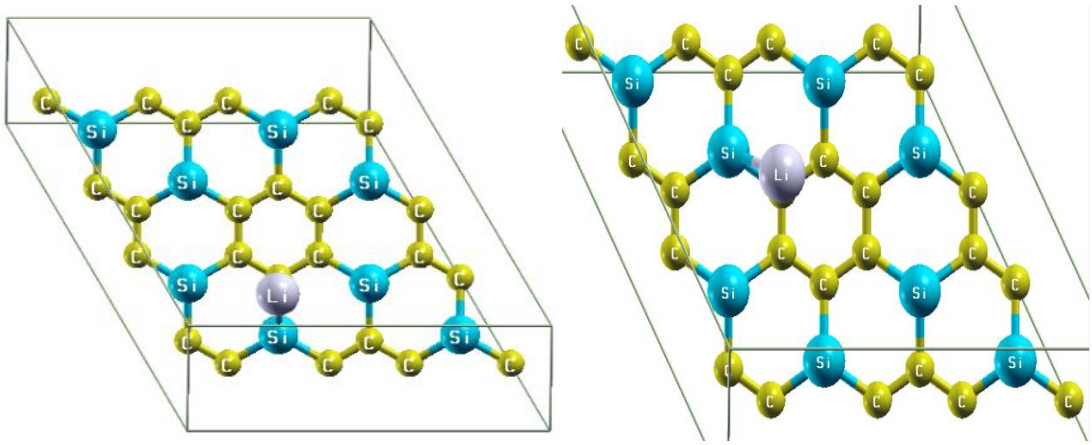

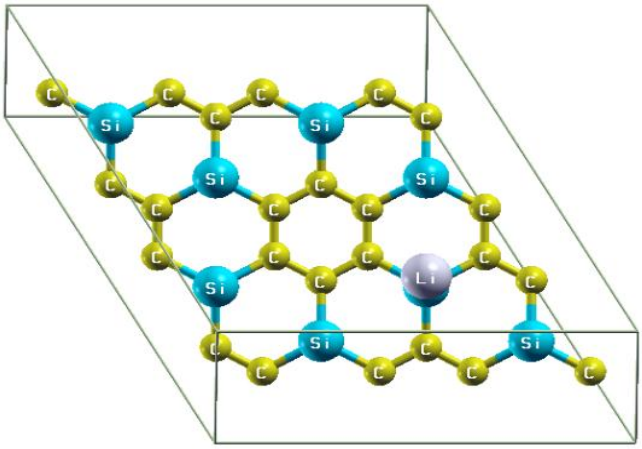

Table 1. Absolute binding energies *E*b at different adsorption sites, vertical distance (*h*) at the H-site.

	system (Ry)	substrat (Ry)	Eb (Ry)	Eb (eV)
H1	-335,95747831	-335,22843455	-0,17262468	-2,3486792748
T1 (C)	-335,88921143	-335,22843455	-0,1043578	-1,4198607176
B2 (C-Si)	-335,82106147	-335,22843455	-0,03620784	-0,4926329387
T2 (Si)	-335,33632645	-335,22843455	0,44852718	6,1025253855
H2	-335,84680505	-335,22843455	-0,06195142	-0,8428923153

II.2 Li Diffusion Process

The actual applications of Lithium batteries are necessities the study at first the Li mobility on Siligraphene and the study of the energy barrier and the possible diffusion path of Li on siligraphene. Before, calculating the diffusion of lithium ion on siligraphene, it's necessary to deduce the most stable site of Li on siligraphene. We have

four principal sites: two bridge, between atoms C-C and between Si-C and two hole in hexagonal constructed with Carbone atoms called H_1 and the second Hole called H_2 is constituted an hexagonal with silicon and Carbone atoms. For calculating the diffusion between two adjacent sites; their difference is in level potential energy exists in this two sites. The diffusion barrier as small as the top of carbon atoms is about 0.095eV but for top of silicon atoms is about 0.223 eV.

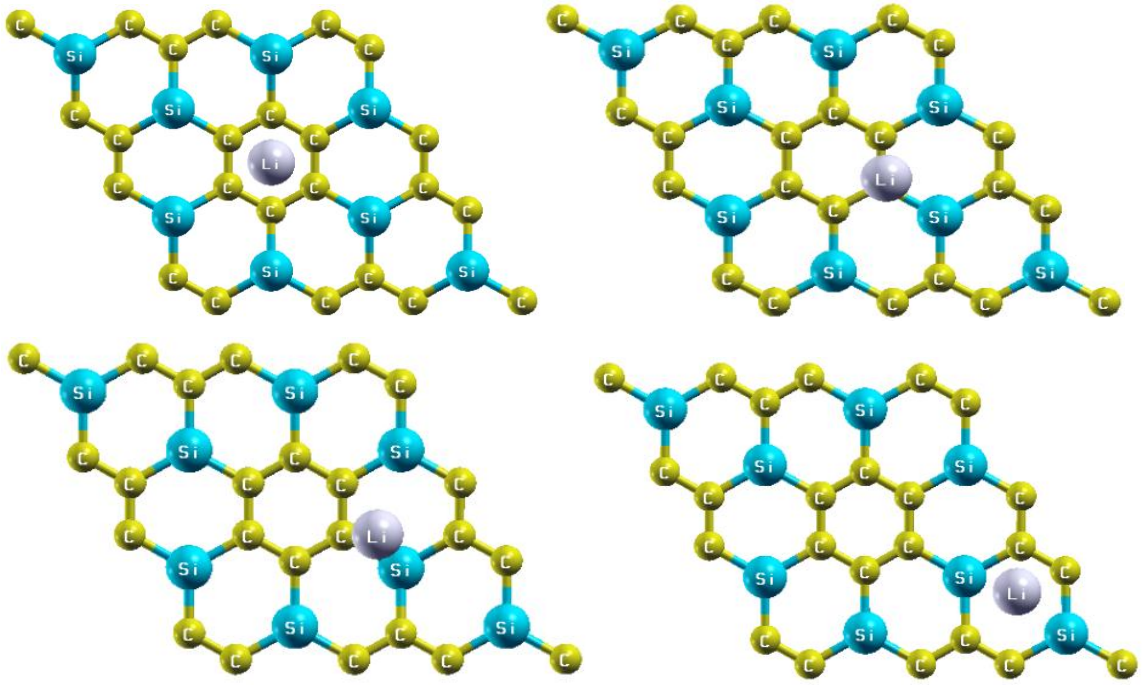

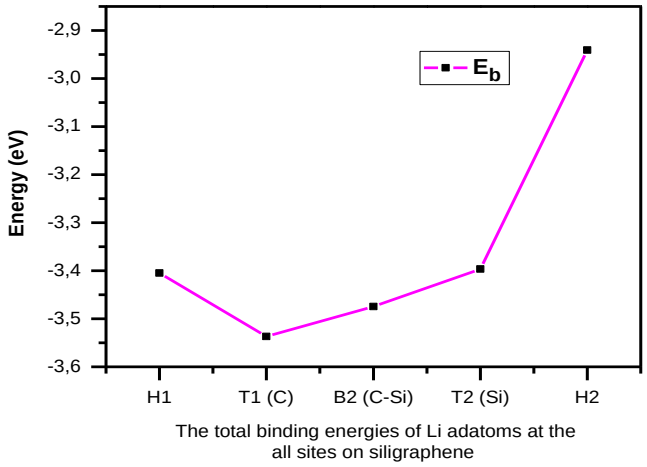

Figure 72: The total binding energies of Li ad-atoms at all sites on siligraphene

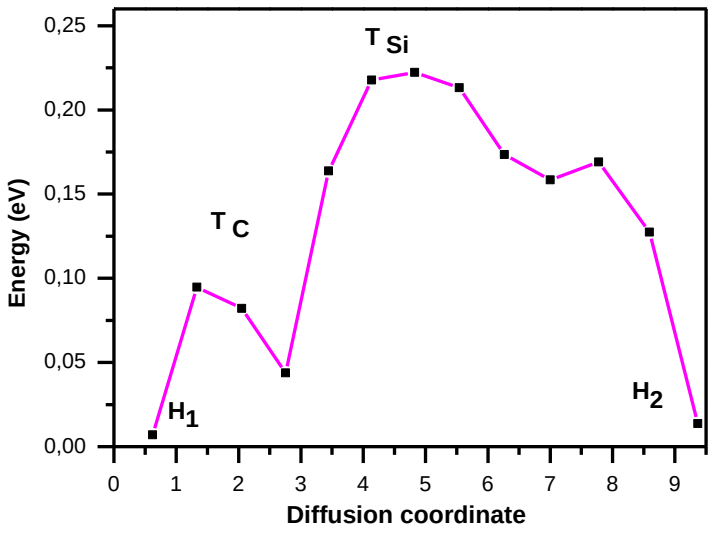

Figure 73: The diffusion barriers

The diffusion barriers along H-H, b -H and H-B-H direction are 0.09 eV and 0.223eV, respectively, which is consistent with previous study and suggesting that Li can diffuse faster along the groove than between two adjacent grooves, like the water flow inside the groove.

IV. Conclusion

To sum up, we have investigated in this paper first-principal calculation based on density functional theory in order to examine the potential of Siligraphene as a new anode material for battery applications by investigating the adsorption and diffusion of Li atom on siligraphene monolayer. We indicated that the structural anisotropy in Siligraphene highly affects the diffusion of Lithium giving an attracting privilege to the diffusion along the all positions.From those observations, it is suggested that Siligraphene can be a strong anode candidate compared to other 2D materials such as graphene and thus it is expected to be efficiently used in the battery applications.

General Conclusion and Outlook

This work was divided into three parts. Thefirst part tackled Generalitieson synthesis and applications of the graphene, siligraphene and its derivatives. The second Part II dealtwith the methods of modeling and simulation. The last Part focused on the physical properties of Siligraphene and its derivatives for application to solar cell or Li-Battery or flexible materials.

We have introduced some allotropes of carbon. We started by Diamond and we finalized by siligraphene. The latter is a new type of 2D materials constituted of graphene doped by silicon atoms with various concentrations. The silicon atoms doped graphene change the metallic character of graphene to semiconductor materials with specific positions and concentrations of silicon atoms in the crystalline structure of graphene.

Part III was dividing into eight chapters: The first chapter presented the optical properties of silicon carbide nanosheet. At this phase, we calculatedin this chapter the dielectric function, reflectivity spectrum, absorption coefficient, optical conductivity and refraction index for both perpendicular and parallel electric field polarizations. We foundthat all result of optical properties is in good argument with one compared with graphene. That is why the silicon carbide nanosheet can be replaced by graphene because it has higher chemical stability. After our full-course on SiC nanosheet, we come up to conclusionthat it can be used to fabricate nano-optoelectronicsdevices. The second Chapter is a theoretically processes the optical conductivity enhancement and band gap opening with Silicon doped graphene. At this point, we have studied the electronic structure of pure and silicon-doped graphene within three approaches GGA, TB-mBJ and GW. Due to the hexagonal symmetries, all the optical properties are different in parallel and perpendicular electric field direction then the graphene is anisotropic material. In addition, we can control the value of band gap as a function of Si concentration. As a consequence, all the optical properties are changed (absorption, transmission). Additionally, the band gap of graphene is gapless, and its optical conductivity starts at very low energy while it has an enhancement because of Si doped graphene in the visible region.

All in all, we concluded that silicon doping increases the optical conductivity of graphene in visible region and it allows the graphene to be used in photovoltaic cells. Chapter three has investigated the Magnetic behavior of Mn doped silicon carbide nanosheet. We studied the electronic structure, the optical and the magnetic properties of Silicon carbide nanosheet pure and doped by Mn. The silicon carbide nanosheet is a semiconductor with a wide band gap equal to 2.51eV. The effects of Manganese doped SiC nanosheet on magnetic and optical properties (absorption coefficient, optical conductivity) were also studied. We obtained that Mn induced the magnetic in SiC nanosheet and increases the absorption coefficient of Silicon carbide nanosheet in the visible light region. Chapter 4, focused on the Electrical property of Siligraphene and its derivatives. In this chapter, the thermal, the electrical and the optical properties of two structures of siligraphene are calculated within wien2kand Boltztrap packages. Our results predict that these two siligraphene have a direct band gap. We concluded that the optical properties are dependent on silicon concentration in siligraphene, and the reflectivity of SiC7 is lower than the reflectivity of SiC3 following xx and zz direction.

Accordingly, we have come up to a number of finding first and foremost the electrical conductivity of g-SiC3 is better than the electrical conductivity of g-SiC7. In this regard, we assume that siligraphene has a potential to be used in solar cell application. In chapter 5 for instance, we have studied the electronic properties and electrical conductivity of the siligraphene (g-SiC3) by using quantum espressoand Boltztrap packages. Second, various percentages of strain effected the electronic properties. So, the electronic band gap is opened under -9% and -10% strains. Third, the geometry structure also altered. We observed that the bond length between C-Si atoms is an increase under strain 10%, which is leads to buckle geometrical structure of the g-SiC3. Another fascinating result is that the electrical conductivity of g-SiC3 increases too, when we apply various percentages of strain. Then we could get a higher value of electrical conductivity at strain equal to -9 % when the siligraphene (g-SiC3) changes its properties semimetal to semiconductor. The bottom line is that siligraphene (g-SiC3) is a flexible nanomaterial and it can be used at smart nanomaterial such as in a smartphone. In chapter 6 for example,wetheoretically studied the electrical and stability properties of the structures of siligraphene as function strain effects using the Boltztrap packages and

quantum espresso code. Here we found that the band gap of Siligraphene changes under biaxial (compressive and tensile) strains. In other words, it decreases under biaxial (compressive and tensile). The electrical conductivity of Siligraphene g-SiC7 becomes higher under biaxial (compressive and tensile) compared to it without strains.

Eventually, in chapter 7 proposeda new anode based on siligraphene used for industrialized Li-ion batteries (LIBs). Based on the first principle calculations, we found that this novel anode has a diffusion of li ion batteries. This important theoretical result pushes experimental research to create this anode.

Bibliography

[1] W. Heath, J. R. Kroto, S. C. OBrien, R. F. Curl et R. E. Smalley, *Nature,* p. 132, 1991.

[2] S. Iijima., *Nature,* vol. 354, p. 56, 1991.

[3] «Novoselov S., Geim A.K., Morozov SV., Jiang D., Zhang Y., Dubonos SV. et al. Electric field effect in atomically thin carbon films,» *Science,* vol. 306, pp. 666-669, 2004.

[4] «Novoselov K.S, Jiang D, Schedinetal F. et al. Two dimensional atomic crystals,» *PNAS,* vol. 102, pp. 10451-10453, 2005.

[5] «JMB Lopes dos Santos, NMR Peres, AH. Castro Neto et al. Graphene bilayer with a twist : electronic structure,» *Phys. Rev Lett.,* vol. 99, p. 256802, 2007.

[6] «H. C. Schniepp et al. Functionalized single graphene sheets derived from splitting graphite oxide,» *J. Phys. Chem. B,* vol. 110, pp. 8535-8539, 2006.

[7] «C. Berger, Z. Song, T. Li, X. Li, A.Y, Ogbazghi, R. Feng, al. et Ultrathin Epitaxial Graphite: 2D Electron Gas Properties and a Route toward Graphene-based Nanoelectronics,» *J. Phys. Chem. B,* vol. 108, pp. 19912-19916, 2004.

[8] «Zhang Y., Y.Tan, Stormer, W. Kim, L. et a. Experimental observation of the quantum Hall effect and Berry's phase in graphene,» *Nature,* vol. 438, p. 201–204, 2005.

[9] «KS. Novoselov, et al. Two-dimensional gas of massless Dirac fermions in graphene,» *Nature,* vol. 438, p. 197–200, 2005.

[10] «KI Bolotin, KJ Sikes, et al. Ultrahigh electron mobility in suspended graphene,» *Solid State Communications,* vol. 146, pp. 351-355, 2008.

[11] «A. S. Mayorov et al.,» *Nano Lett.,* vol. 11, p. 2396, 2011.

[12] «K. Kinam, YC. Jae, K. Taek al. et A role for graphene in silicon-based semiconductor devices,» *Nature,* vol. 479, pp. 338-344, 2011.

[13] «A. S. Mayorov et al.,» *Nano Lett.,* vol. 11, p. 2396, 2011.

[14] «M, Abb; P, Albella; J, Aizpurua; L., Muskens O. All-optical Control of a Single Plasmonic Nanoantenna-ITO Hybrid,» *Nano Lett.,* vol. 11, p. 2457−2463, 2011.

[15] «Naji S, Belhaj A; H, Labrim; M, Bhihi; A, Benyoussef; A., El Kenz, Adsorption of Co and Ni on Graphene with a double Hexagonal Symmetry: Electronic and Magnetic Properties,» *J.*

Phys. Chem. C, vol. 118, p. 4924−4929, 2014.

[16] S. Naji, A. Belhaj, H. Labrim, M. Bhihi, A. Benyoussef et A. E. Kenz, « Electronic and Magnetic Properties of Iron Adsorption on Graphene with Double Hexagonal Geometry,» *Int. J. Quantum Chem.,* vol. 114, pp. 463-467, 2014.

[17] «M, Huang F.; J., Baumberg J. et al. Actively Tuned Plasmons on Elastomerically Driven Au Nanoparticle,» *Nano Lett,* vol. 10, p. 1787−1792, 2010.

[18] «Wang, F., Zhang, Y., Tian C., Girit C., et al. Gate-Variable Optical Transitions in graphene,» *Science,* vol. 320, pp. 206-209, 2008.

[19] X. Wang, Y. Ouyang, X. Li, H. Wang, J. Guo et H. Dai, «Room-temperature all-semiconducting sub-10-nm graphene nanoribbon field-effect transistors,» *Phys. Rev. Lett.,* vol. 100, p. 206803, 2008.

[20] P. Denis, «Band gap opening of monolayer and bilayer graphene doped with aluminium, silicon, phosphorus, and sulfur,» *Chemical Physics Letters,* vol. 492, p. 251–257, 2010.

[21] M. Azdeh, A. Kokabi, M. Housseini and M. Fardmanesh, "Tunable bandgap opening in the proposed structure of silicon-doped graphene," *Micro & Nano Letters,* vol. 6, p. 582, 2011.

[22] M. Escaño, T. Nguyen et H. Kasai, «Analysis of band gap formation in graphene by Si impurities: Local bonding interaction rules,» *Chemical Physics Letters,* vol. 515, p. 85–90, 2011.

[23] M. Houmad, H. Zaari, A. Benyoussef, A. E. Kenz et H. Ez-Zahraouy, *Carbon,* vol. 94, p. 1021 – 1027 , 2015.

[24] H. Park, S. Chang, X. Zhou, J. Kong, T. Palacios et S. Gradečak, «Flexible graphene electrode-based organic photovoltaics with record-high efficiency,» *Nano Lett.,* vol. 14, pp. 5148-54, 2014.

[25] J. C. Charlier, X. Blase and S. Roche, *Carbon,* vol. 677 , p. 79, 2007.

[26] L. A. Girifalco et R. A. Lad, *J. Chem. Phys,* vol. 693, p. 25, 1956.

[27] N. KS, *The rise of graphene. Nature materials,* vol. 6, pp. 183-91, 2007.

[28] «D. Li, R. B. Kaner et al. Materials science. Graphene-based materials,» *Science,* vol. 320, pp. 1170-1, 2008.

[29] «A. K. Geim et al.,» *Science,* vol. 324, p. 1530, 2009.

[30] « P. R. Wallace et al.,» *Phys. Rev.,* vol. 71, p. 622, 1947.

[31] «J. W. McClure et al.,» *Phys. Rev.,* vol. 108, p. 612, 1957.

[32] «J. S. Slonczewski , P. R. Weiss et al.,» *Phys. Rev.,* vol. 109, p. 272, 1958.

[33] «M. A. H. Vozmediano, F. Guinea et al.,» *arXiv:1108.0580,* 2011.

[34] «A. Reina et al. few-layer graphene films on arbitrary substrates by chemical vapor deposition,» *Nano Lett.,* vol. 1, n° %110.1021/nl801827v, p. 30–35, 2009.

[35] «S. Park, R.S. Ruoff et al. Chemical methods for the production of graphenes,» *Nat. Nanotechnol.,* vol. 4, n° %110.1038/nnano.2009.58, p. 217–224, 2009.

[36] « D.V., Kosynkin A.L., Higginbotham A., Sinitskii J.R., Lomeda A., Dimiev B.K., Price J.M. Tour Longitudinal unzipping of carbon nanotubes to form graphene nanoribbons,» *Nature,* vol. 7240, n° %110.1038/nature07872, p. 872–876, 2009.

[37] «L.Y. Jiao, L. Zhang, X.R. Wang, G. Diankov, H. J. Dai et al. Narrow graphene nanoribbons from carbon nanotubes,» *Nature,* vol. 7240, n° %110.1038/nature07919, p. 877–880, 2009.

[38] «Q. Xin G., Hwang W., Kim N., Cho S. M., Chae H. et al. A graphene sheet exfoliated with microwave irradiation and interlinked by carbon nanotubes for high-performance transparent flexible electrodes,» *Nanotechnology,* vol. 21, n° %110.1088/0957-448, p. 40, 2010.

[39] «Xuesong Li, et al. Large-area synthesis of high-quality and uniform graphene films on copper foils,» *science,* vol. 324.5932, pp. 1312-1314, 2009.

[40] «P.W. Sutter, I.J. Flege,E.A. Sutter,» *Nat. Mater.,* vol. 7, p. 406, 2008.

[41] «S.Y. Kwon, C.V. Ciobanu, V. Petrova et al.,» *Nano Lett.,* vol. 9, p. 3985, 2009.

[42] «C. N. R. Rao and A. K. Sood. et al. Synthesis Properties and Phenomena,» *2013 Wiley-VCH Verlag GmbH & Co. KGaA.*

[43] «A., Reina; X., Jia; J., Ho; D., Nezich; Bulovic, Son H.; Dresselhaus, V.; Kong, M.S.,» *Nano Lett.,* vol. 9, p. 30, 2008.

[44] «Wang Z., Li P., Chen Y., Liu J., Zhang W., Guo Z., Dong M., Li Y.,» *J. Mater. Chem. C,* n° %110.1039/C5TC00563A, 2015.

[45] «Ji L., Lin Z., Alcoutlabi M., Zhang X.,» *Energy & Environmental Science,* vol. 4, pp. 2682-2699, 2011.

[46] «Yoo E., Kim J., Hosono E., Zhou H.s., Kudo T., Honma I.,» *Nano letters,* vol. 8, pp. 2277-2282, 2008.

[47] «Idota Y., Kubota T., Matsufuji A., Maekawa Y., Miyasaka T.,» *Science,* vol. 276, pp. 1395-1397, 1997.

[48] «Oyama, N.; Tatsuma, T.; Sato, T.; Sotomura, T.,» 1995.

[49] «X., Li; W., Cai; J., An; S., Kim; J., Nah; D., Yang; al., et,» *Science,* vol. 324, p. 1312, 2009.

[50] «K.S., Kim; Y., Zhao; H., Jang; S.Y., Lee; J.M., Kim; K.S., Kim; J.H., Ahn; P., Kim; J.Y., Choi; B.H., Hong,» *Nature,* vol. 457, p. 706, 2009.

[51] «S.Y., Kwon; C.V., Ciobanu; V., Petrova; V.B., Shenoy; J., Bareno; V., Gambin; I., Petrov; S., Kodambaka,» *Nano Lett.,* vol. 9, p. 3985, 2009.

[52] «Wang, Z.; Li, P.; Chen, Y.; Liu, J.; Zhang, W.; Guo, Z.; Dong, M.; Li, Y.,» *J. Mater. Chem. C,* n° %110.1039/C5TC00563A, 2015.

[53] «Born, D.; Oppenheimer, J.R.,» *Ann. Phys. Rev.,* vol. 84, p. 457, 1927.

[54] «Hartree, D. R. "The wave mechanics of an atom with non-Coulombic central I, II, III, volume 24: 89,111,426 Proc. Cambridge Phil. Soc. Vol. 30. 1928.».

[55] «V. Fock. Z. Phys, 65:209,1930.».

[56] «P. Hohenberg et W. Khon. Phys. Rev., 136, B864, (1964)».

[57] «P. Hohenberg et W. Khon. Phys. Rev., 136, B864, (1964).».

[58] «W. Khon et L. J. Sham. Phys. Rev. A, 140, 1133, (1964).».

[59] «F. Herman, J. P. Van Dyke, and I. P. Ortenburger, Phys. Rev. Lett. 22:807, (1969).».

[60] «J. P. Perdew, J. A. Chevary, S. H. Vosko, K. A. Jackson, M. R. Pederson, D. J. Singh and C. Fiolhais, Physical Review B, Vol. 46, No. 23,1992, pp. 6671-6687.».

[61] «J. P. Perdew and A. Zunger, Phys. Rev. B 23, 5048(1981)».

[62] «P. Blaha and K. Schwarz, “WIEN2k,” Vienna University of Technology, Austria, 2006».

[63] «Koelling and Harmon, 1977».

[64] «MacDonald et al., 1980».

[65] «Nov´ak, 1997.».

[66] «Desclaux, 1969».

[67] «Warren E.Pikett. Computer Physics Report 9. 115, (1989)».

[68] «J.C. Phillips and L. Kleinman, Phys Rev 116, 1959».

[69] «C. Fiolhais, F. Nogeuira, M.A.L. Marques, A Primer in Density-Functional Theory, Lecture notes in Physics, Vol. 620, Springer, Berlin, 2003, chapitres 1 et 6.».

[70] «F.Tran and P.Blaha, Phys Rev.Lett 102, 226401 (2009)».

[71] «W. Kohn and L. J. Sham, Phys. Rev. 140, A1133 (1965)».

[72] «J. P. Perdew and K. Burke, Int. J. Quantum Chem. 57, 309 (1996)».

[73] «A. D. Becke and E. R. Johnson, J. Chem. Phys. 124, 221101 (2006)».

[74] «P.T.B. Schaffer, R.G. Naum ,J. Opt. Soc. Am. (USA) vol.59 (1969) p.1498».

[75] «A. Solangi, M.I. Chaudhry ,J. Mater. Res. (USA) vol.7 no.3 (1992) p.539-54».

[76] «S. Nishino, H. Matsunami, T. Tanaka ,Jpn. J. Appl. Phys. (Japan) vol.14 (1975)».

[77] «N.I. Medvedeva, E.I. Yuryeva, A.L. Ivanovski I, Semiconductors 36 (2002)751–754.».

[78] «X.M. Yu, W.C. Zhou, F. Luo, W.J. Zheng, D.M. Zhu, J. AlloysCompd. 479 (2009)L1–L3.».

[79] «J.S. Lee, Y.K. Byeun, S.H. Lee, S.C. Choi, J. AlloysCompd. 456 (2008) 257–263».

[80] «S. Novoselov, A.K. Geim, S.V. Morozov, D. Jiang, Y. Zhang, S.V. Dubonos, I.V. Grigorieva, A.A. Firsov, Science 306 (2004) 666.».

[81] «K.S. Novoselov and al., PNAS 102,10451 (2005)».

[82] «Huang, F. M.; Baumberg, J. J. Nano Lett. 2010, 10, 1787−1792.».

[83] «Xu, G.; Huang, C. M.; Tazawa, M.; Jin, P.; Chen, D. M. J. Appl. Phys. 2008, 104, 053102».

[84] «Abb, M.; Albella, P.; Aizpurua, J.; Muskens, O. L. Nano Lett. 2011, 11, 2457−2463.».

[85] «Berthelot, J.; Bouhelier, A.; Huang, C. J.; Margueritat, J.; Colasdes-Francs, G.; Finot, E.; Weeber, J. C.; Dereux, A.; Kostcheev, S.; El Ahrach, H. I.; Baudrion, A. L.; Plain, J.; Bachelot, R.; Royer, P.; Wiederrecht, G. P. Nano Lett. 2009, 9, 3914−3921».

[86] «Kim, J.; Son, H.; Cho, D. J.; Geng, B. S.; Regan, W.; Shi, S. F.; Kim, K.; Zettl, A.; Shen, Y. R.; Wang, F. Nano Lett. 2012, 12, 5598−5602».

[87] «A. Wander, F. Schedin, P. Steadman, A. Norris, R. McGrath,T. S. Turner, G. Thornton and N. M. Harrison, Phys. Rev.Lett., 2001, 86, 3811».

[88] «Y. Miyamoto and B. D. Yu, Appl. Phys. Lett., 2002, 80, 586».

[89] «F. Claeyssens, C. L. Freeman, N. L. Allan, Y. Sun,M. N. R. Ashfolda and J. H. Hardingb, J. Mater. Chem. ,2005, 15, 139–148».

[90] «C. L. Freeman, F. Claeyssens and N. L. Allan, Phys. Rev. Lett.,2006, 96, 066102».

[91] «M. Peterson, F. Wanger, L. Hufnagel, M. Scheffler, P. Blaha and K. Schwarz, Computer Physics Communications, Vol. 126, No. 3, 2000, pp. 294-309. doi:10.1016/S0010-4655(99)00495-6».

[92] «W.Y. Ching et al., Materials Science and Engineering (2006)».

[93] «von Munch et al. ,New Series Springer ,Berlin, (1982)».

[94] «J. P. Perdew, J. A. Chevary, S. H. Vosko, K. A. Jackson, M. R. Pederson, D. J. Singh and C. Fiolhais, Physical Review B, Vol. 46, No. 23,1992, pp. 6671-6687.».

[95] «R. Khenata, A. Bouhemadou , M. Sahnoun , Ali. H. Reshak,H. Baltache, M. Rabah, Computational Materials Science 38 (2006) 29–38».

[96] «G. Murtaza, B.amin, S.Arif, M.Maqbool, I. Ahmed, A.Afaq, S. Nazir , M. Imran, M. Haneef, Computational Materials Science, Vol. 58, p. 71-76, 2012».

[97] «H. Salehi, H. Tolabinejad, Optics and Photonics Journal, 2011, 1, 75-80».

[98] «Ming Liu et al., nature letter, 2011».

[99] «H. Salehi, H. Tolabinejad, Optics and Photonics Journal, 2011, 1, 75-80».

[100] «Lopes dos Santos JMB , Peres NMR, Castro Neto AH. Graphene bilayer with a twist :

electronic structure. Phys. Rev Lett. 2007; (99) p. 256802».

[101] «Schniepp HC, Li JL, McAllister MJ, Sai H, Herrera AM, Adamson DH, et al. Functionalized single graphene sheets derived from splitting graphite oxide. J. Phys. Chem. B 2006; (110): 8535-8539».

[102] «Berger C, Song Z, Li T, Li X, Ogbazghi A.Y, Feng R, et al. Ultrathin Epitaxial Graphite: 2D Electron Gas Properties and a Route toward Graphene-based Nanoelectronics. J. Phys. Chem. B 2004; (108): 19912-19916».

[103] «Zhang Y, Tan Y, Stormer W, Kim H. L. P, Experimental observation of the quantum Hall effect and Berry's phase in graphene. Nature 2005; (438): 201–204».

[104] «Abb M, Albella P, Aizpurua J, Muskens O. L. All-optical Control of a Single Plasmonic Nanoantenna-ITO Hybrid. Nano Lett. 2011; (11): 2457−2463».

[105] «Huang F. M, Baumberg J. J. Actively Tuned Plasmons on Elastomerically Driven Au Nanoparticle. Nano Lett. 2010; (10): 1787−1792».

[106] «Wang X.R, Ouyang Y.J, Li X.L, Wang H.L, Guo J, Dai H.J. Room-temperature all-semiconducting sub-10-nm graphene nanoribbon field-effect transistors. Phys. Rev. Lett. 2008; (100) p. 206803».

[107] «Wang X, Zhi L. X, Mullen K. Transparent Conductive graphene Electrodes for Dye-Sensitized Solar Cells. Nano Lett. 2008; (8): 323-327».

[108] «Khenfouch M, Wéry J , Baïtoul M, Maaza M. Photoluminescence and dynamics of excitation relaxation in graphene oxide-porphyrin nanorods composite. Journal of Luminescence 2014; (145): 33-37».

[109] C. DW, C. HJ, F. A et B. JB, «Graphene in photovoltaic applications: organic photovoltaic cells (OPVs) and dye-sensitized solar cells (DSSCs),» *J. Mater. Chem. A,* vol. 2, pp. 12136-12149, 2014.

[110] «Kumar R, et al. Antireflection properties of graphene layers on planar and textured silicon surfaces. Nanotechnology 2013; (24):165402».

[111] «Nath P, et al. Ab-initio calculation of electronic and optical properties of nitrogen and boron doped graphene nanosheet. Carbon 2014;(73): 275-282».

[112] «Nair R. R, et al. Fine Structure Constant Defines Visual Transparency of Graphene. Science 2008; (320) p. 1308».

[113] «Stauber T, et al. Optical conductivity of graphene in the visible region of the spectrum Physical Review B 2008; (78) p. 085432».

[114] «Avouris P, Graphene: Electronic and Photonic Properties and Devices. Nano Lett. 2010; (11): 4285–4294».

[115] «Yao Y, Kats MA, Shankar R, Song Y, Kong J, et al. wide wavelength Tuning of Optical Antennas on Graphene with Nanosecond Response Time. Nano Lett. 2014; (14): 214−219».

[116] «Yao Y, Kats MA, Genevet P, Yu NF, Song Y, Kong J, Capasso F. Broad Electrical Tuning of graphene-Loaded Plasmonic Antennas. Nano Lett. 2013; (13):1257−1264».

[117] «Wu M, Cao C, Jiang JZ. Electronic structure of substitutionally Mn-doped graphene. New Journal of Physics 2010; (12) p. 063020».

[118] «Wang SJ, Geng Y, Zheng Q, Kim JK. Fabrication of highly conducting and transparent graphene films. Carbon 2010; (48):1815-1823».

[119] «X. Wang, L.X. Zhi, K. Mullen. Transparent, Conductive graphene Electrodes for Dye-Sensitized Solar Cells. Nano Lett. 2008, 323-327».

[120] «Chen, S.; Wu, Q.; Mishra, C.; Kang, J.; Zhung, H.; Cho, K. et al. Thermal conductivity of isotopically modified graphene. Nat. Mater. 2012, pp 203–207.».

[121] «M.R. Tchalala, H. Enriquez, H. Yildirim, A. Kara, A.J. Mayne, G. Dujardin, M. Air Ali and H. Oughaddou, Appl. Surf. Sci. 2014, 61».

[122] «Balandin, A.A. Thermal properties of graphene and nanostructured carbon materials. Nat. Mater. 2011, 10, 569–581».

[123] «Feng Wang, Yuanbo Zhang, Chuanshan Tian, Caglar Girit et al. Gate-Variable Optical Transitions in graphene. Science 2008, 206-209».

[124] «Leibo Hu, Xianru Hu, Xuebin Wu, Chenlei Du, Yunchuan Dai, Jianbo Deng , Physica B 405 (2010) 3337–3341».

[125] «M. Houmad, O. Dakir, A. Abbassi , A. Benyoussef , A. El Kenz, H. Ez-Zahraouy. Optik -Int. J. Light Electron Opt. (2015).».

[126] «M Wu , C Cao, J Z Jiang. New Journal of Physics 12 (2010) 063020».

[127] «G. Murtaza, B.amin, S.Arif, M.Maqbool, I. Ahmed, A.Afaq et al. Structural, electronic and

optical properties of CaxCd1_xO and its conversion from semimetal to wide bandgap semiconductor. Computational Materials Science 2012, Vol. 58, p. 71-76».

[128] «C. Berger, Z. Song, T. Li, X. Li, A.Y. Ogbazghi, R. Feng, et al., Ultrathin epitaxial graphite: 2D electron gas properties and a route toward graphene-based nanoelectronics, J. Phys. Chem. B 108, 2004, 19912–19916.».

[129] «Y. Zhang, Y. Tan, W. Stormer and H.L.P. Kim, Experimental observation of the quantum Hall effect and Berry's phase in graphene, Nature 20 (438), 2005, 1–204.».

[130] «K.I. Bolotin, K.J. Sikes, et al., Ultrahigh electron mobility in suspended graphene, Solid State Commun. 146, 2008, 351–355.».

[131] «K. Kinam, Y.C. Jae, K. Taek, et al., A role for graphene in silicon-based semiconductor devices, Nature 479, 2011, 338–344.».

[132] «S. Tongay, T. Schumann, X. Miao, B.R. Appleton and A.F. Hebard, Tuning Schottky diodes at the many-layer-graphene semiconductor interface by doping, Carbon 49, 2011, 2033–2038».

[133] «Deji Akinwande, Nicholas Petrone and James Hone, Hone two-dimensional flexible nanoelectronics, Nat. Commun. 5678, 2014, 6678.».

[134] «W. Xiong, C. Xia, X. Zhao, T. Wang and Y. Jia, Effects of strain and electric field on electronic structures and Schottky barrier in graphene and SnS hybrid heterostructures, Carbon 2016, https://doi.org/10.1016/j.carbon.2016.08.082».

[135] «Satoshi Moriyama, Yoshifumi Morita, Eiichiro Watanabe,, et al., Fabrication of quantum-dot devices in graphene, Sci.Technol. Adv. Mater. 11 (5), 2010, 054601».

[136] «H. Bi, H. Cui, T. Lin and F. Huang, Graphene wrapped copper-nickel nanospheres on highly conductive graphene film for use as counter electrodes of dye-sensitized solar cells, Carbon 2015, https://doi.org/10.1016/j.carbon.2015.04.051.».

[137] «Q. Chang, L. Huang, J. Wang, Z. Ma, P. Li, Y. Yan, J. Zhu, S. Xu, L. Shen, Q. Chen, Q. Yu and W. Shi, Nanoarchitecture of variable sized graphene nanosheets incorporated into three-dimensional graphene network for dye sensitized solar cells, Carbon 2014,».

[138] «F. Xu, T. Lin, H. Bi and F. Huang, Graphene-like carbon with three-dimensional periodicity prepared from organic-inorganic templates for energy storage application, Carbon 111, 2017, 128–132.».

[139] «J. Ye, Z. Yu, W. Chen, Q. Chen, S. Xu and R. Liu, Facile synthesis of molybdenum

disulfide/nitrogen-doped graphene composites for enhanced electrocatalytic hydrogen evolution and electrochemical lithium storage, Carbon 2016, https://doi.org/10.1016/j.carb».

[140] «Y.O.O. Eunjoo, Taichi Habe and Junji Nakamura, Possibilities of atomic hydrogen storage by carbon nanotubes or graphite materials, Sci. Technol. Adv. Mater. 6 (no 6), 2005, 615–619.».

[141] «P.A. Denis, Mono and dual doped monolayer graphene with aluminum, silicon, phosphorus and sulfur, Comput. Theor. Chem. 2016, https://doi.org/10.1016/j.comptc.2016.10.002.».

[142] «C. Tayran, S. Aydin, M. Çakmak and Ş Ellialtioğlu, Structural and electronic properties of AB- and AA-stacking bilayer-graphene intercalated by Li, Na, Ca, B, Al, Si, Ge, Ag and Au atoms, Solid State Commun. 2016, https://doi.org/10.1016/j.ssc.2016.02.007».

[143] «M. Shahrokhi and C. Leonard, Tuning the band gap and optical spectra of silicon doped graphene: many-body effects and excitonic states, Alloys Compd. 2016, https://doi.org/10.1016/j.jallcom.2016.10.101.».

[144] «G.P. Dai, M.H. Wu, D.K. Taylor and K. Vinodgopal, Square-shaped, single-crystal, monolayer graphene domains by low-pressure chemical vapor deposition, Mater. Res. Lett. 1 (2), 2013, 67–76.».

[145] «S.S. Lin, Light-emitting two-dimensional ultrathin silicon carbide, J. Phys. Chem. C 116, 2012, 3951–3955.».

[146] «Z. Shi, Z. Zhang, A. Kutana and B.I. Yakobson, Predicting two dimensional silicon, ACS Carbide Monolayers Nano 2015, https://doi.org/10.1021/acsnano.5b02753.».

[147] «H. Dong, L. Zhou, T. Frauenheim, T. Hou, S. Lee and Y. Li, SiC7 siligraphene novel donor material with extraordinary sunlight absorption, Nanoscale 2016, https://doi.org/10.1039/C6NR00046K.».

[148] «Liu-Jiang Zhou, Yong-Fan Zhang and Li-Ming Wu, SiC2 siligraphene and nanotubes novel donor materials in excitonic solar cells, Nano Lett. 2013, https://doi.org/10.1021/nl403010s.».

[149] «A. Kheyri, Z. Nourbakhsh and E. Darabi, Effect of Fe, Co, Si and Ge impurities on optical properties of graphene sheet, Thin Solid Films 2016, https://doi.org/10.1016/j.tsf.2016.06.007».

[150] «R.R. Nair, et al., Fine structure constant defines visual transparency of graphene, Science 320, 2008, 1308.».

[151] «T. Stauber, et al., Optical conductivity of graphene in the visible region of the spectrum, Phys. Rev. B 78, 2008, 085432.».

[152] «P. Nath, et al., Ab-initio calculation of electronic and optical properties of nitrogen and boron doped graphene nanosheet, Carbon 73, 2014, 275–282, (Y. Li, F., Li, Z. Zhou.».

[153] «S. Bhattacharyya and A.K. Singh, Lifshitz transition and modulation of electronic and transport properties of bilayer graphene by sliding and applied normal compressive strain, Carbon 2016, https://doi.org/10.1016/j.carbon.2015.12.025.».

[154] «Muhammad Farooq Khan, Muhammad Zahir Iqbal, Muhammad Waqas Iqbal, et al., Improving the electrical properties of graphene layers by chemical doping, Sci. Technol. Adv. Mater. 15 (5), 2014, 055004.».

[155] «M. Iqbal, M. Iqbal Waqas, M. Zahir, Farooq M. Khan, et al., Modification of the structural and electrical properties of graphene layers by Pt adsorbates, Sci. Technol. Adv. Mater. 15 (5), 2014, 055002».

[156] «S. Tongay, T. Schumann, X. Miao, B. Appleton, and A. Hebard, "Tuning Schottky diodes at the many-layer-graphene/semiconductor interface by doping," Carbon, vol. 49, pp. 2033-2038, 2011.».

[157] «S. Feng, Z. Lin, X. Gan, R. Lv, and M. Terrones, "Doping two-dimensional materials: ultra-sensitive sensors, band gap tuning and ferromagnetic monolayers," Nanoscale Horizons, vol. 2, pp. 72-80, 2017.».

[158] «H. Bi, H. Cui, T. Lin, and F. Huang, "Graphene wrapped copper–nickel nanospheres on highly conductive graphene film for use as counter electrodes of dye-sensitized solar cells," Carbon, vol. 91, pp. 153-160, 2015.».

[159] «T. M. Marques, C. Luz-Lima, M. Sacilloti, K. Fujisawa, N. Perea-Lopez, M. Terrones, et al., "Photoluminescence Enhancement of Titanate Nanotubes by Insertion of Rare Earth Ions in Their Interlayer Spaces," Journal of Nanomaterials, vol. 2017, 2017.».

[160] «F. Xu, T. Lin, H. Bi, and F. Huang, "Graphene-like carbon with three-dimensional periodicity prepared from organic-inorganic templates for energy storage application," Carbon, vol. 111, pp. 128-132, 2017.».

[161] «S. H. Choi, J.-K. Lee, and Y. C. Kang, "Three-dimensional porous graphene-metal oxide composite microspheres: Preparation and application in Li-ion batteries," Nano Research,

vol. 8, pp. 1584-1594, 2015.».

[162] «S. Liu, Q. Liao, S. Lu, X. Zhang, Z. Zhang, G. Zhang, et al., "Triboelectricity-assisted transfer of graphene for flexible optoelectronic applications," Nano Research, vol. 9, pp. 899-907, 2016.».

[163] «L. Wang, L. Gao, and H. Song, "High-Performance Top-Gated Monolayer SnS2 Field-Effect Transistors," in Advanced Optoelectronics for Energy and Environment, 2013, p. ASa3A. 55.».

[164] «M. H. Al-Abboodi, F. N. Ajeel, and A. M. Khudhair, "Influence of oxygen impurities on the electronic properties of graphene nanoflakes," Physica E: Low-dimensional Systems and Nanostructures, vol. 88, pp. 1-5, 2017.».

[165] «M. H. Mohammed, "Controlling the electronic properties of the graphene nanoflakes by BN impurities," Physica E: Low-dimensional Systems and Nanostructures, vol. 95, pp. 86-93, 2018.».

[166] «M. H. Mohammed, "Designing and engineering electronic band gap of graphene nanosheet by P dopants," Solid State Communications, vol. 258, pp. 11-16, 2017.».

[167] «P. A. Denis, "Mono and dual doped monolayer graphene with aluminum, silicon, phosphorus and sulfur," Computational and Theoretical Chemistry, vol. 1097, pp. 40-47, 2016.».

[168] «Z. Wang, P. Li, Y. Chen, J. Liu, W. Zhang, Z. Guo, et al., "Synthesis, characterization and electrical properties of silicon-doped graphene films," Journal of Materials Chemistry C, vol. 3, pp. 6301-6306, 2015.».

[169] «D. W. Chang, H.-J. Choi, A. Filer, and J.-B. Baek, "Graphene in photovoltaic applications: organic photovoltaic cells (OPVs) and dye-sensitized solar cells (DSSCs)," Journal of Materials Chemistry A, vol. 2, pp. 12136-12149, 2014.».

[170] «S. Bai and X. Shen, "Graphene–inorganic nanocomposites," Rsc Advances, vol. 2, pp. 64-98, 2012.».

[171] «F. Lopez-Urias, M. Terrones, and H. Terrones, "Beryllium doping graphene, graphene-nanoribbons, C 60-fullerene, and carbon nanotubes," Carbon, vol. 84, pp. 317-326, 2015.».

[172] «H. Dong, L. Zhou, T. Frauenheim, T. Hou, S.-T. Lee, and Y. Li, "SiC 7 siligraphene: a novel donor material with extraordinary sunlight absorption," Nanoscale, vol. 8, pp. 6994-6999, 2016.».

[173] «H. I. Sirikumara, E. Putz, M. Al-Abboodi, and T. Jayasekera, "Symmetry induced semimetal-semiconductor transition in doped graphene," Scientific reports, vol. 6, 2016.».

[174] «C. Berger, Z. Song, T. Li, X. Li, A. Y. Ogbazghi, R. Feng, et al., "Ultrathin epitaxial graphite: 2D electron gas properties and a route toward graphene-based nanoelectronics," The Journal of Physical Chemistry B, vol. 108, pp. 19912-19916, 2004.».

[175] «F. Huang and J. J. Baumberg, "Actively tuned plasmons on elastomerically driven Au nanoparticle dimers," Nano letters, vol. 10, pp. 1787-1792, 2010.».

[176] «F. Wang, Y. Zhang, C. Tian, C. Girit, A. Zettl, M. Crommie, et al., "Gate-variable optical transitions in graphene," science, vol. 320, pp. 206-209, 2008.».

[177] «I. Meric, M. Y. Han, A. F. Young, B. Ozyilmaz, P. Kim, and K. L. Shepard, "Current saturation in zero-bandgap, top-gated graphene field-effect transistors," Nature nanotechnology, vol. 3, pp. 654-659, 2008.».

[178] «K. Kim, J.-Y. Choi, T. Kim, S.-H. Cho, and H.-J. Chung, "A role for graphene in silicon-based semiconductor devices," Nature, vol. 479, p. 338, 2011.».

[179] «H. Bi, H. Cui, T. Lin, and F. Huang, "Graphene wrapped copper–nickel nanospheres on highly conductive graphene film for use as counter electrodes of dye-sensitized solar cells," Carbon, vol. 91, pp. 153-160, 2015.».

[180] «D. Akinwande, N. Petrone, and J. Hone, "Two-dimensional flexible nanoelectronics," Nature communications, vol. 5, p. 5678, 2014.».

[181] «J. Ye, Z. Yu, W. Chen, Q. Chen, S. Xu, and R. Liu, "Facile synthesis of molybdenum disulfide/nitrogen-doped graphene composites for enhanced electrocatalytic hydrogen evolution and electrochemical lithium storage," Carbon, vol. 107, pp. 711-722, 2016.».

[182] «H. Park, S. Chang, X. Zhou, J. Kong, T. s. Palacios, and S. Gradečak, "Flexible graphene electrode-based organic photovoltaics with record-high efficiency," Nano letters, vol. 14, pp. 5148-5154, 2014.».

[183] «M. H. Mohammed, F. N. Ajeel, and A. M. Khudhair, "Adsorption of gas molecules on graphene nanoflakes and its implication as a gas nanosensor by DFT investigations," Chinese Journal of Physics, 2017.».

[184] «W. Li, M. Guo, G. Zhang, and Y.-W. Zhang, "Gapless MoS 2 allotrope possessing both massless Dirac and heavy fermions," Physical Review B, vol. 89, p. 205402, 2014.».

[185] «B. Marco, M. Palummo, and J. C. Grossman. Nano letters 13, no. 8 (2013): 3664-3670».

[186] «H. Feng, C. C. Stoumpos, R. P. Chang, and M. G. Kanatzidis.136, no. 22 (2014): 8094-8099».

[187] «Furchi, Marco M., Armin A. Zechmeister, Florian Hoeller, Stefan Wachter, Andreas Pospischil, and Thomas Mueller. IEEE Journal of Selected Topics in Quantum Electronics 23, no. 1 (2017): 1-11.».

[188] «H. Wei, L. Lin, C. Yang, J. Dai, and J.Yang. Nano letters 16, no. 3 (2016): 1675-1682.».

[189] «M. Khuili, N. Fazouan, H. A. El Makarim, E. H. Atmani, Physics Letters A, 380 (36) (2016) 2881-2887.».

[190] «Zakrajsek, Luke, Erik Einarsson, Ngwe Thawdar, Michael Medley, and Josep Miquel Jornet. IEEE Antennas and Wireless Propagation Letters 15 (2016): 1553-1556.».

[191] «Sun, Chen, Jiangnan Si, Zhewei Dong, and Xiaoxu Deng. Optics express 24, no. 11 (2016): 11466-11474.».

[192] «Merthe, Daniel J., and Vitaly V. Kresin. Physical Review B 94, no. 20 (2016): 205439.».

[193] «Li, Si-Yu, Mei Zhou, Jia-Bin Qiao, Wenhui Duan, and Lin He. Physical Review B 94, no. 8 (2016): 085419.».

[194] «Takashima, Kengo, Satoru Konabe, and Takahiro Yamamoto. Surface and Interface Analysis 48, no. 11 (2016): 1214-1216.».

[195] «J. Dai, J. Yuan, P. Giannozzi, Appl. Phys. Lett. 95 (2009) 232105.».

[196] «Yin, Renli, Wanqian Guo, Juanshan Du, Xianjiao Zhou, Heshan Zheng, Qinglian Wu, Joshu Chang, and Nanqi Ren. Chemical Engineering Journal (2017).».

[197] «Z. Shi, Z. Zhang, A. Kutana, B I. Yakobson. Acs nano (2015)».

[198] «Wang, Zegao, Pingjian Li, Yuanfu Chen, Jingbo Liu, Wanli Zhang, Zheng Guo, Mingdong Dong, and Yanrong Li. Journal of Materials Chemistry C 3, no. 24 (2015): 6301-6306».

[199] «Pablo A. Denis. Chemical Physics Letters 492 (2010) 251–257».

[200] «J. Choi, K.-J. Kim, B. Kim, H. Lee, S. Kim, J. Phys. Chem. C 113 (2009) 9433.».

[201] «I. Zanella, S. Guerini, S.B. Fagan, J. Mendes Filho, A.G. Souza Filho, Phys. Rev. B 77 (2008) 073404.».

[202] «H. Dong, L. Zhou,T. Frauenheim, T. Hou, S. Lee and Y. Li, SiC7 Siligraphene: Novel Donor Material with Extraordinary Sunlight Absorption, Nanoscale, 2016, DOI: 10.1039/C6NR00046K».

[203] «Liu-Jiang Zhou, Yong-Fan Zhang, Li-Ming Wu, SiC2 Siligraphene and Nanotubes: Novel Donor Materials in Excitonic Solar Cells, Nano Lett. 2013, doi: 10.1021/nl403010s».

[204] «Madsen, G. K. H.; Singh, D. J. Comput. Phys. Commun. 2006, 175, 67-71.».

[205] «Yazami, R., and Ph Touzain. "A reversible graphite-lithium negative electrode for electrochemical generators." Journal of Power Sources 9.3 (1983): 365-371.».

[206] «L. Ji, Z. Lin, M. Alcoutlabi and X. Zhang, Energy & Environmental Science, 2011, 4, 2682-2699».

[207] «E. Yoo, J. Kim, E. Hosono, H.-s. Zhou, T. Kudo and I. Honma, Nano letters, 2008, 8, 2277-2282».

[208] «N. Oyama, T. Tatsuma, T. Sato and T. Sotomura, 1995.».

[209] «Wang X.R, Ouyang Y.J, Li X.L, Wang H.L, Guo J, Dai H.J. Room-temperature all-semiconducting sub-10-nm graphene nanoribbon field-effect transistors. Phys. Rev. Lett. 2008; (100) p. 206803».

[210] «K. F. Mak, C.H. Lui, J. Shan, T. F. Heinz, Phys. Rev. Lett. 102 (2009) 256405.».

[211] «Z. Shi, Z. Zhang, A. Kutana, B I. Yakobson, Predicting Two Dimensional Silicon Carbide Monolayers. Acs nano 2015».

[212] «. Choi, K.-J. Kim, B. Kim, H. Lee, S. Kim, J. Phys. Chem. C 113 (2009) 9433.».

[213] «A. D. Becke and E. R. Johnson, J. Chem. Phys. 124, 221101 (2006)».

[214] «Nair R. R, et al. Fine Structure Constant Defines Visual Transparency of Graphene. Science 2008; (320) p. 1308».

[215] «P. Nath, et al., Ab-initio calculation of electronic and optical properties of nitrogen and boron doped graphene nanosheet, Carbon 73, 2014, 275–282, (Y. Li, F., Li, Z. Zhou.».